Martin-CR-65-70 Copy No. 5

CONTRACT NAS8-11300

DCN 1-4-50-0144-01 and S1 (1F)
CPB 02-1198-64

FINAL REPORT

DETERMINATION OF LOW-TEMPERATURE FATIGUE PROPERTIES OF STRUCTURAL METAL ALLOYS

(JULY 1964 THRU AUGUST 1965)

October 1965

prepared for:

NATIONAL AERONAUTICS AND SPACE ADMINISTRATION
GEORGE C. MARSHALL SPACE FLIGHT CENTER
HUNTSVILLE, ALABAMA

prepared by:

MARTIN COMPANY
DENVER, COLORADO

Martin CR-65-70 Copy No. 5

Contract NAS8-11300
DCN 1-4-50-01144-01 and S1 (1F)
CPB 02-1198-64

FINAL REPORT
DETERMINATION OF LOW-TEMPERATURE FATIGUE PROPERTIES OF STRUCTURAL METAL ALLOYS
(July 1964 thru August 1965)

October 1965

Authors

T. F. Kiefer
R. D. Keys
F. R. Schwartzberg

Approved

A. A. Ezra, Manager
Aeromechanics and Materials Laboratory

MARTIN COMPANY
Denver, Colorado
Aerospace Division of Martin-Marietta Corporation

FOREWORD

This report was prepared by Martin-Marietta Corporation under Contract NAS8-11300, for the George C. Marshall Space Flight Center of the National Aeronautics and Space Administration. The work was administered under the technical direction of the Propulsion and Vehicle Engineering Laboratory, Materials Division of the George C. Marshall Space Flight Center with W. B. McPherson acting as project manager.

CONTENTS

Figure

Table

ABSTRACT

The results of a one-year fatigue program that is supplemental to a previous contract are presented in this final report.

During the program the following aluminum stainless steel and nickel structural sheet alloys were evaluated under the conditions noted.

Aluminum Alloys	Test Conditions
2014-T6	Parent (R = 0.01), Notch (K_t = 8.0)
7039-T6	Parent (R = 0.01), Notch (K_t = 8.0)
7106-T6	Parent (R = -1.0, 0.01), Notch (K_t = 3.5), Weld
Stainless Steel	
A-286	Parent (R = -1.0), Notch (K_t = 3.5), Weld
Nickel Alloys	
Inconel 718	Parent (R = -1.0), Notch (K_t = 3.5), Weld
Hastelloy C	Parent (R = -1.0), Notch (K_t = 3.5), Weld

Properties for these materials were determined at 70, -320, and -423°F for fatigue life in the 10^3 to 10^7 cycle range.

Data obtained from the final report of the previous fatigue contract, NAS8-2631, are included in this report for comparison.

From an analysis of the complied test results, the following materials appear to be satisfactory for cyclic service at cryogenic temperatures.

Aluminum Alloys	Stainless Steel	Nickel Alloys
2014-T6	321	Inconel 718
2219-T87	A-286	Hastelloy C
2219-T62		
7039-T6		
7106-T6		
5456-H343		

I. INTRODUCTION

Selection of the proper materials for booster and space vehicle systems that use cryogenic propellants is a challenge because of the behavior of structural materials at low temperatures. Routine mechanical properties, such as tensile and compressive strength, modulus of elasticity, and ductility are usually determined to assess the behavior of a candidate material. Behavior under stress concentration and cyclic loading conditions must also be studied to evaluate a potential material adequately.

Cryogenic literature reveals some data on the routine properties, but there is a significant lack of reliable information on fatigue or cyclic loading. Cryogenic fatigue data on welded material are virtually nonexistent. The experimental program presented in this report was prepared to fill this requirement for sound engineering data.

Fatigue tests can best be described by the method used to apply loads. Repeated loading to both a constant-stress amplitude and a constant-strain amplitude are used. With the first method, direct axial loading is employed, and with the second, plane or rotational bending techniques are used. For axial testing, the entire cross section is uniformly loaded. Stress is determined by load/area. In bending, the stress varies throughout the cross section of the test specimen, from a maximum at the outer fiber through zero at the neutral axis, to a maximum negative value at the opposite outer surface. With this technique, stress must be obtained by calculating from the moment formula, $S = (Mc)/I$.

Although these bending tests have been the most popular fatigue techniques in the past, they are being replaced by the axial-loading method because of certain disadvantages in bending.

As shown by the formula, bending stress is calculated with the bending moment and section modulus. The bending moment, M, is a function of the modulus of elasticity of the test material. Accuracy of the stress calculation is, therefore, directly proportional to the accuracy of the modulus value. Although moduli of common engineering materials at room temperature are known, there is little information in the literature on values at cryogenic temperatures.

The endurance limit obtained by bending techniques may be as much as 30% higher than values obtained by axial loading. Although the reasons for this are not fully understood, certain state-of-stress theories have been proposed. One explanation is the possible development of favorable transverse stresses in the elongated or compressed surface layers and an outer-layer resistance to deformation caused by the underlying material during bending load tests.

Another shortcoming of the bending technique is that when plastic yielding occurs, stresses in the member cannot be readily calculated. Even in tests performed in the elastic range, minute localized plastic deformation may change the outer fiber stress.

There is a greater chance of failure from minor surface defects in bending than in axial loading. These defects may also create larger scatter with a limited number of specimens.

In calculating stress, the simple moment formula can be used only on specimens free from holes, grooves, and outline or surface discontinuities, such as weld beads. Therefore, to evaluate the bending fatigue of welded specimens, it would be more desirable to machine the weld bead flush. However, this would detract from the validity of the joint information since it eliminates stress concentrations.

The axial loading method was selected for this program because of the superiority of the technique and its ability to simulate anticipated structural loads. The axial-loading machines use a rotating mass to apply a controlled dynamic load sinusoidally about a static-load level.

Tension/compression tests of sheet materials under axial loading are not often performed, since these tests are normally restricted to bar materials. Fortunately, the sheet gage selected by NASA allowed complete reversal of stresses without having to resort to the bending technique. The success of such an approach depends on the flatness of the sheet products available. The aluminum, stainless steel, and nickel alloys used for this research were sufficiently flat to permit fully reversed stressing.

Testing at liquid hydrogen temperature was conducted at the Denver laboratories. All equipment was designed and constructed at this location. Evaluation of fatigue properties at 70 and -320°F was conducted at the Baltimore laboratories.

The experimental program described in this report represents the third year's effort of a program initiated in April 1962, under Contract NAS8-2631. The results of the first two years' research, conducted under the above contract, were reported in Determination of Low-Temperature Fatigue Properties of Structural Metal Alloys, Martin-CR-64-74, dated October 1964.

During the NAS8-2631 work, testing equipment was developed and a fatigue evaluation of 11 materials was performed for various specimen conditions at temperatures from 70 to -423°F. The work performed during the current effort is a further study of several materials previously investigated, plus evaluation of new compositions.

II. MATERIALS AND TEST PROGRAM

Materials selected for evaluation in this program include those that are being considered for structural service at cryogenic temperatures.

Material condition was selected to give the high strength levels normally considered for aerospace construction. Specimen test conditions used for this program were unnotched, notched, and welded.

The materials selected for evaluation during the past year's effort are listed in Table 1. Chemical analyses for these alloys are given in Table 2.

Aluminum, stainless steel, and nickel alloys were welded with the tungsten inert gas (TIG) process and automatic welding heads. Table 3 lists details of the procedure used for each material.

All weld panels were radiographically inspected. The aluminum panels exceeded the Class II requirements of MSFC Drawing 10509310. Weld quality approximated the requirements displayed in the NASA specifications for Class I welds. Similarly, the stainless steel and nickel alloys were of high quality.

The test program for the past year and a review of the previous work are listed in Table 4.

Table 1 List of Materials Selected for Experimental Program

Alloy Base	Designation	Temper	Nominal Thickness (in.)	Producer	Heat Number
Aluminum	2014	-T6	0.100	Reynolds	
Aluminum	7039	-T6	0.125	Kaiser	
Aluminum	7106	-T6	0.125	Alcoa	
Stainless Steel	321	Annealed	0.090	Republic	3342058
Stainless Steel	A-286 (AMS-5525)	Solution-Treated	0.125	Eastern Stainless Steel	E-93432
Nickel	Inconel 718	Solution-Treated	0.100	International Nickel	HT-6509-E
Nickel	Hastelloy C	Solution-Treated	0.100	Haynes Division, Union Carbide	CA-3648

Table 2 Composition of Alloys Evaluated

Material	Heat Number	Certification	Composition (Wt%)									
			Si	Fe	Cu	Mn	Mg	Zn	Cr	Others	Aℓ	
2014 Aluminum	--	Nominal	0.5 to 1.2	1.0	3.9 to 5.0	0.40 to 1.2	0.20 to 0.80	0.25	0.10	--	Balance	
2020 Aluminum	--	Nominal	0.40	0.40	4.0 to 5.0	0.30 to 0.80	0.03	0.25	--	--	Balance	
2219 Aluminum	--	Nominal	0.20	0.30	5.8 to 6.8	0.20 to 0.40	0.02	0.10	--	--	Balance	
5456 Aluminum	--	Nominal	0.40 Si and Fe		0.10	0.50 to 1.0	4.47 to 5.5	0.25	0.05 to 0.25	--	Balance	
7039 Aluminum	--	Nominal	0.30	0.40	0.25	0.10 to 0.40	2.3 to 3.3	3.5 to 4.5	0.15 to 0.25	--	Balance	
7075 Aluminum	--	Nominal	0.50	0.70	1.2 to 2.0	0.30	2.1 to 2.9	5.1 to 6.1	0.18 to 0.40	--	Balance	
7106 Aluminum	--	Nominal	0.35 Si and Fe		0.10	0.10 to 0.40	1.7 to 2.8	3.7 to 4.8	0.06 to 0.20	Zr=0.08 to 0.25	Balance	
			C	Mn	Si	Ni	Cr	Mo	Fe	W	Ti	Others
321 Stainless Steel	3342058	Nominal	0.08	2.00	1.00	8.0 to 11.0	17.0 to 19.0	--	Balance	--	6xC to 0.7	--
A-286 Stainless Steel	E-93432	Actual	0.054	1.30	0.69	25.78	14.70	1.2	Balance	--	1.89	Al = 0.15
Inconel 718 Nickel	HT-6509-E	Actual	0.04	0.20	0.20	52.5	19.0	3.0	18.0	--	0.80	Cb = 5.20 Al = 0.60
Hastelloy C Nickel	CA-3648	Actual	0.05	0.48	0.64	56.6	15.5	16.2	5.7	3.8	--	--

Table 3 Welding Procedure for Stainless Steel, Nickel, and 7106 Aluminum Alloys

Alloy	Filler Wire	Wire Diameter (in.)	Voltage (v)	Current (amp)	Speed (in./min)
A-286 Stainless Steel	Hastelloy W	0.062	11	90	6
Inconel 718 Nickel	718	0.062	11	60	6
Hastelloy C Nickel	Hastelloy C	0.062	11.5	70	6
7106-T6 Aluminum	X5180	0.096	13	110	18

Table 4 Test Program for Past Year

Material	Test Condition				
	Unnotched		Notched		
	R = -1	R = 0.01	K_t = 3.5	K_t = 8.0	Welded
2014-T6	*	†	*	†	*
2219-T87	*	--	*	--	*
2219-T62	*	--	*	--	*
7039-T6	*	†	*	†	*
7106-T6	†	†	†	--	†
5456-H343	*	--	*	--	*
7075-T6	*	--	*	--	--
2020-T6	*	--	--	--	--
Ti-5Al-2.5Sn	--	*	*	--	*
Ti-6Al-4V	--	*	*	--	*
Ti-13V-11Cr-3Al	--	*	*	--	*
AISI 321	*	--	*	--	*
A-286	†	--	†	--	†
Inconel 718	†	--	†	--	†
Hastelloy C	†	--	†	--	†

*Work performed under Contract NAS 8-2631.
†Work performed under present Contract NAS8-11300.

III. SPECIMENS

Tensile specimens were machined to specifications shown in Fig. 1 and designed specifically for use with the multiple-linkage system described by Keys (Ref 1).

Unnotched and welded fatigue specimens were machined according to the sketch in Fig. 2a. Aluminum specimens were machined to 0.375-in. gage width (A dimension), and stainless steel and nickel materials to a gage width of 0.200 in. In contrast to the usual fatigue specimen shapes, the specimen design incorporates a straight-column test-gage section. A constant-width test section was selected to permit proper evaluation of weld bead and heat-affected zone in a short column length.

Notched specimens were machined according to specifications in Fig. 2b. A notch depth of 33% was used. Notch specimens were machined with an elastic stress concentration factor (K_t) of 3.5 or 8.0. Stress concentration factors were calculated according to the data of Peterson (Ref 2).

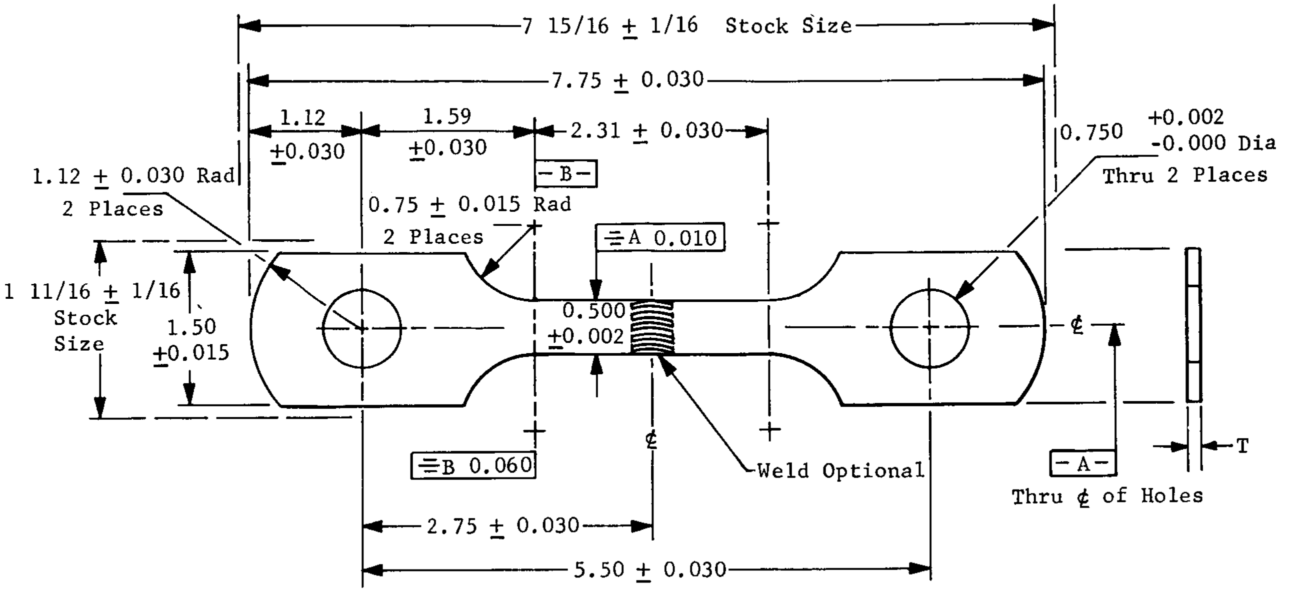

(a) Parent and Weld Tensile Specimen

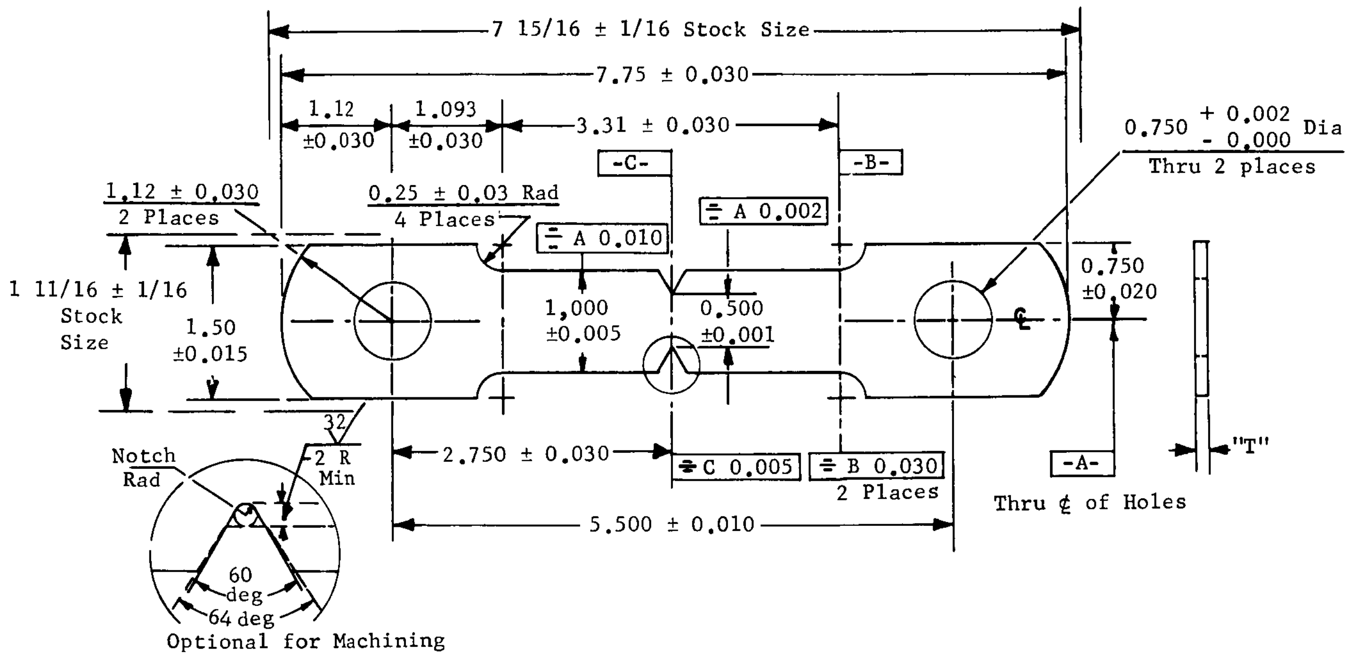

(b) Notched Tensile Specimen

Fig. 1 Specifications for Tensile Specimens

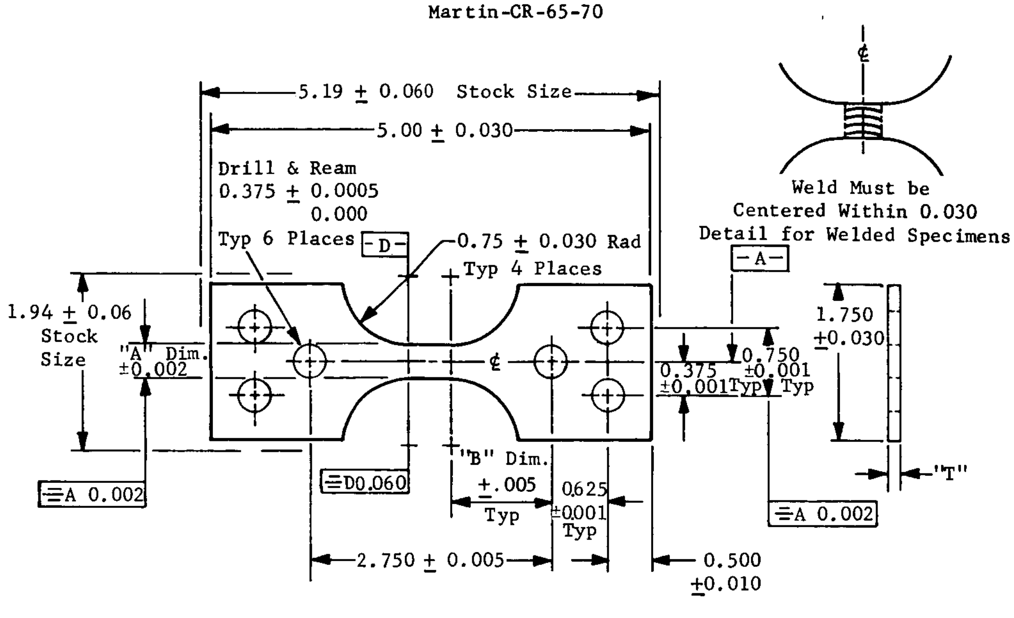

Note:	When "A" = 0.200, "B" = 1.250.
	When "A" = 0.375, "B" = 1.125.

(a) Unnotched and Welded Specimen

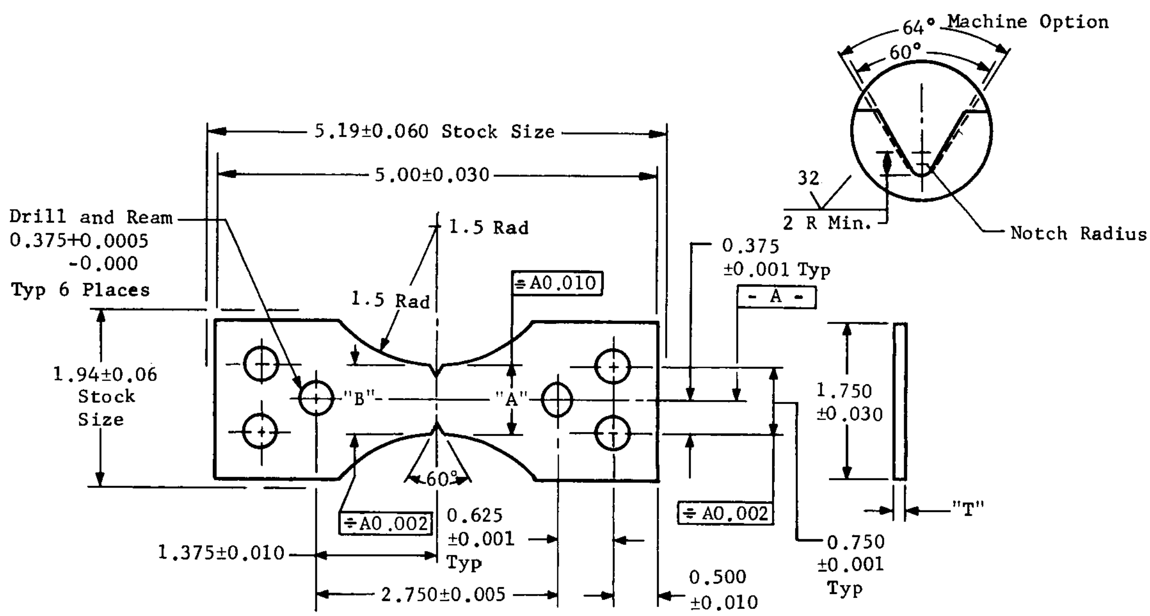

Note:	1. When "A" = 0.600, "B" = 0.400
	±0.005 ±0.001.
	2. When "A" = 0.375, "B" = 0.250.
	3. Notch root center lines ⊥A.0.003.

(b) Notched Specimen

Fig. 2 Specifications for Fatigue Specimens

IV. TEST APPARATUS, FACILITIES, AND TEST PROCEDURE

A. TEST APPARATUS

The fatigue test apparatus used for this work is described in Ref 3 and 4. A cutaway view of the cryostat assembly is shown in Fig. 3. The design incorporates a vacuum-insulated, double-walled, stainless steel container with a tubular loading stem that passes through its central axis. Another tubular loading stem passes through the cryostat lid. The test specimen is gripped between these two stems. The cryostat mounts on the reciprocating platen of the test machine and moves with the platen while the lid, with the liquid supply line, vent line, and instrumentation support attached, remains fixed to the machine head frame.

A detailed discussion of alignment and assembly is given in Ref 3.

B. FACILITIES

Photographs and detailed discussion of the facility for liquid nitrogen and liquid hydrogen testing are in Ref 3.

C. TEST PROCEDURE

Procedure for tension and fatigue testing is the same as previously described for the work performed under Contract NAS 8-2631 (Ref 3).

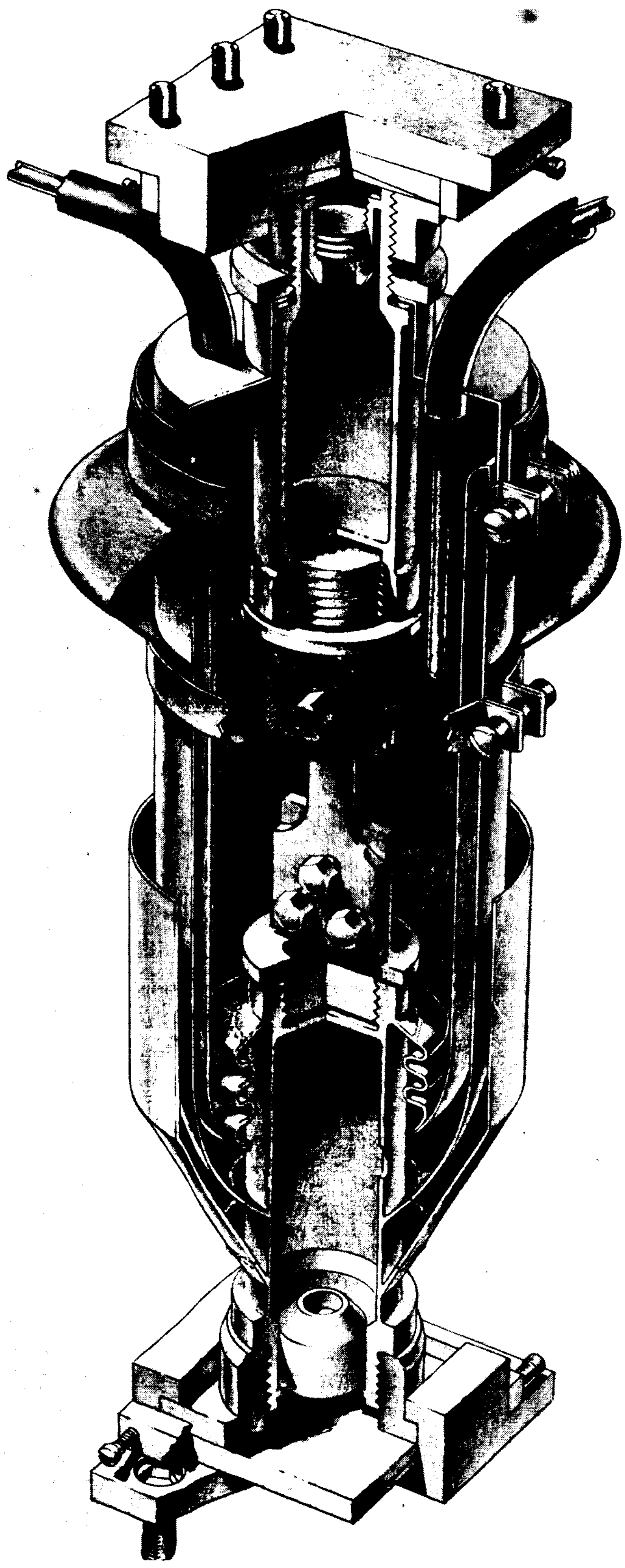

Fig. 3 Cutaway View of Cryostat Assembly Mounted in Fatigue-Testing Machine

V. EXPERIMENTAL RESULTS

Tension testing at all temperatures and liquid hydrogen fatigue testing were performed at the Denver facility. Fatigue testing at room and liquid nitrogen temperatures was performed at the Baltimore Division.

A. TENSION TESTS

Tension tests were performed at 70, -320, and -423°F to provide data on ultimate strength, yield strength, elongation, modulus of elasticity, notch strength, and weld strength.

Triplicate tests were performed for each condition. Results of these tests are shown in Fig. 4 thru 15. Detailed test data are given in Appendix A. Data from Contract NAS 8-2631 are included with the current data to provide complete property information for the entire 3-yr effort.

B. FATIGUE TESTS

Fatigue tests were performed to provide S-N diagrams at 70, -320, and -423°F. A stress ratio (R) of -1 was used for all aluminum, stainless steel, and nickel alloy specimens. The titanium specimens were not sufficiently flat to permit fully reversed stressing and were tested under tension/tension loading at a stress ratio of 0.01. In addition, three of the aluminum alloys (2014-T6, 7039-T6, and 7106-T6) were also tested at a stress ratio of 0.01 to provide sufficient data to determine the effect of stress ratio.

Notched specimens containing an elastic stress concentration factor (K_t) of 3.5 were tested. To determine the effect of notch sharpness on fatigue behavior, two aluminum alloys (2014-T6 and 7039-T6) were also evaluated with a sharper notch, $K_t = 8.0$.

Fatigue test results are given in Fig. 16 thru 53. Circles are used to denote data points of specimens tested for the first time. Discontinued specimens are identified by an arrow extending to the right. Re-runs of discontinued specimens are shown by square symbols. Detailed tabular presentations of these data are given in Appendix B. Data from Contract NAS 8-2631 are included to provide complete property information.

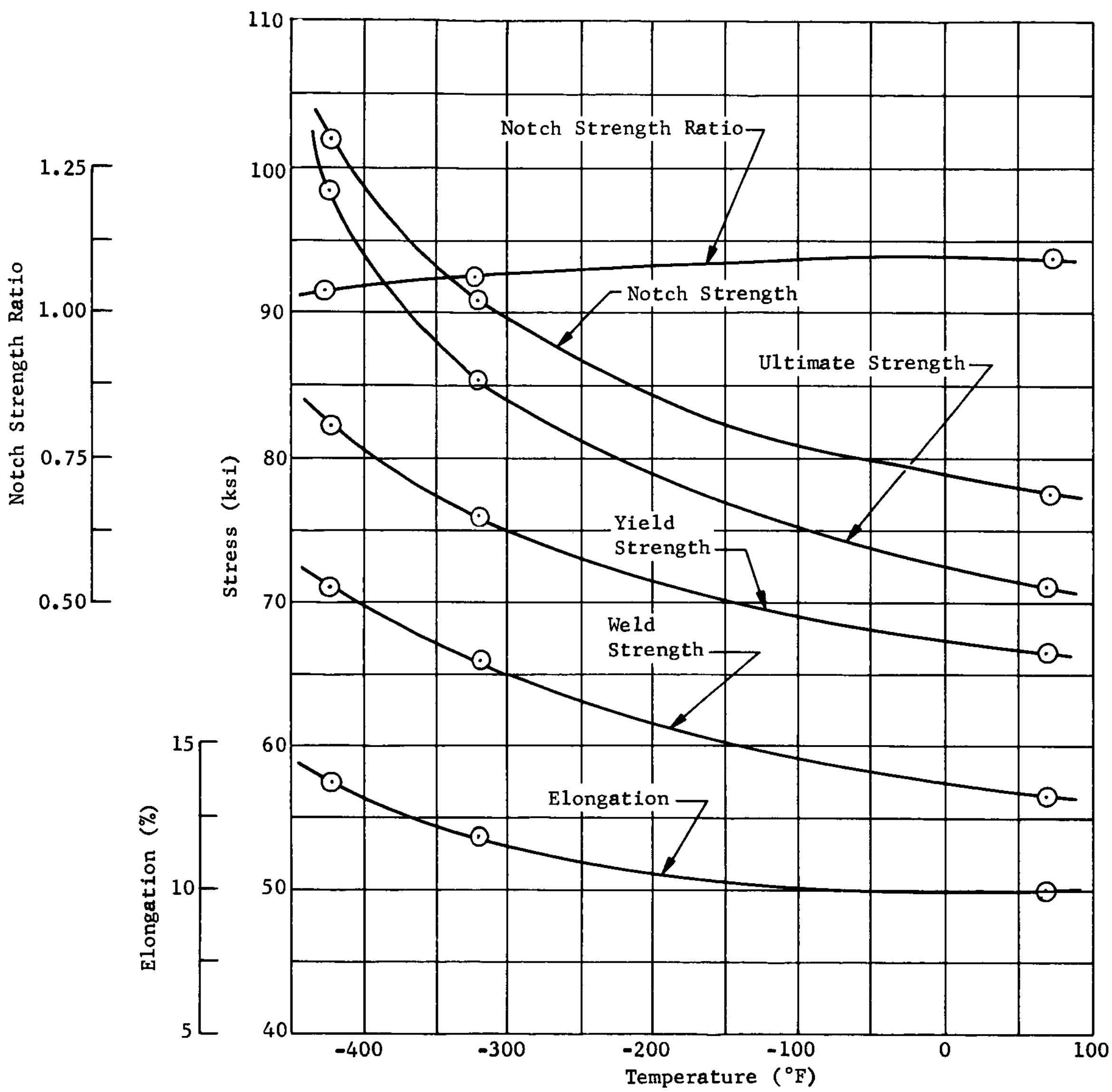

Fig. 4 Tensile Properties of 2014-T6 Aluminum Alloy at Cryogenic Temperatures

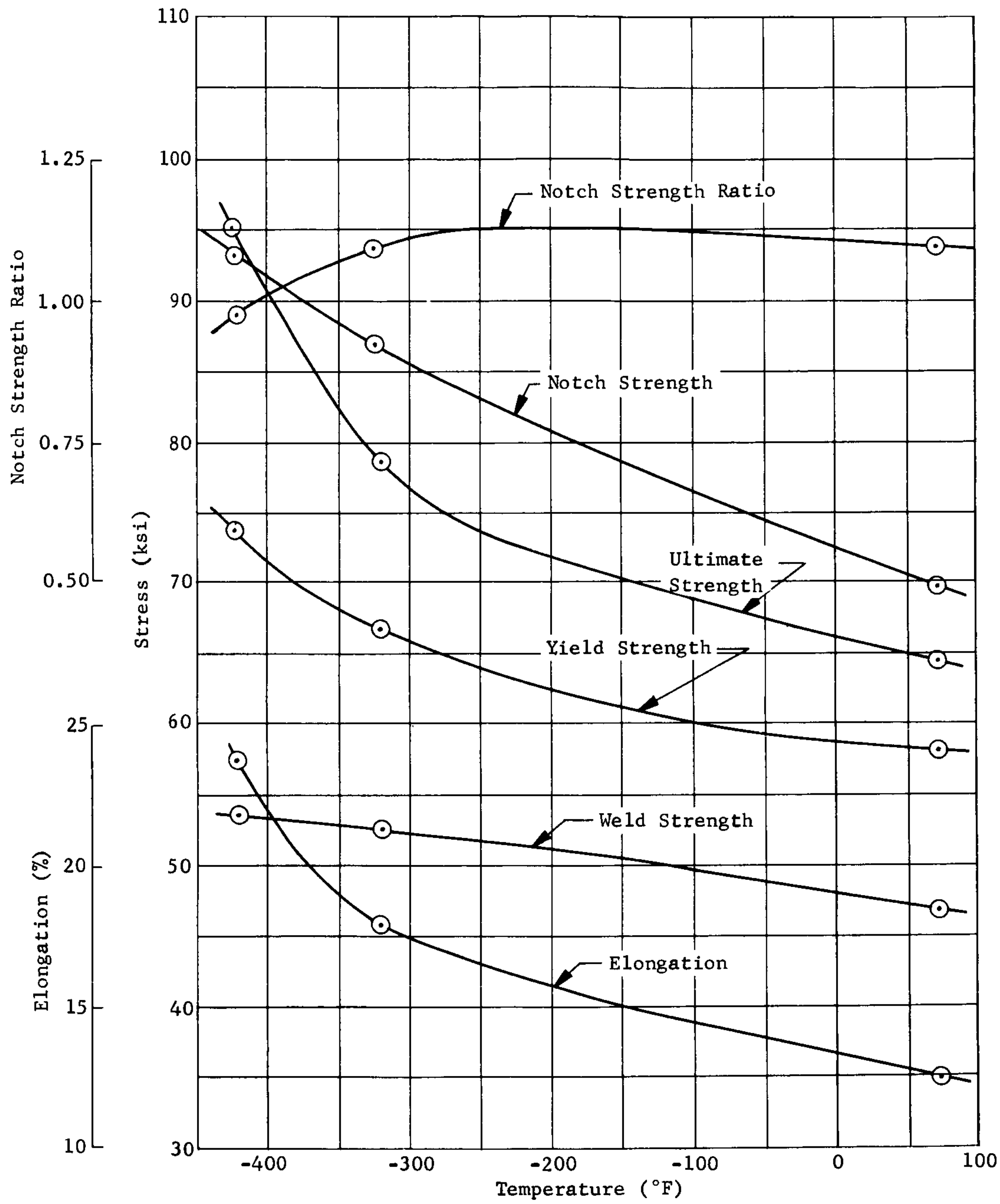

Fig. 5 Tensile Properties of 7039-T6 Aluminum Alloy at Cryogenic Temperatures

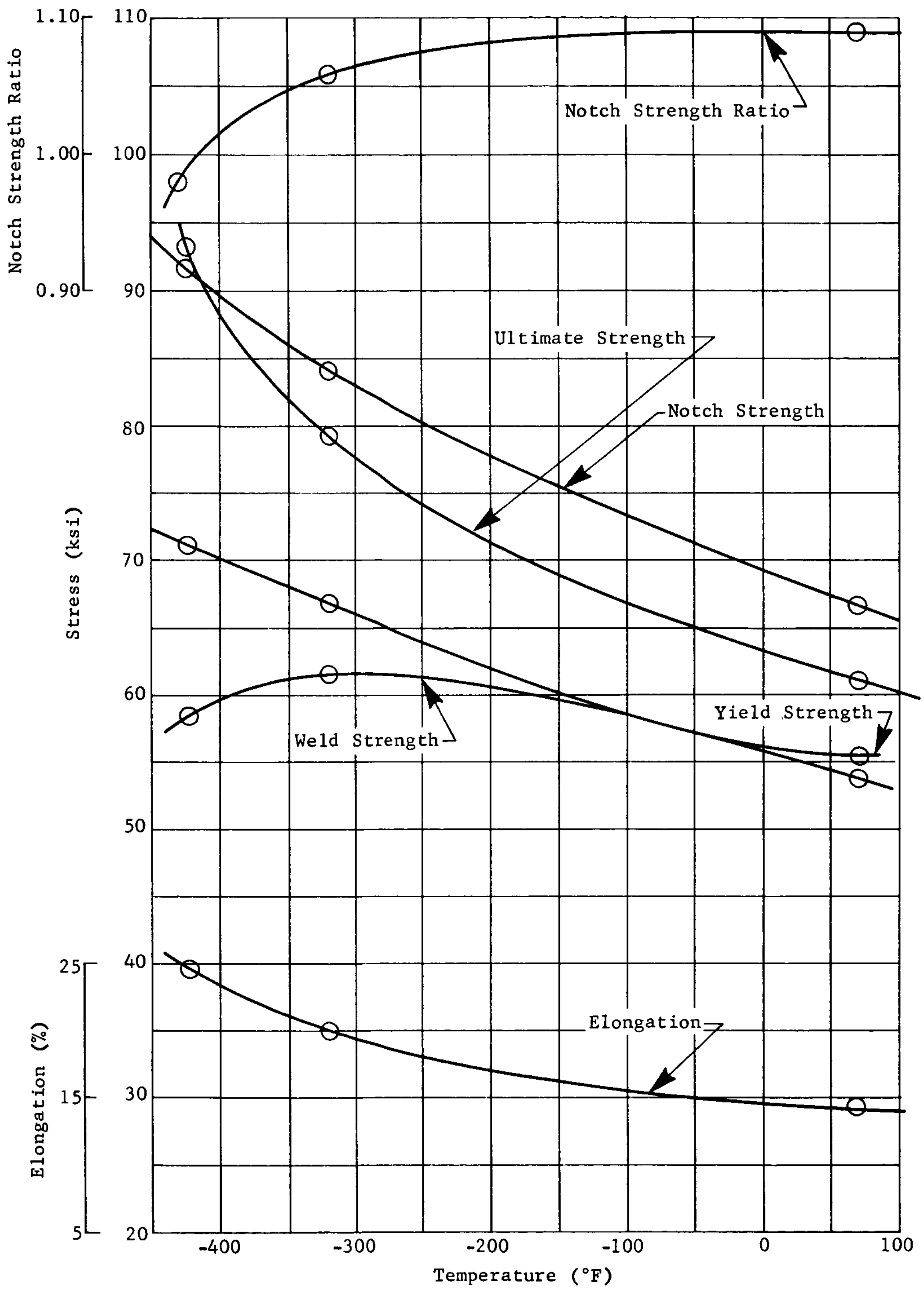

Fig. 6 Tensile Properties of 7106-T6 Aluminum Alloy at Cryogenic Temperatures

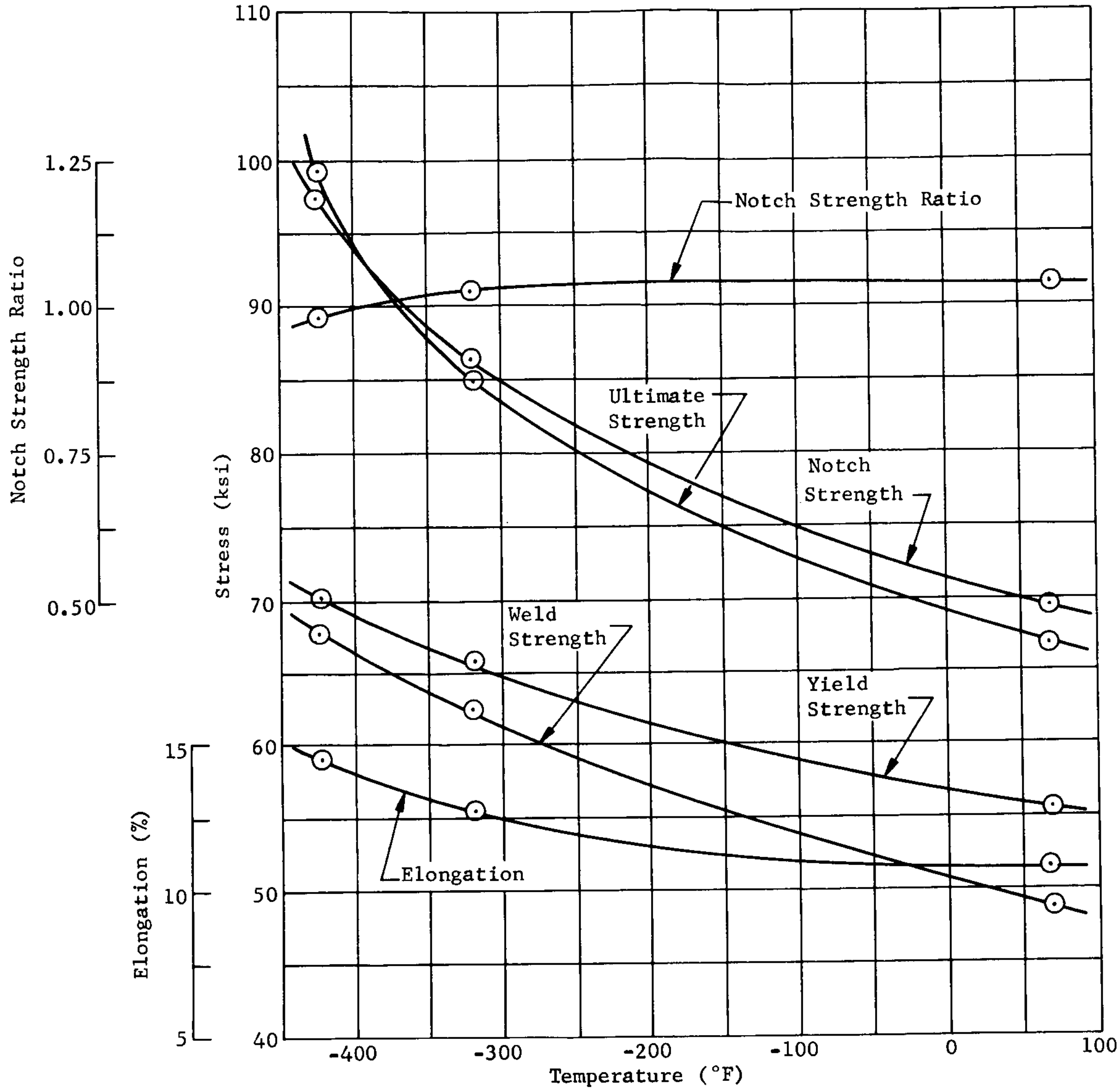

Fig. 7 Tensile Properties of 2219-T87 Aluminum Alloy at Cryogenic Temperatures

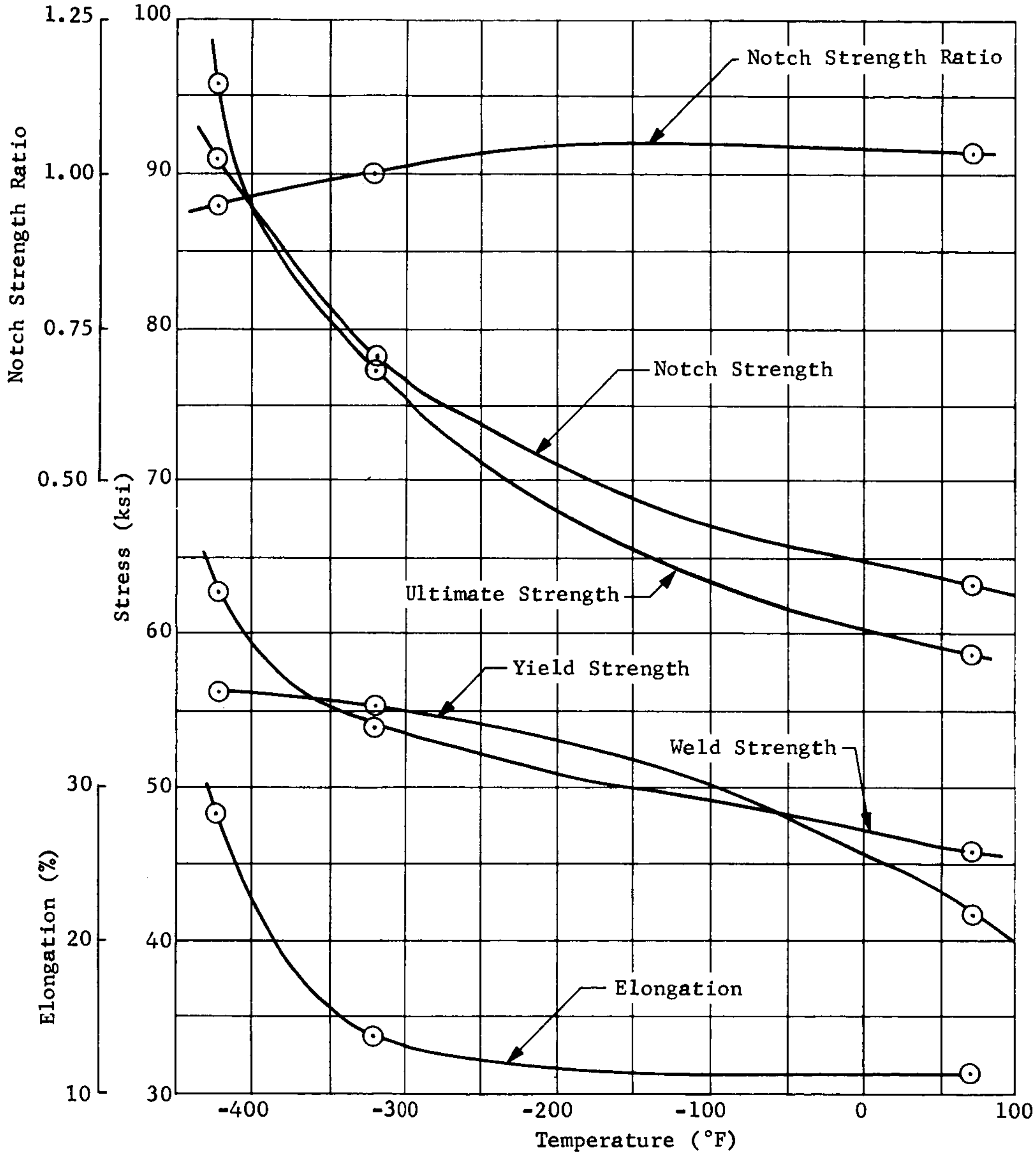

Fig. 8 Tensile Properties of 2219-T62 Aluminum Alloy at Cryogenic Temperatures

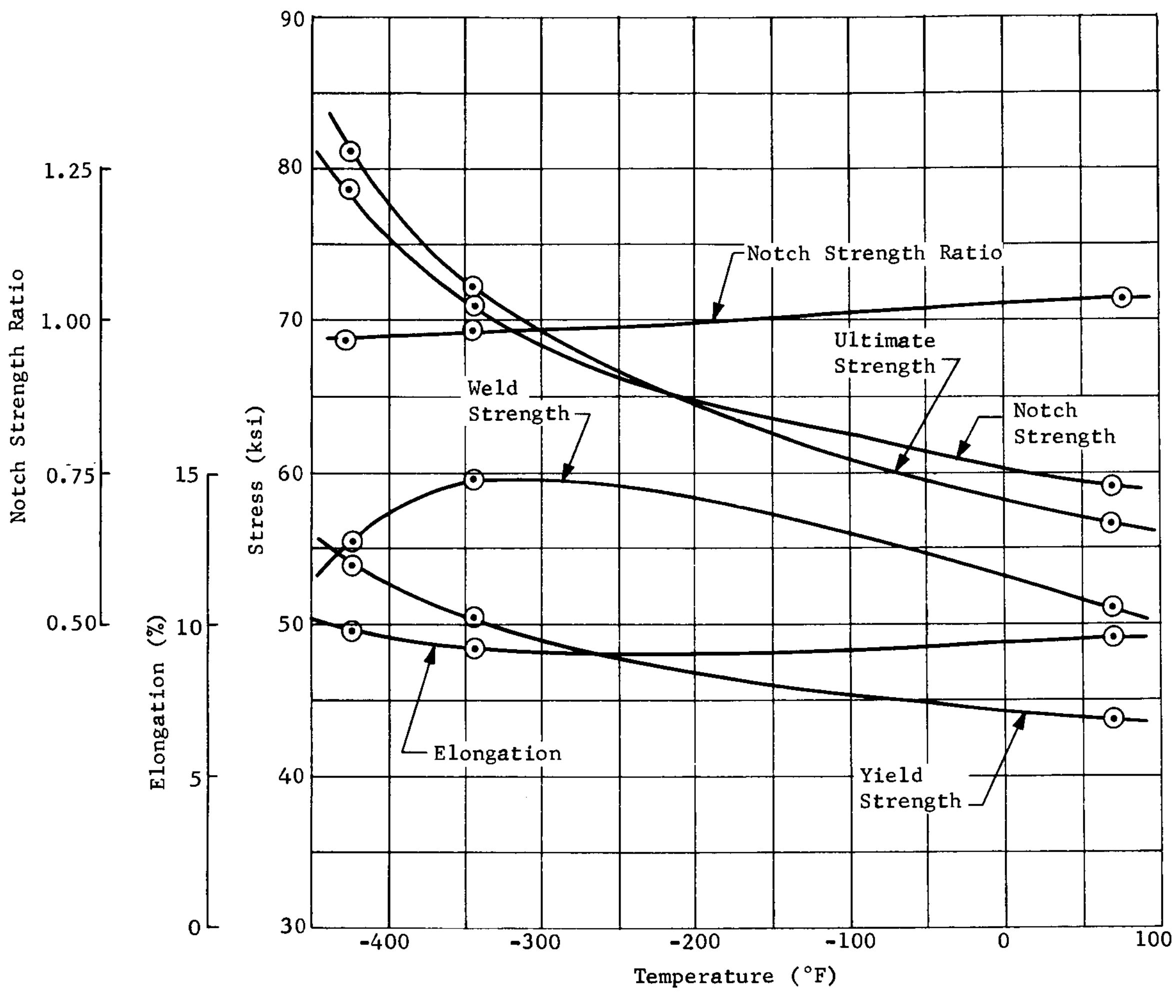

Fig. 9 Tensile Properties of 5456-H343 Aluminum Alloy at Cryogenic Temperatures

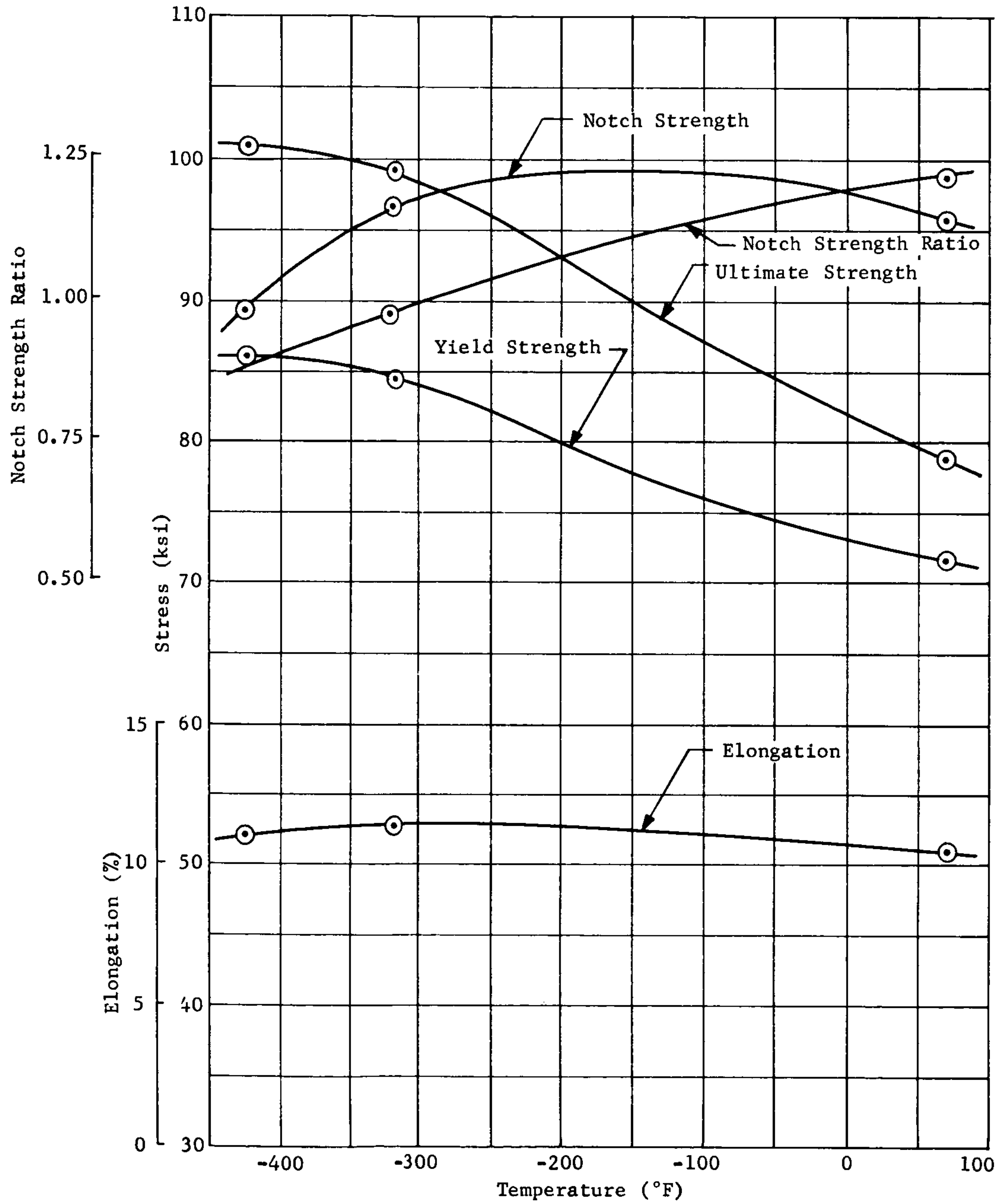

Fig. 10 Tensile Properties of 7075-T6 Aluminum Alloy at Cryogenic Temperatures

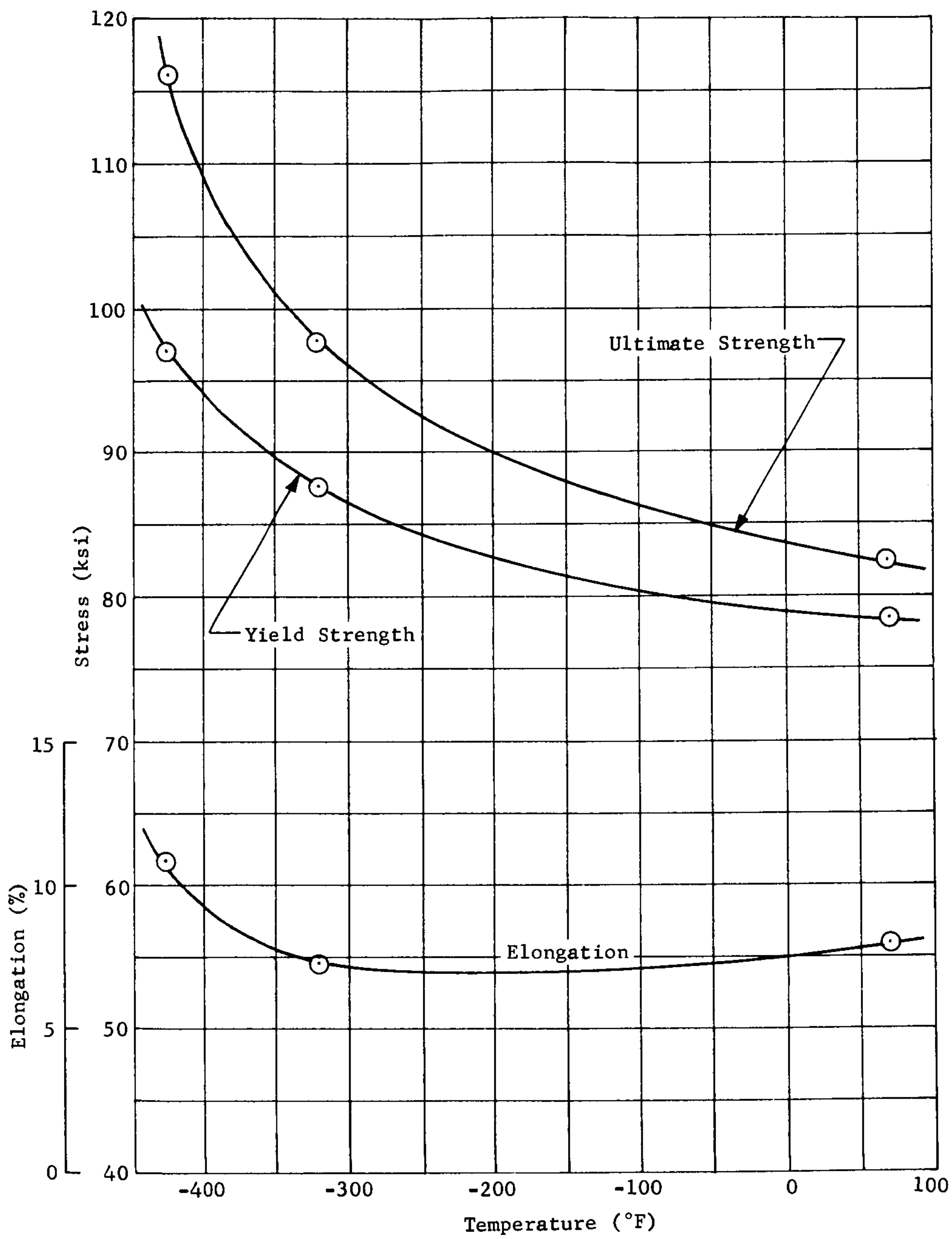

Fig. 11 Tensile Properties of 2020-T6 Aluminum Alloy at Cryogenic Temperatures

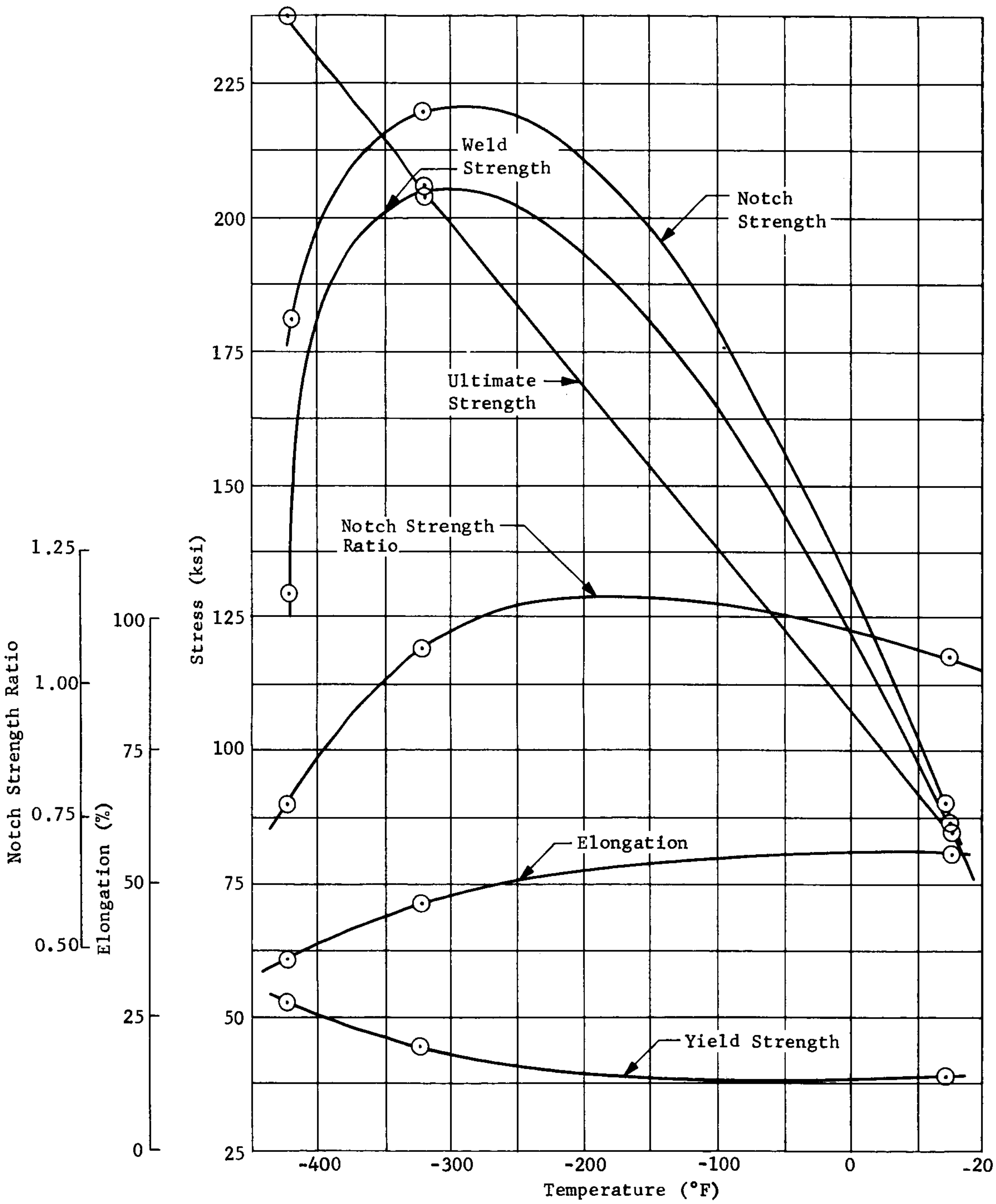

Fig. 12 Tensile Properties of 321 Stainless Steel Alloy at Cryogenic Temperatures

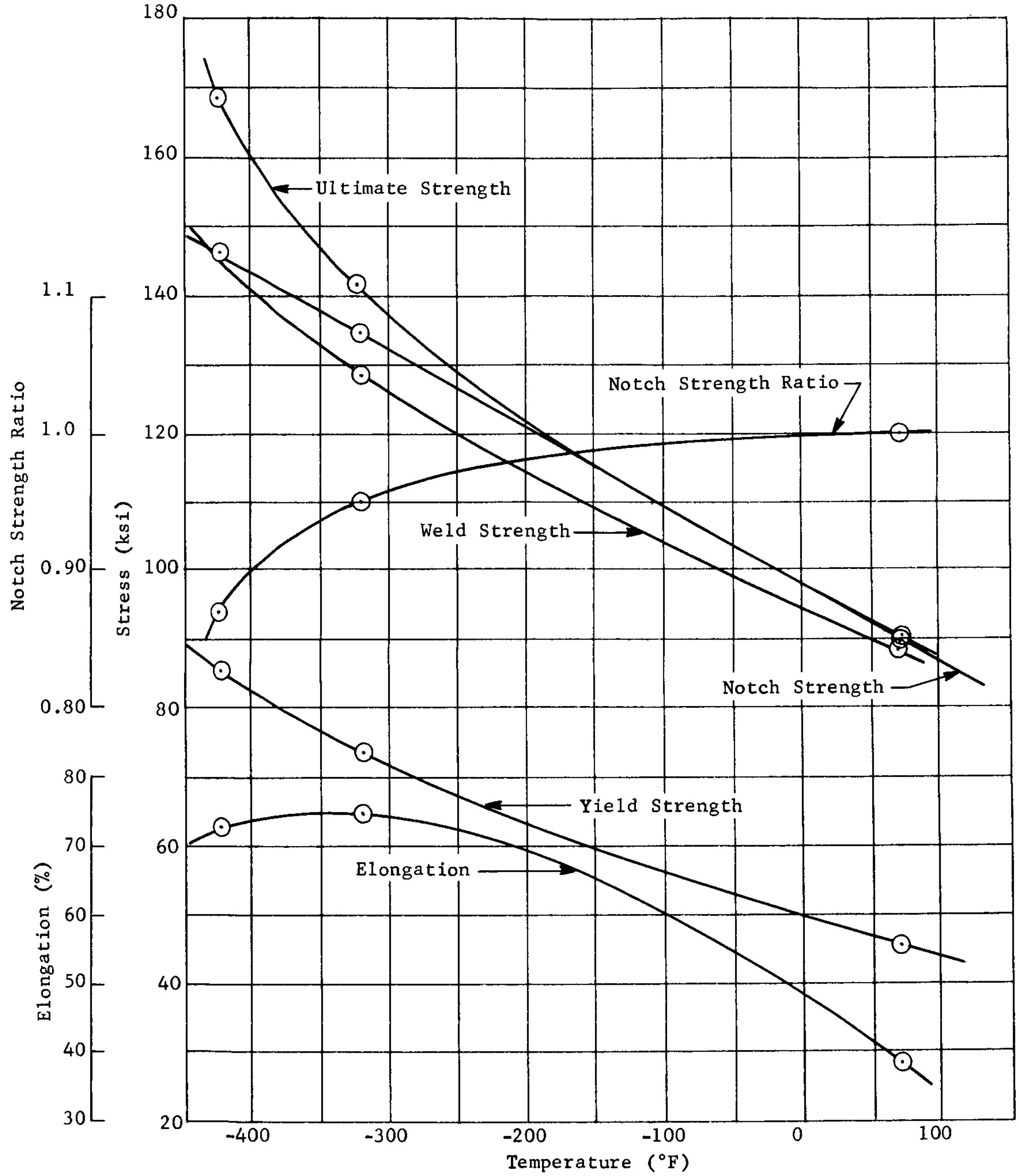

Fig. 13 Tensile Properties of A-286 Stainless Steel Alloy at Cryogenic Temperatures

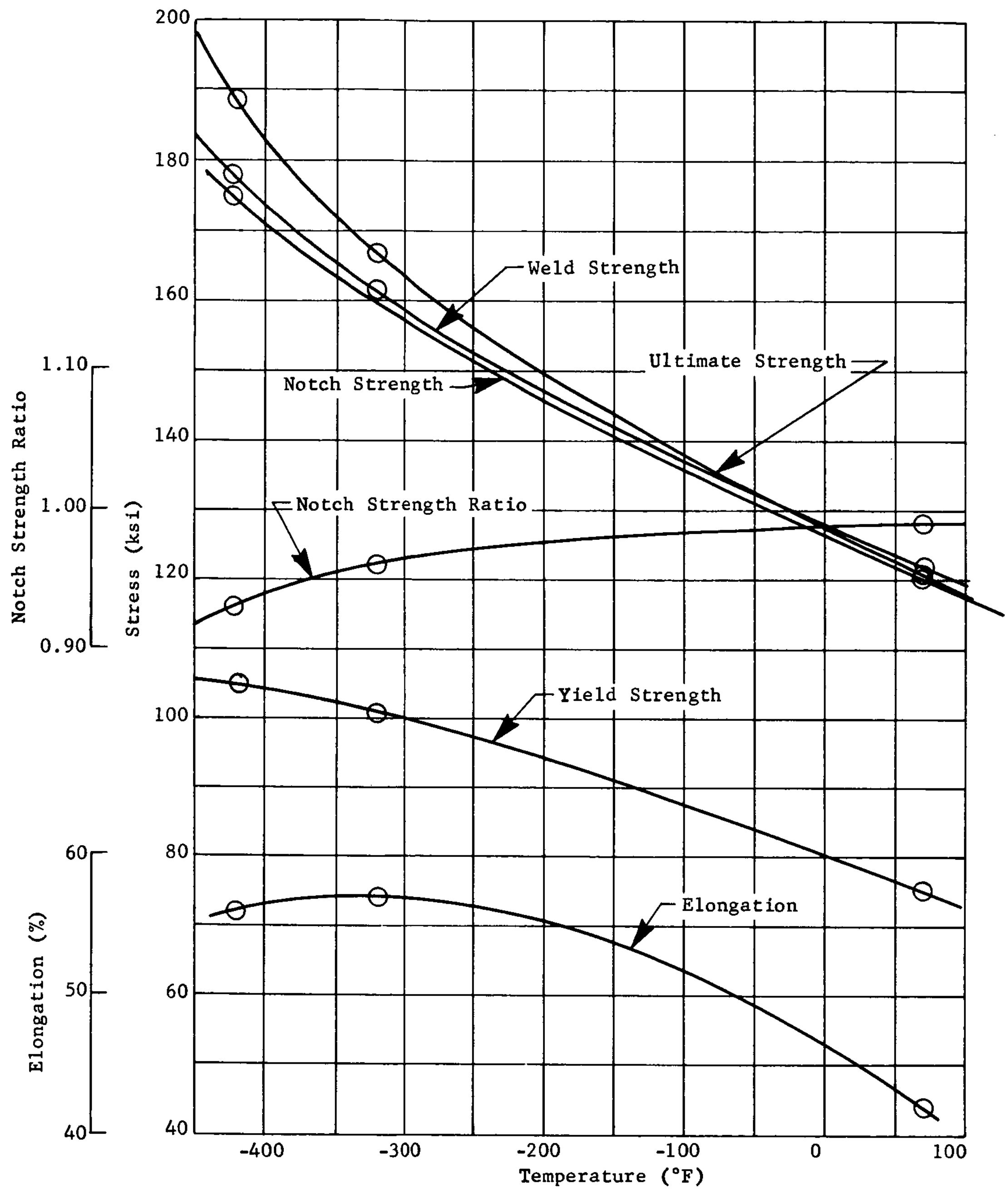

Fig. 14 Tensile Properties of Inconel 718 Nickel Alloy at Cryogenic Temperatures

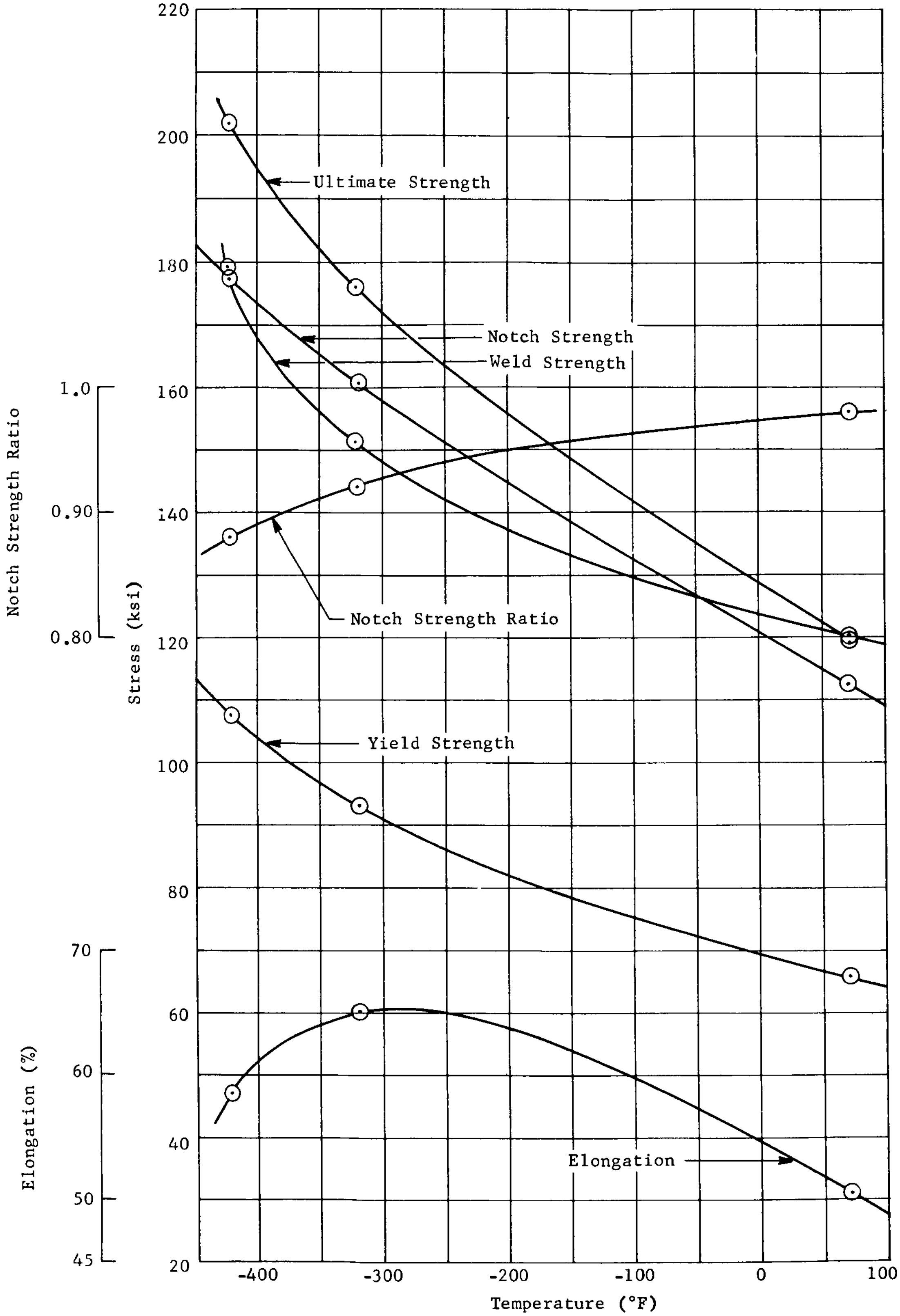

Fig. 15 Tensile Properties of Hastelloy C Nickel Alloy at Cryogenic Temperatures

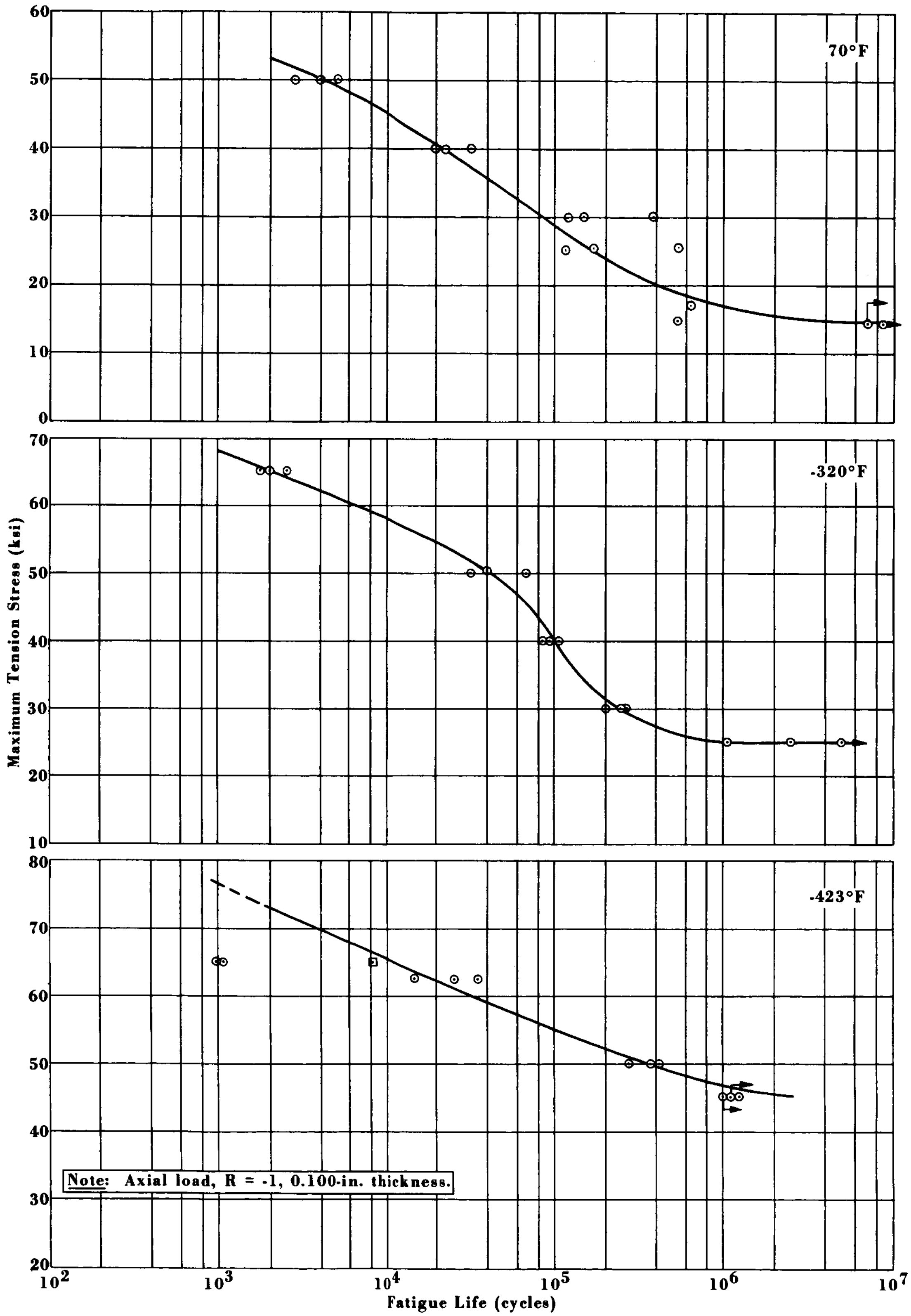

Fig. 16 Fatigue Properties of Unnotched 2014-T6 Aluminum Alloy (R = -1)

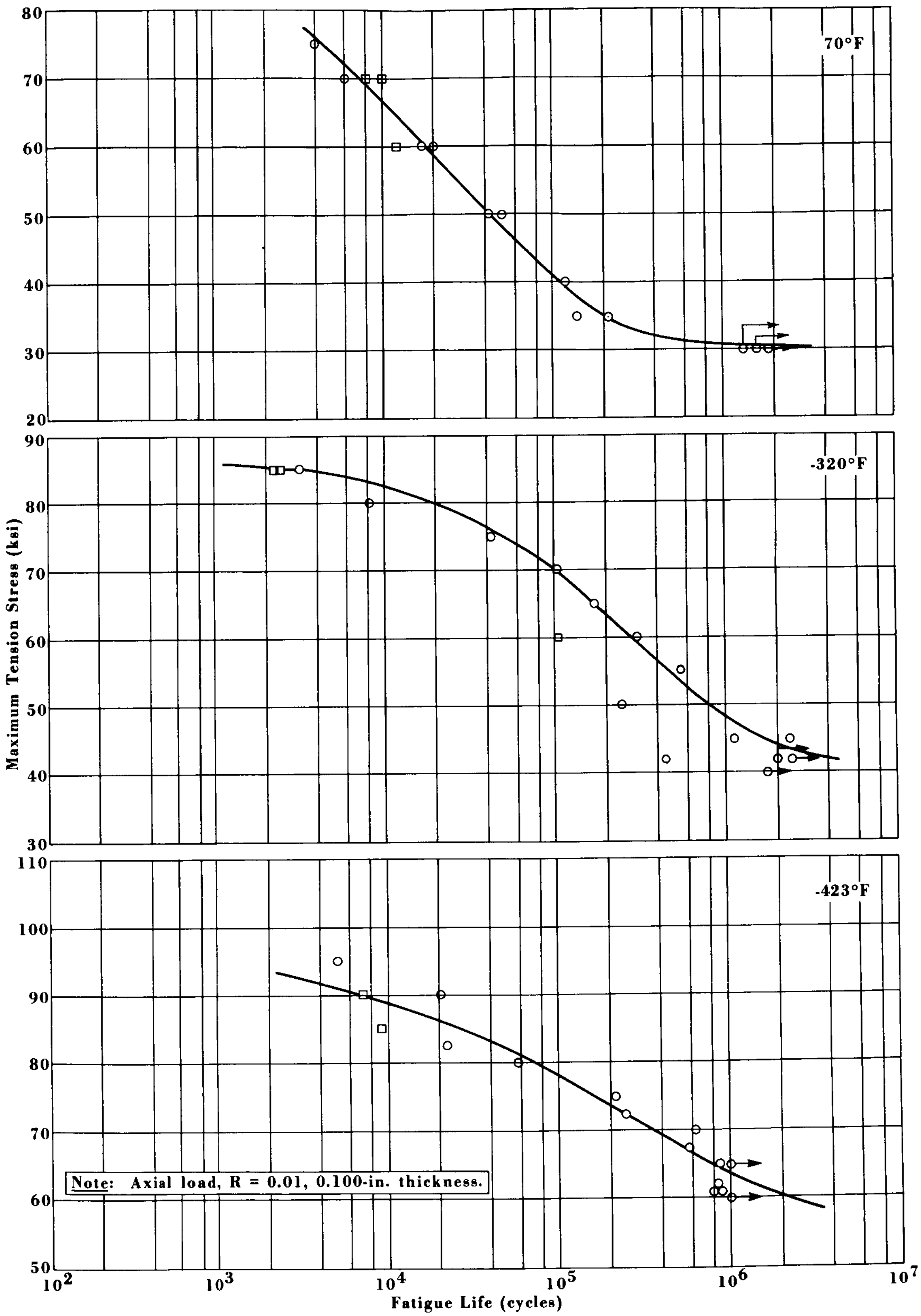

Fig. 17 Fatigue Properties of Unnotched 2014-T6 Aluminum Alloy (R = 0.01)

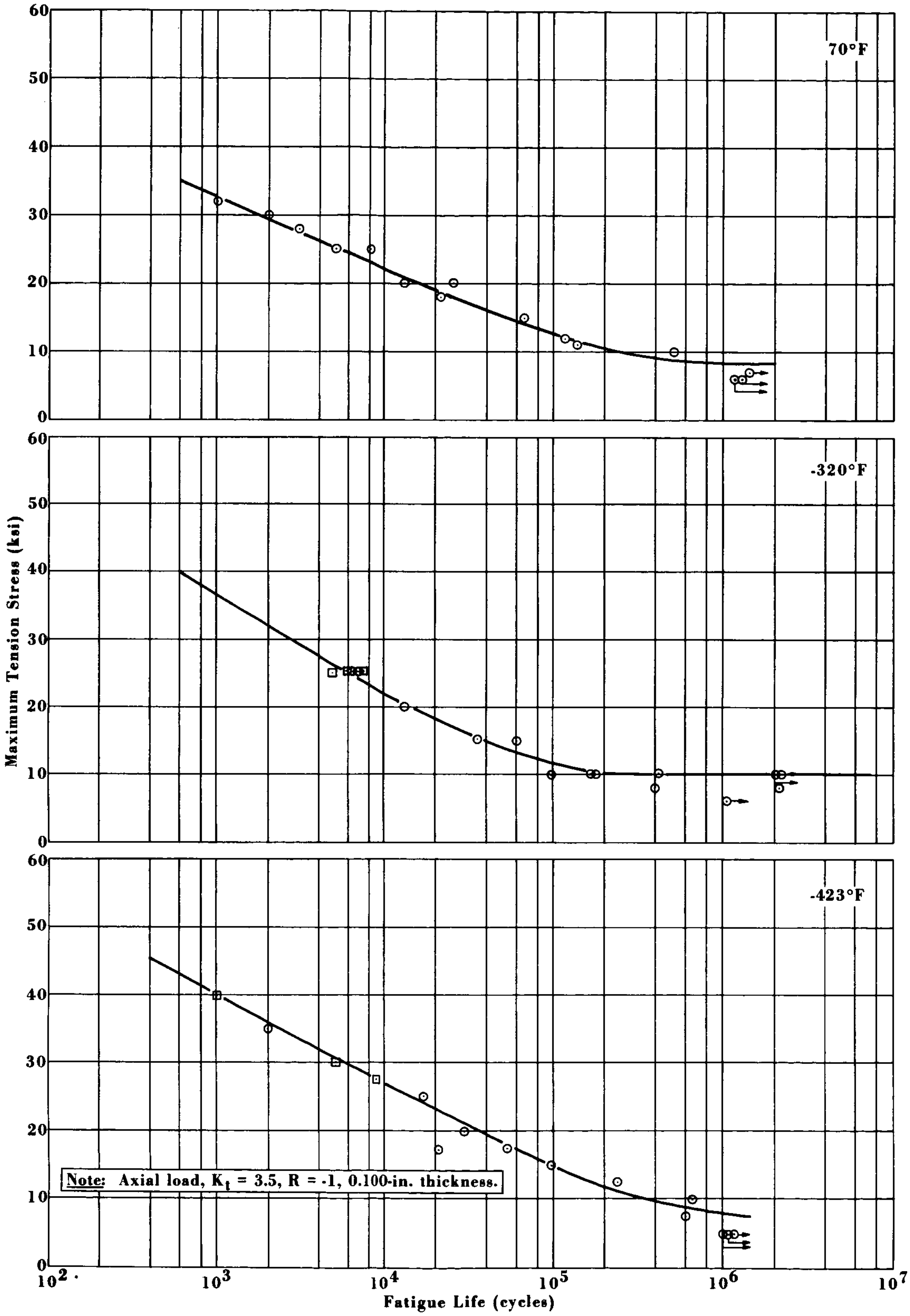

Fig. 18 Fatigue Properties of Notched 2014-T6 Aluminum Alloy (K_t = 3.5)

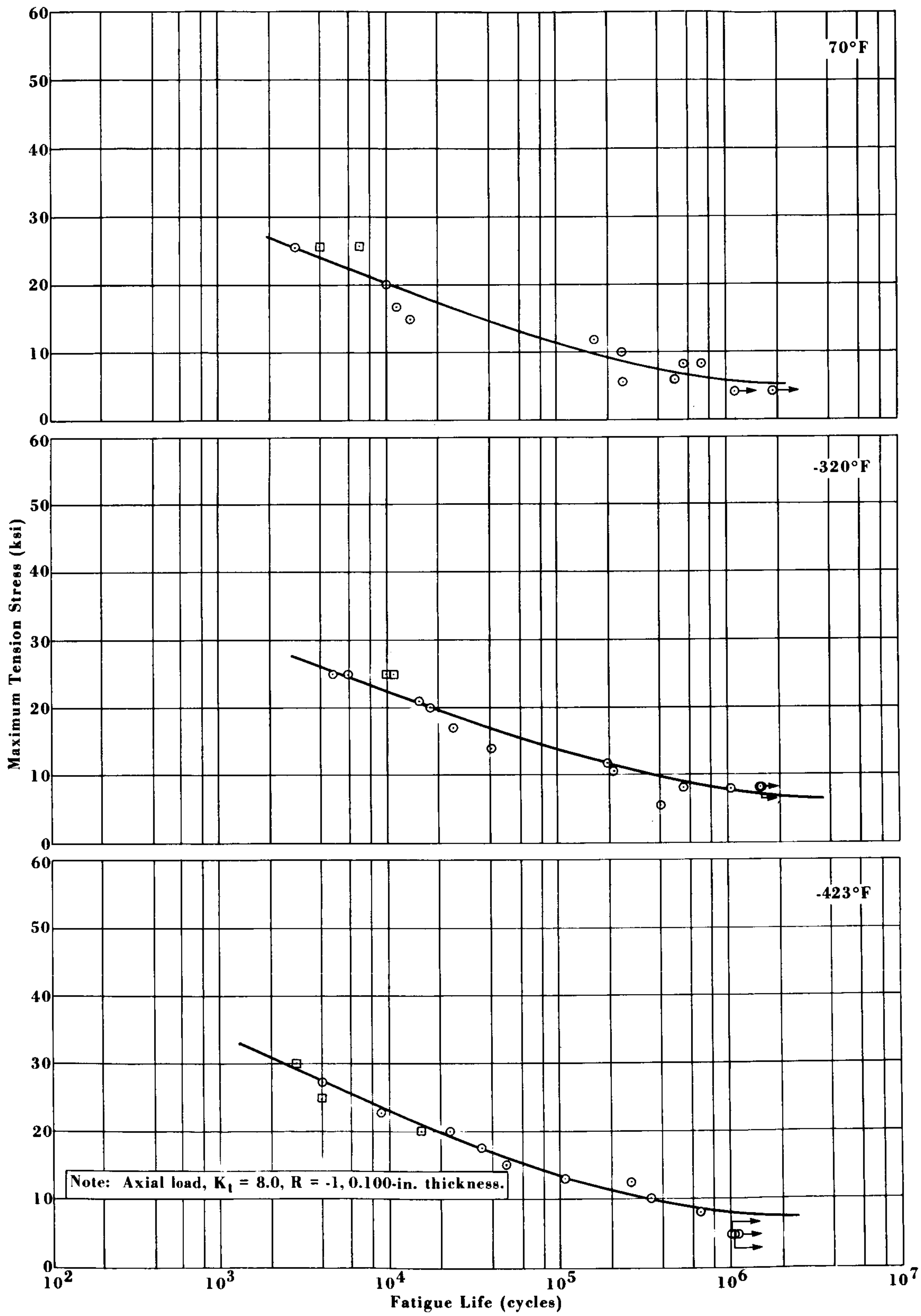

Fig. 19 Fatigue Properties of Notched 2014-T6 Aluminum Alloy (K_t = 8.0)

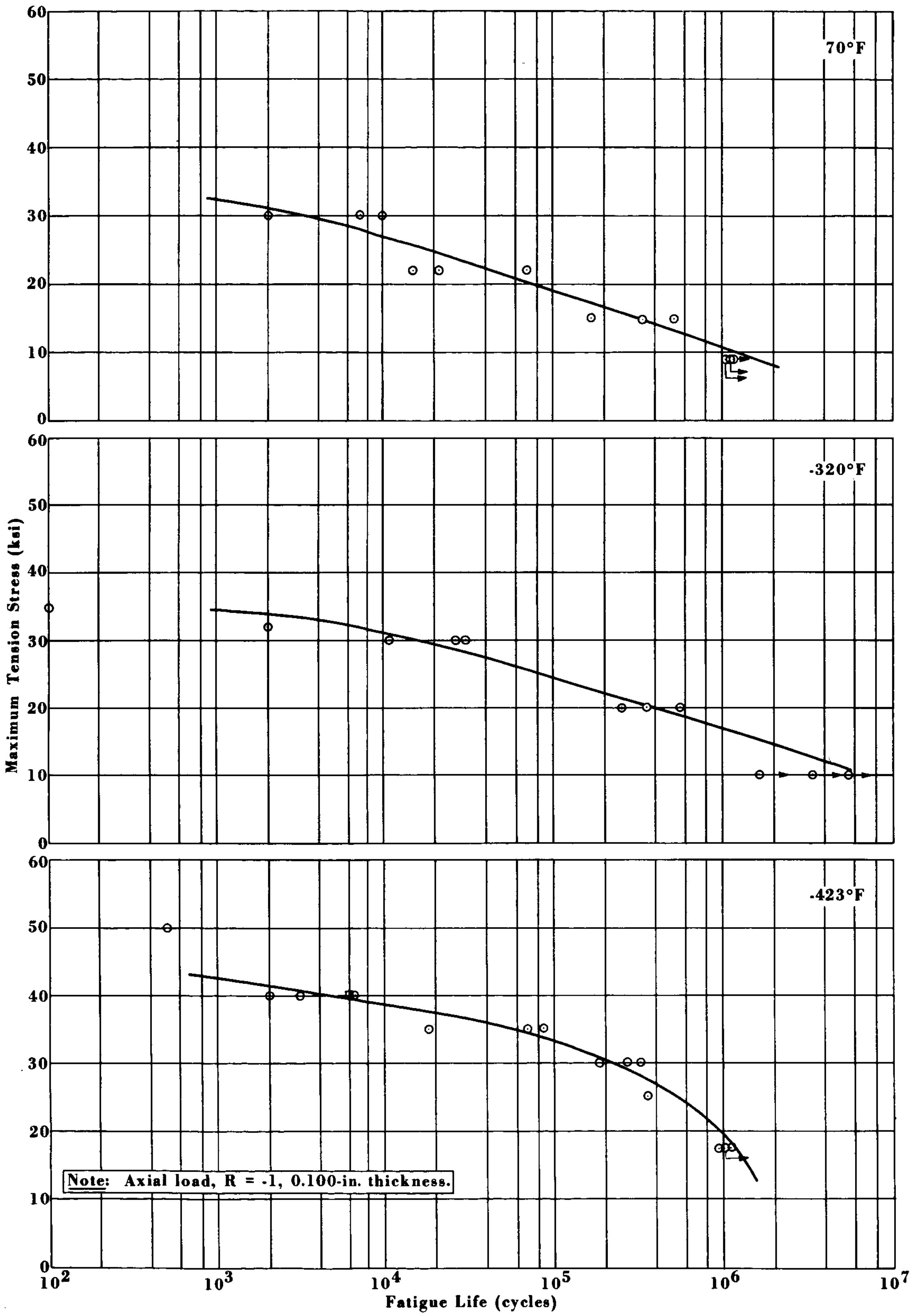

Fig. 20 Fatigue Properties of Welded 2014-T6 Aluminum Alloy

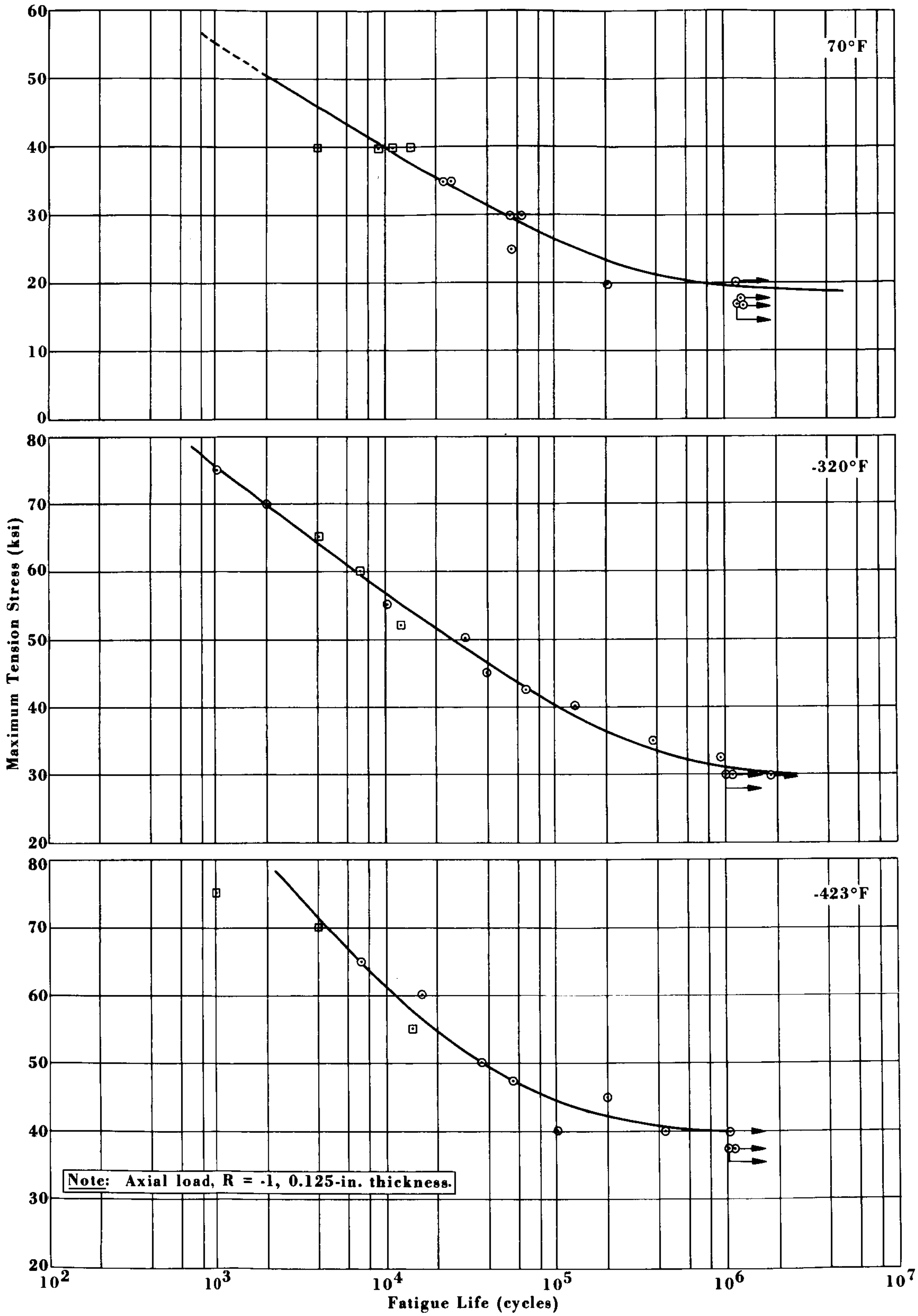

Fig. 21 Fatigue Properties of Unnotched 7039-T6 Aluminum Alloy (R = -1)

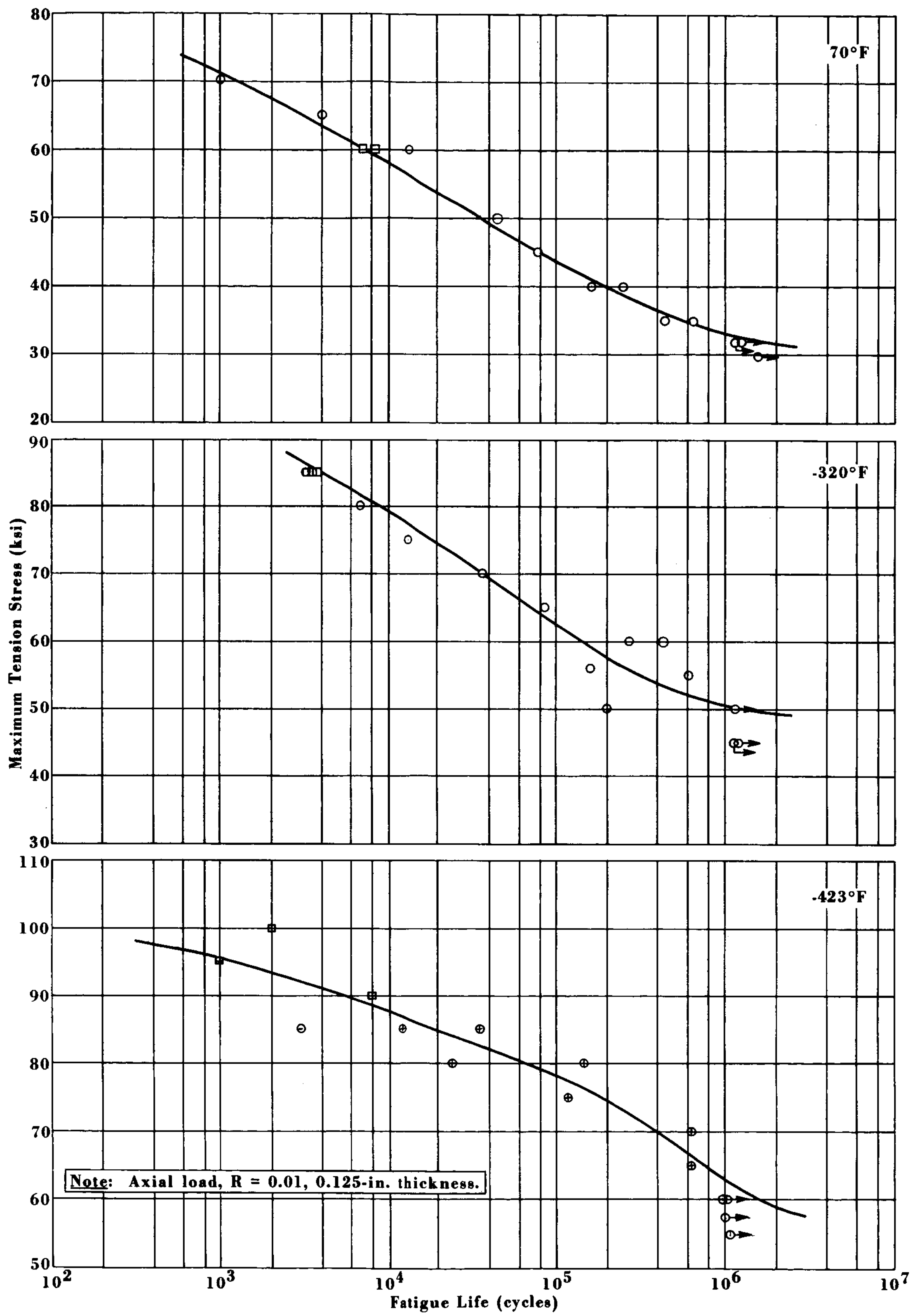

Fig. 22 Fatigue Properties of Unnotched 7039-T6 Aluminum Alloy (R = 0.01)

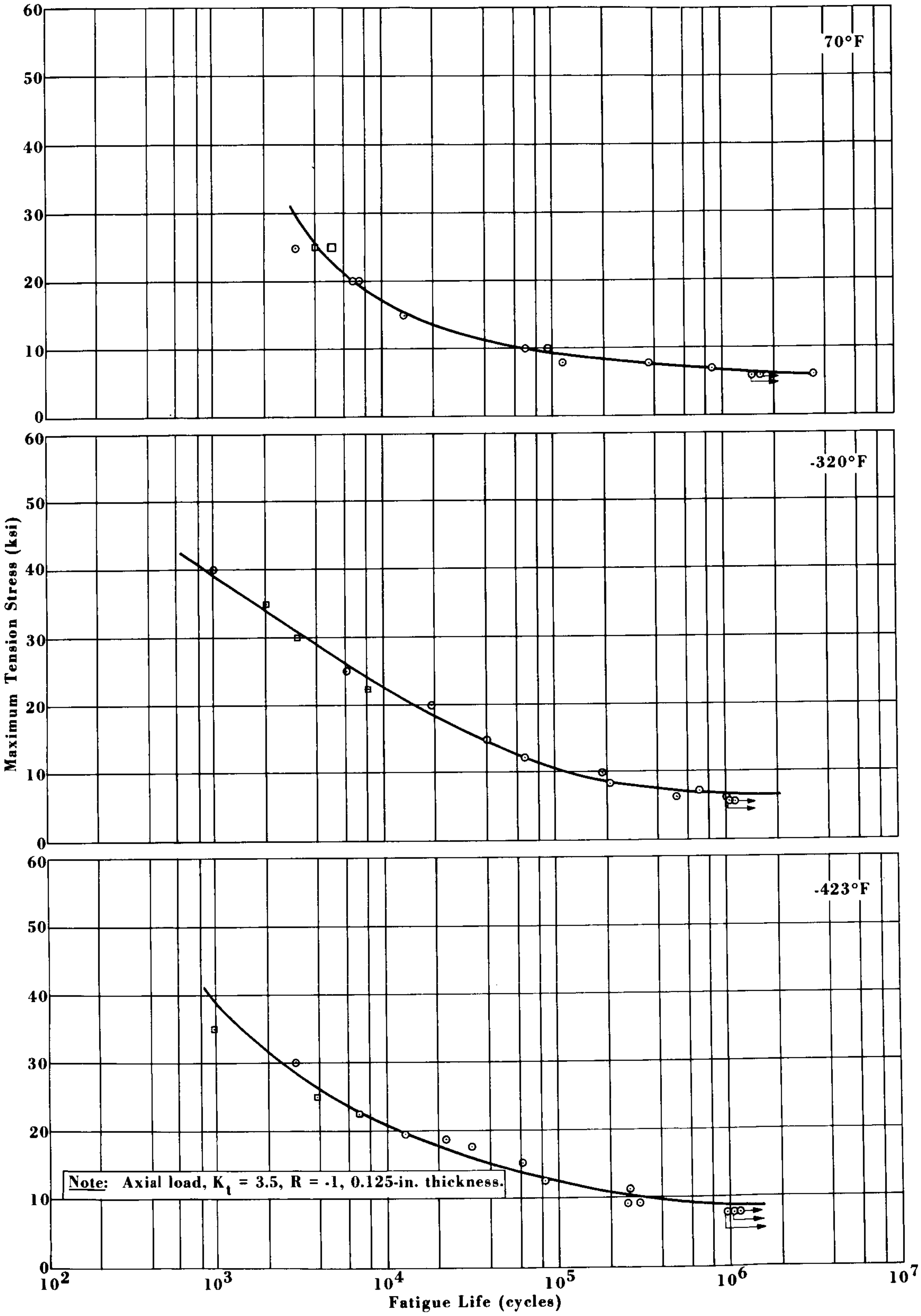

Fig. 23 Fatigue Properties of Notched 7039-T6 Aluminum Alloy (K_t = 3.5)

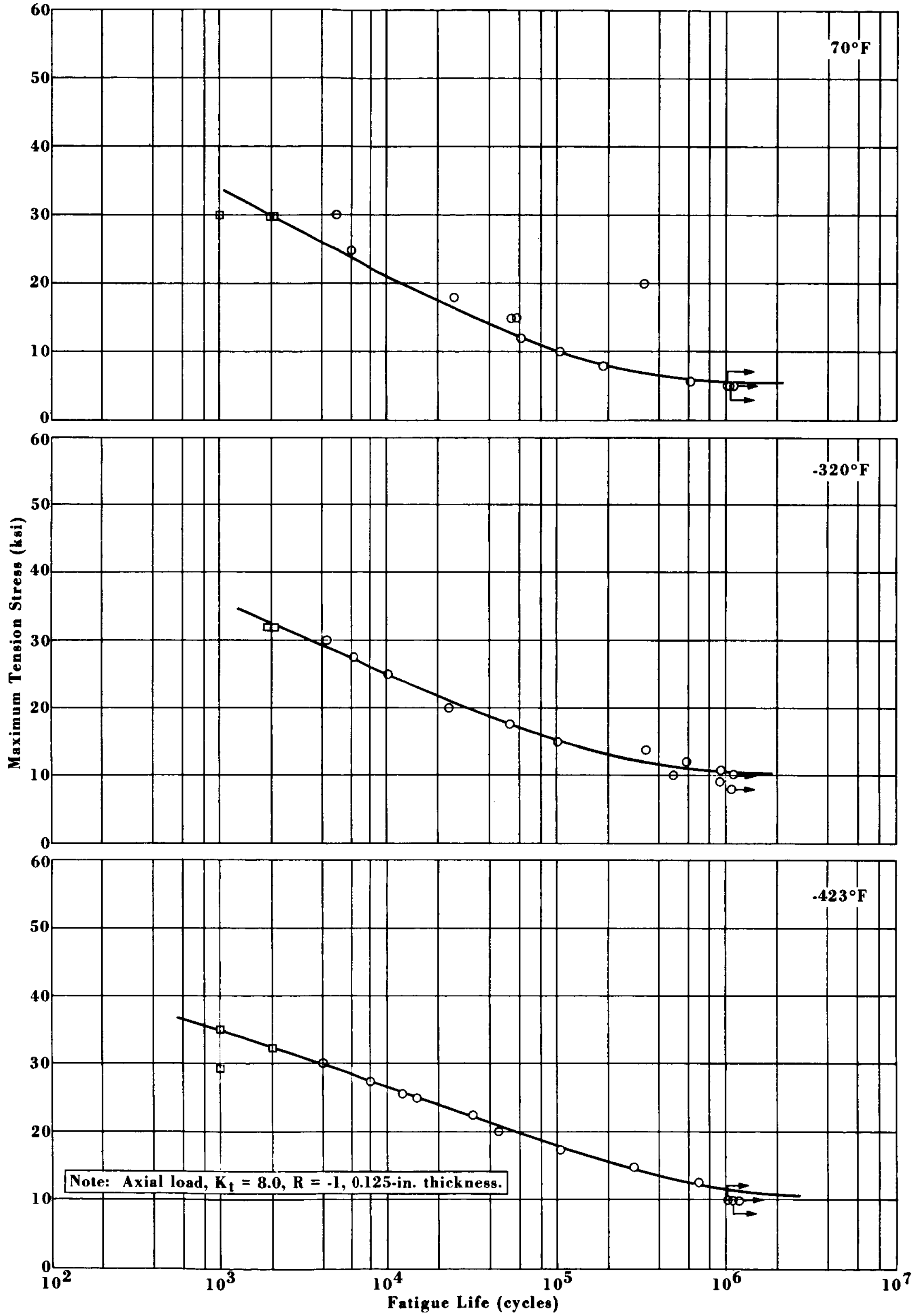

Fig. 24 Fatigue Properties of Notched 7039-T6 Aluminum Alloy (K_t = 8.0)

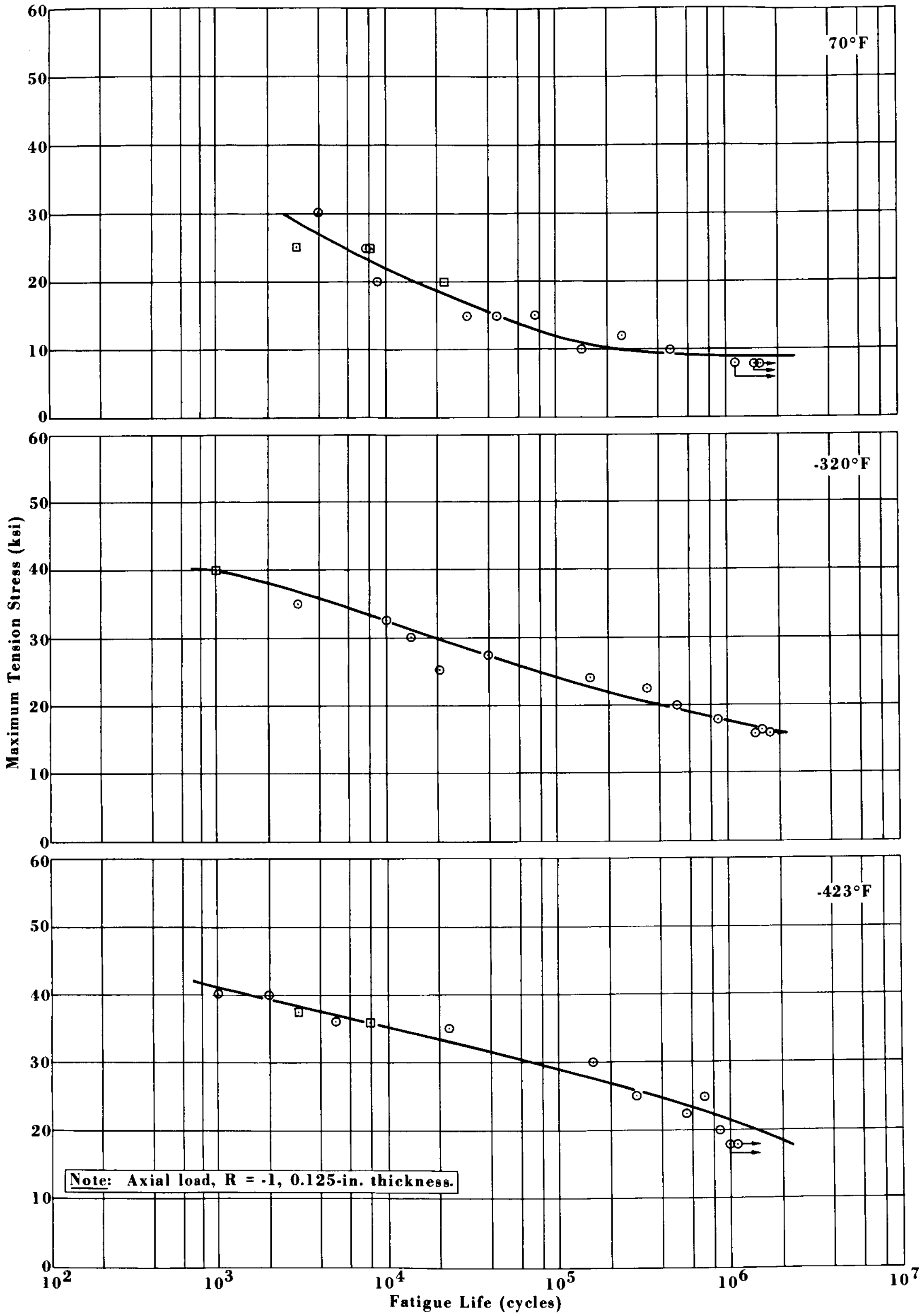

Fig. 25 Fatigue Properties of Welded 7039-T6 Aluminum Alloy

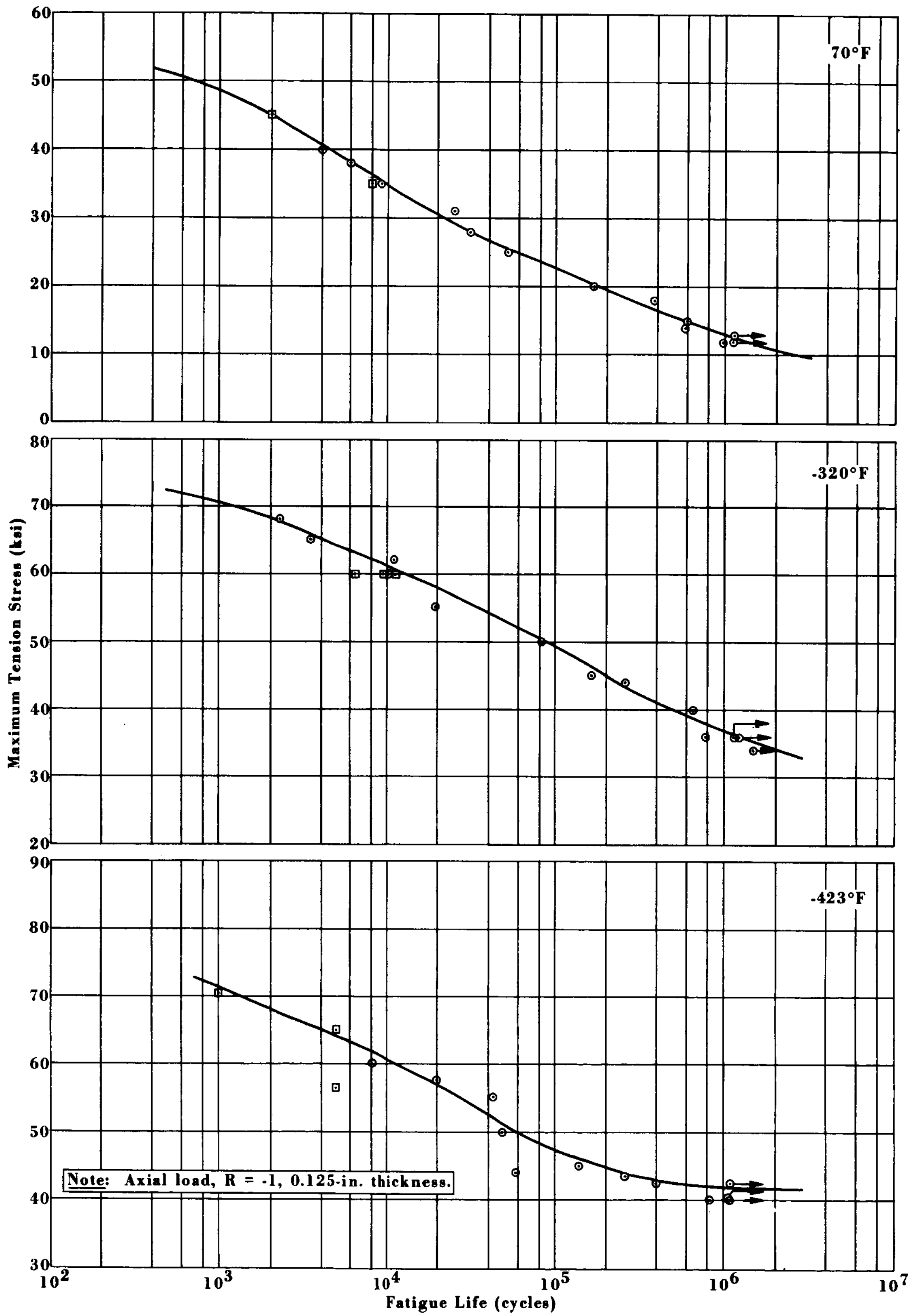

Fig. 26 Fatigue Properties of Unnotched 7106-T6 Aluminum Alloy (R = -1)

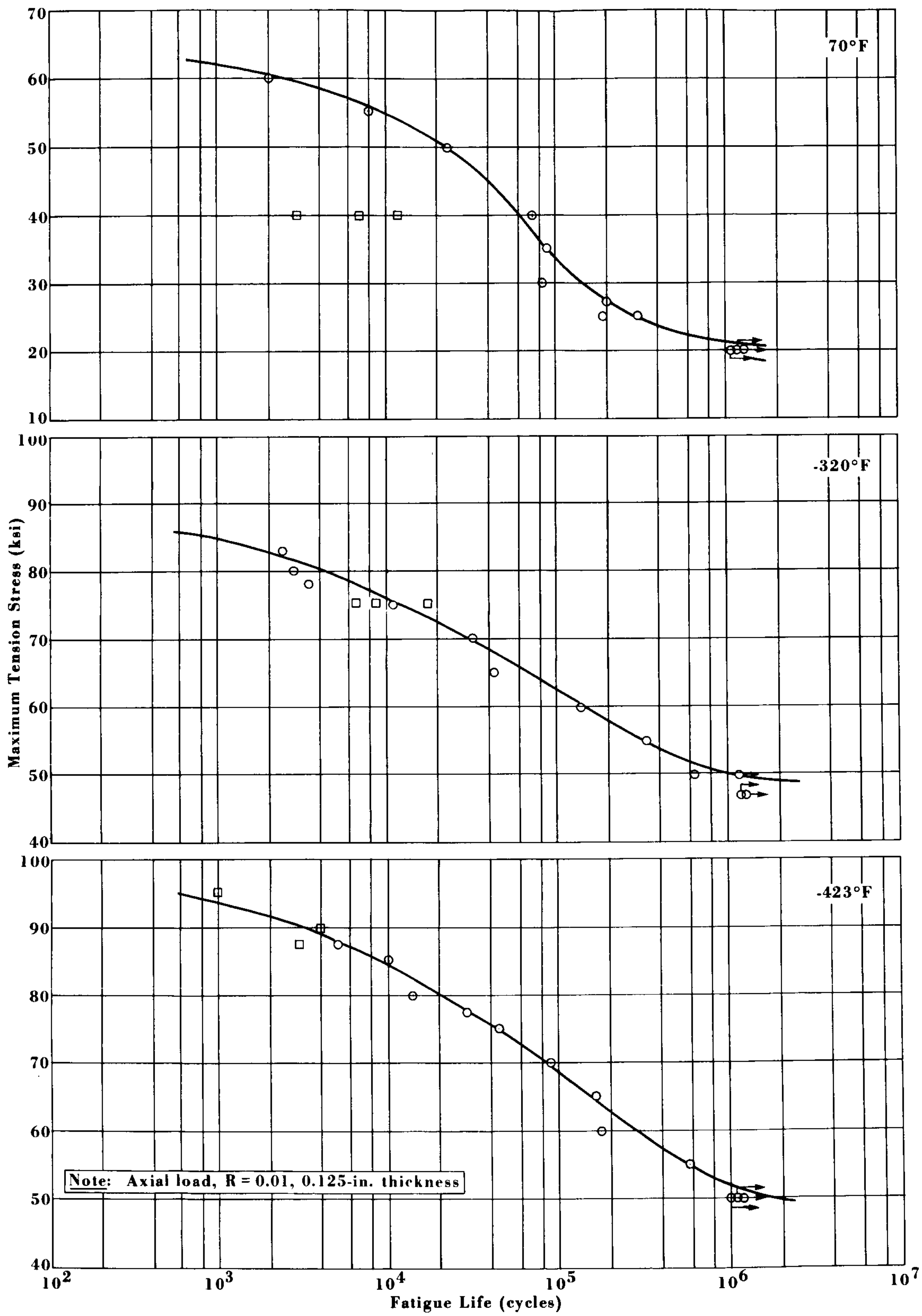

Fig. 27 Fatigue Properties of Unnotched 7106-T6 Aluminum Alloy (R = 0.01)

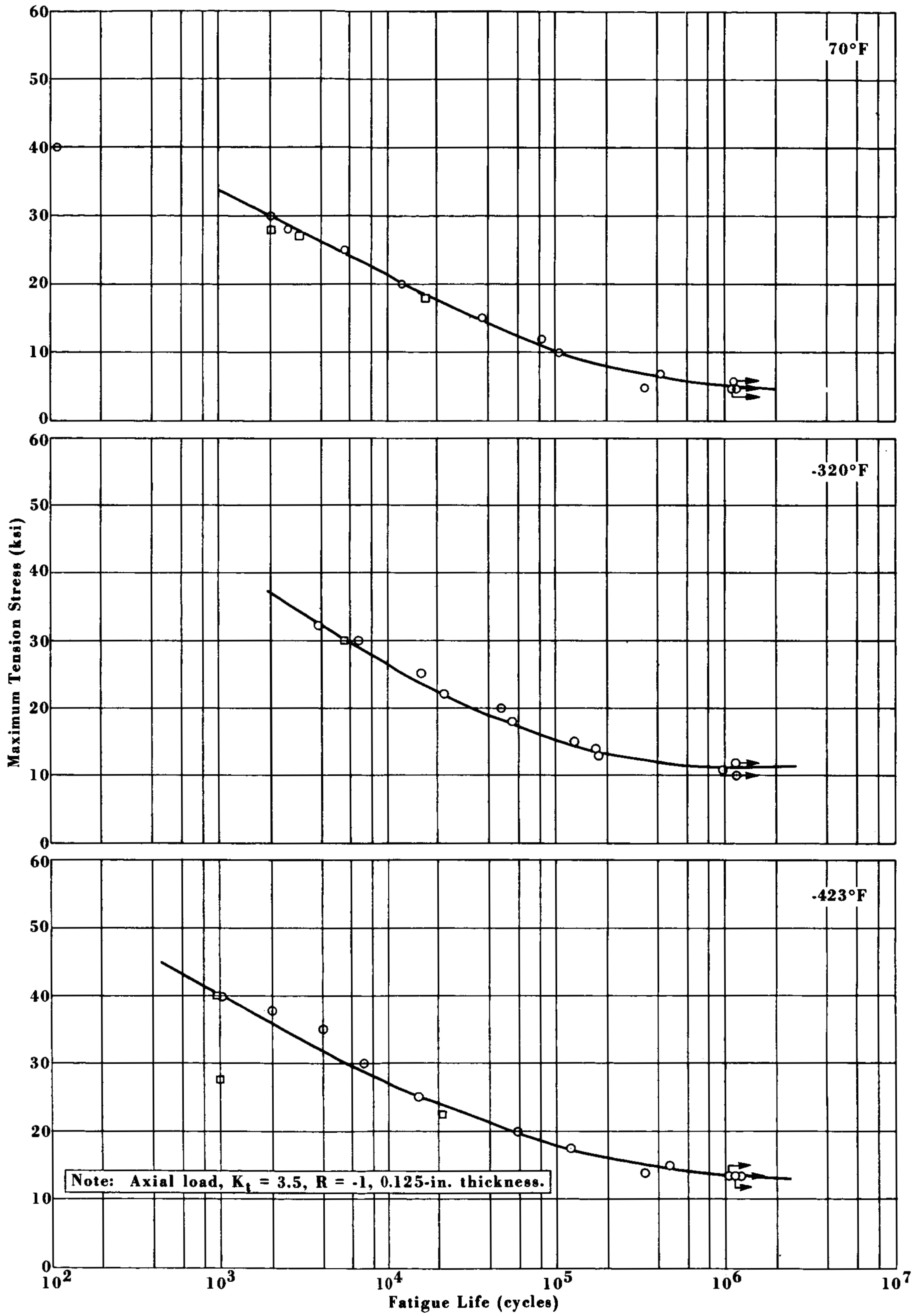

Fig. 28 Fatigue Properties of Notched 7106-T6 Aluminum Alloy

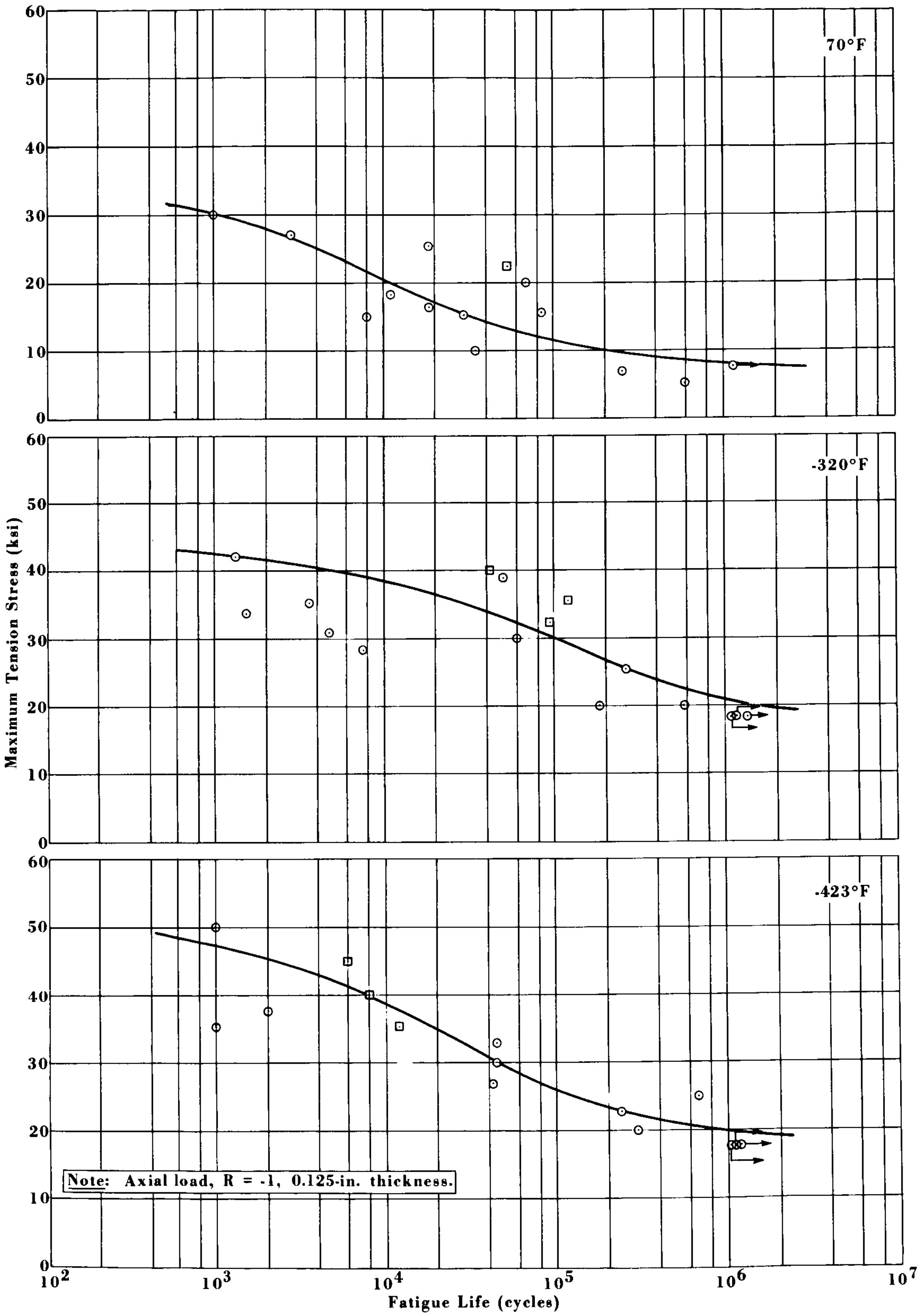

Fig. 29 Fatigue Properties of Welded 7106-T6 Aluminum Alloy

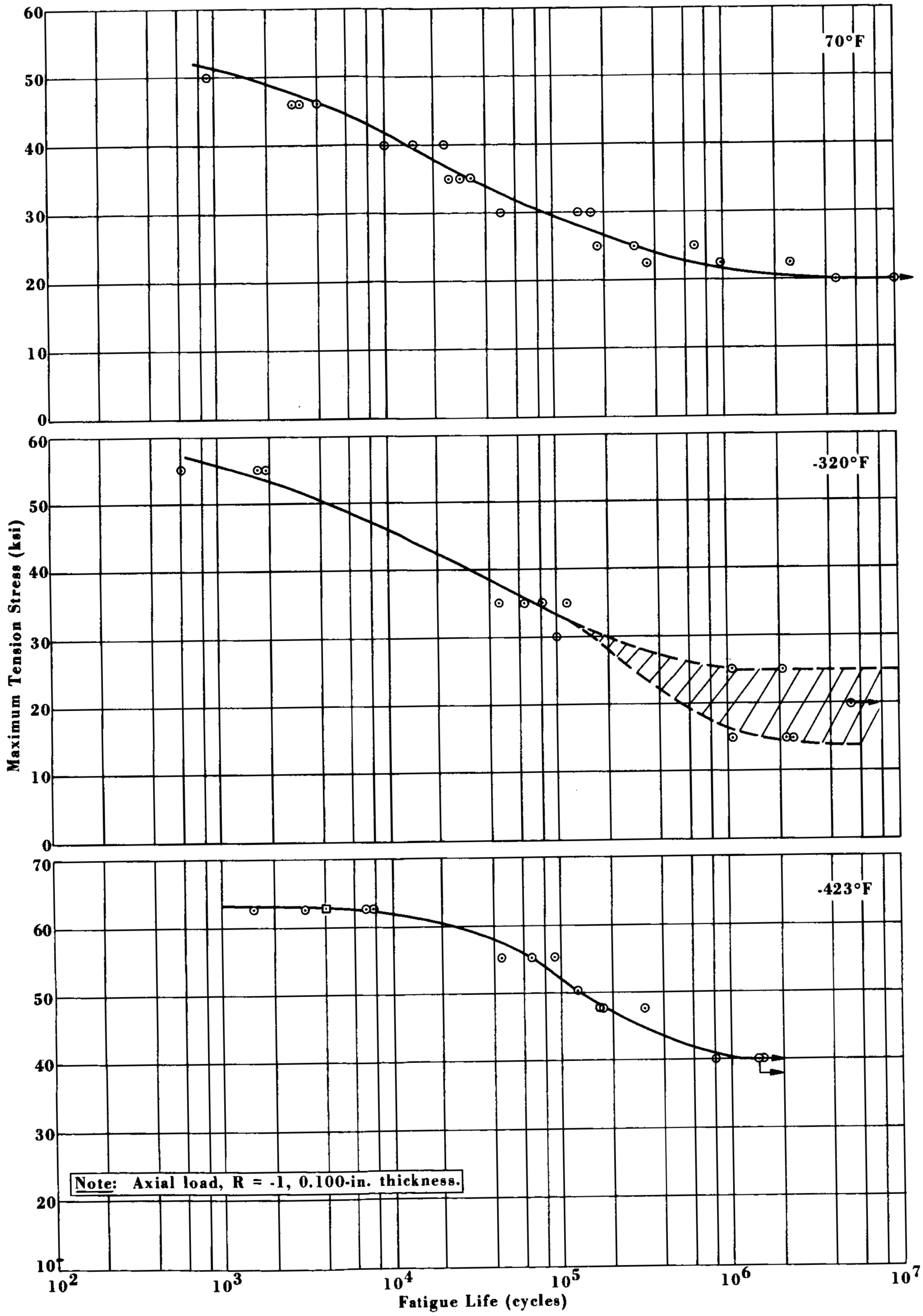

Fig. 30 Fatigue Properties of Unnotched 2219-T87 Aluminum Alloy

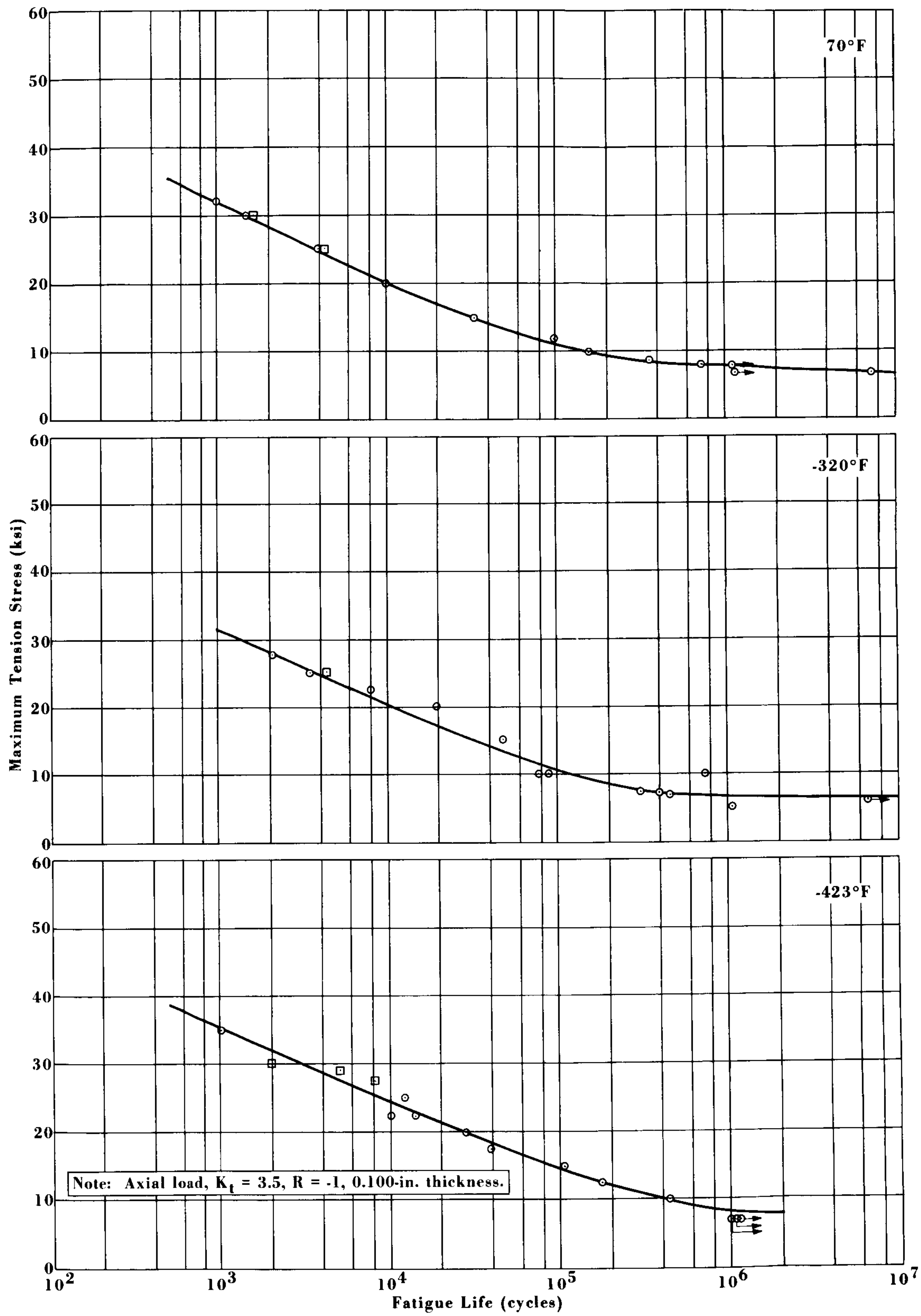

Fig. 31 Fatigue Properties of Notched 2219-T87 Aluminum Alloy

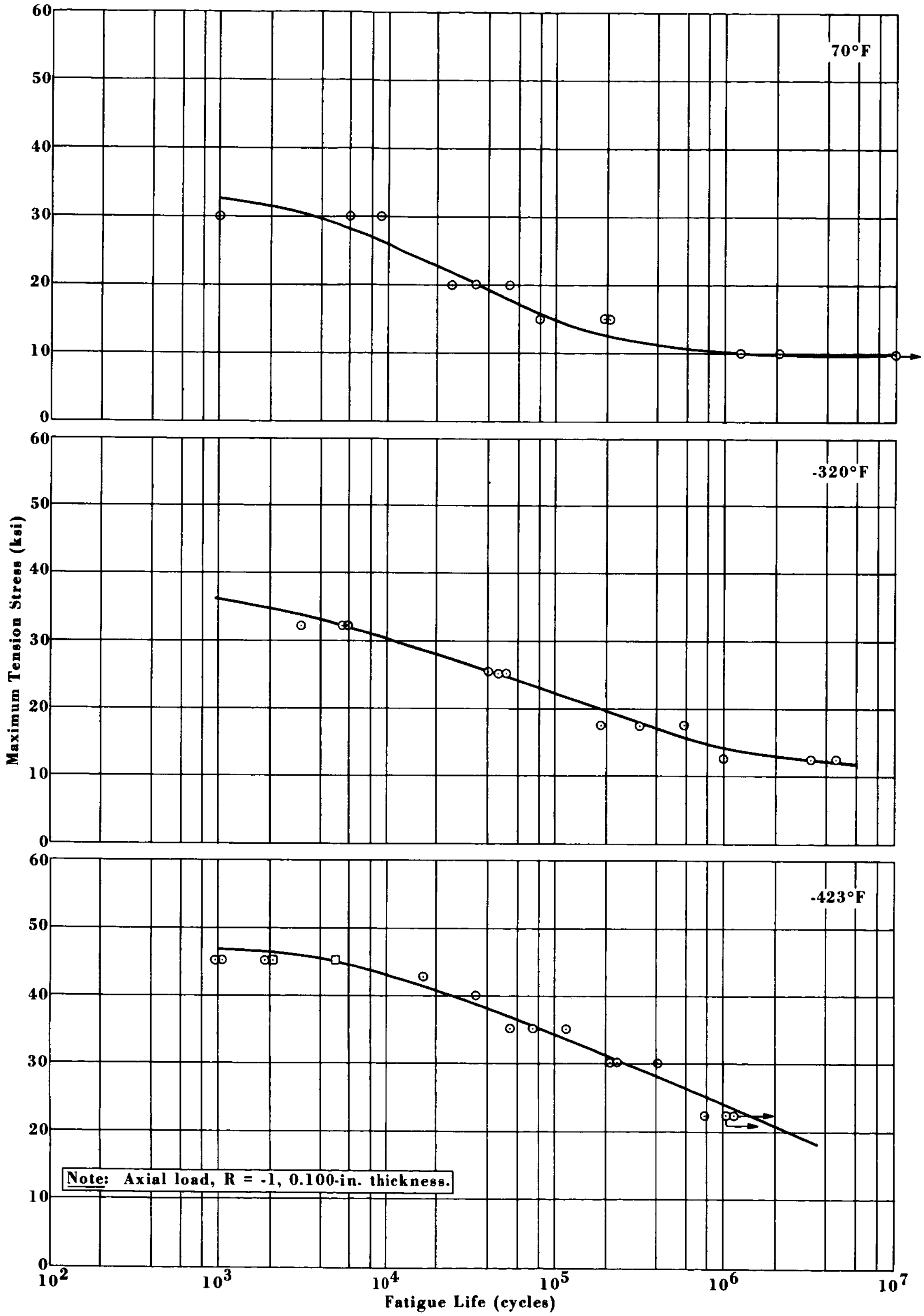

Fig. 32 Fatigue Properties of Welded 2219-T87 Aluminum Alloy

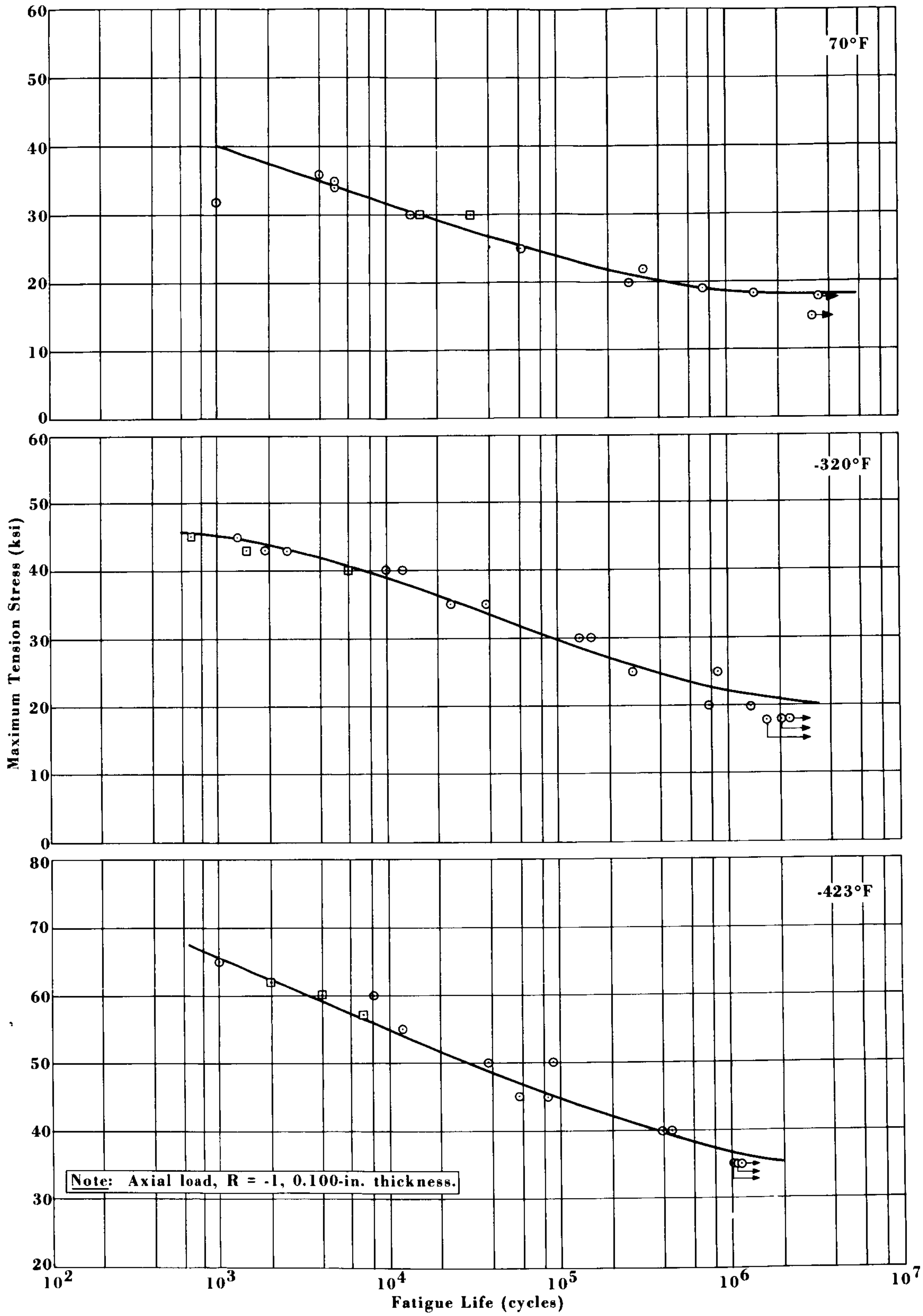

Fig. 33 Fatigue Properties of Unnotched 2219-T62 Aluminum Alloy

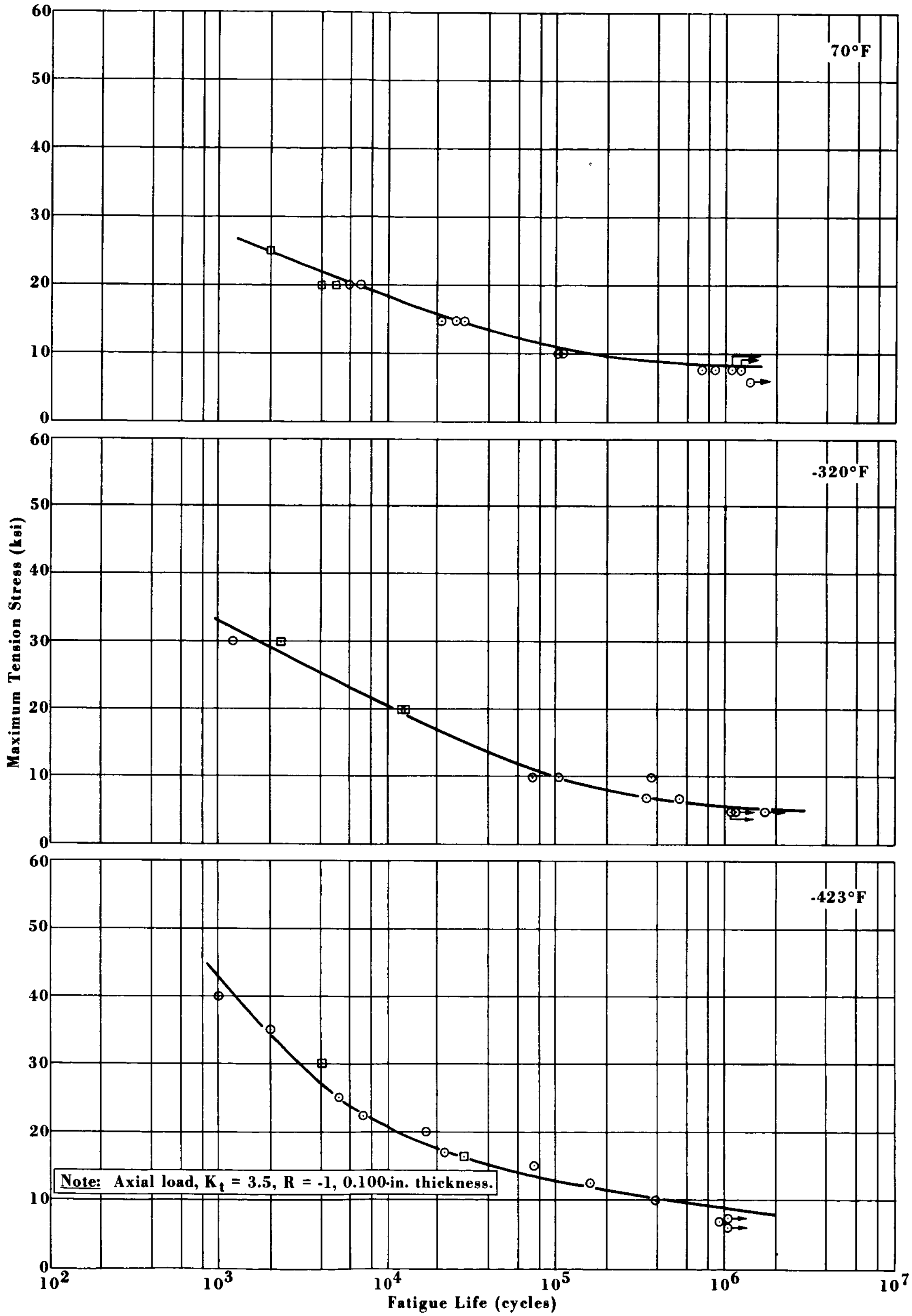

Fig. 34 Fatigue Properties of Notched 2219-T62 Aluminum Alloy

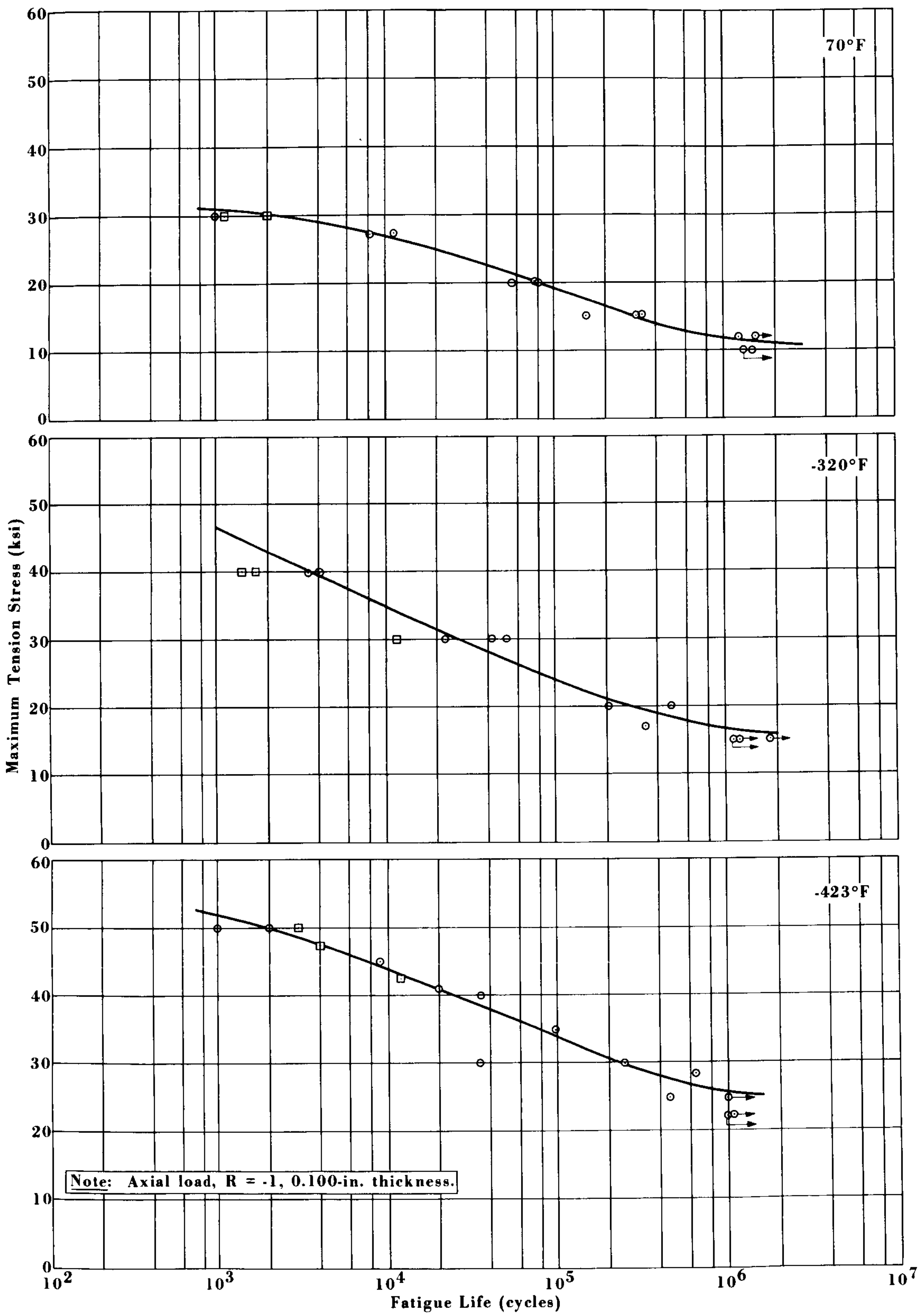

Fig. 35 Fatigue Properties of Welded 2219-T62 Aluminum Alloy

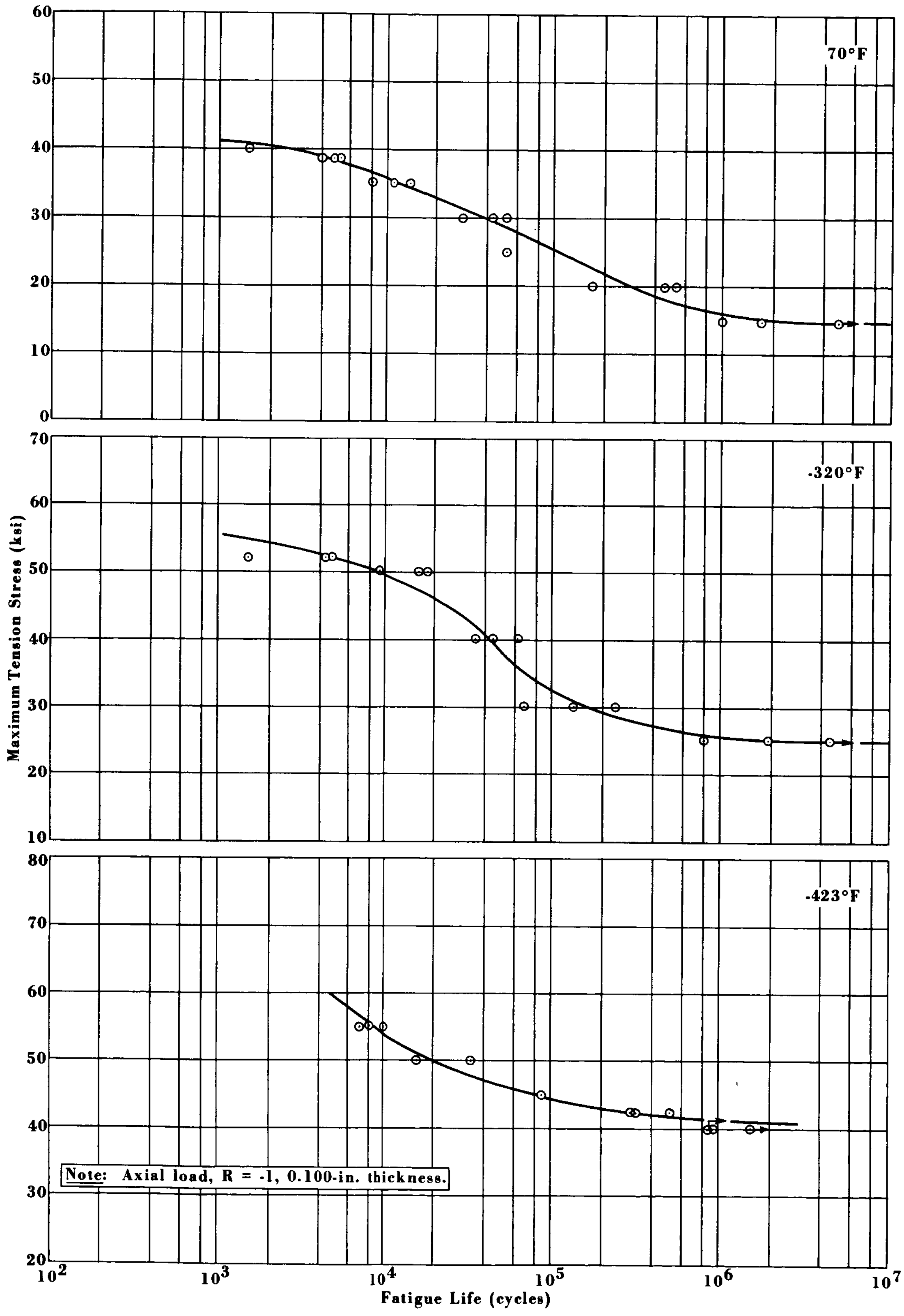

Fig. 36 Fatigue Properties of Unnotched 5456-H343 Aluminum Alloy

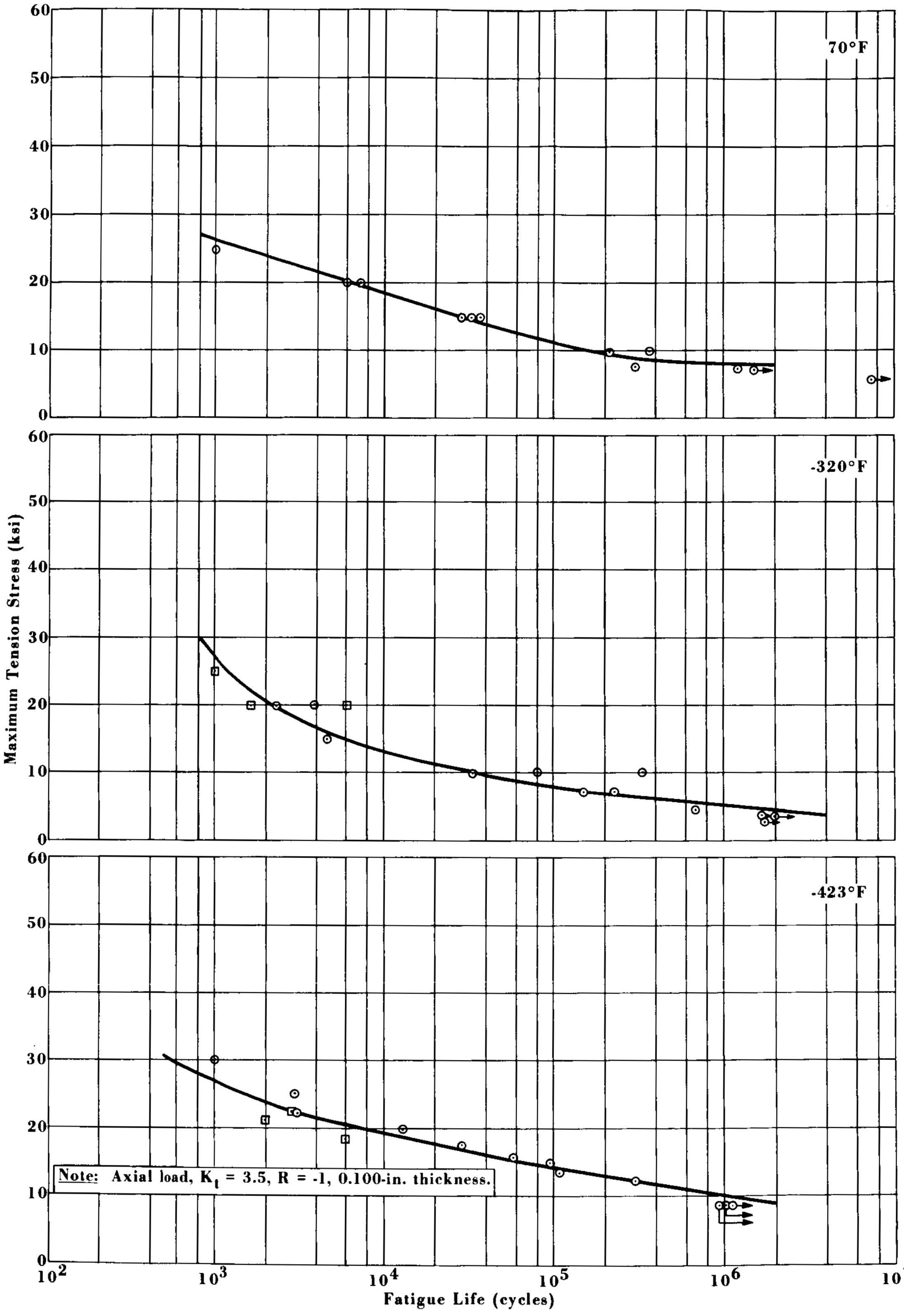

Fig. 37 Fatigue Properties of Notched 5456-H343 Aluminum Alloy

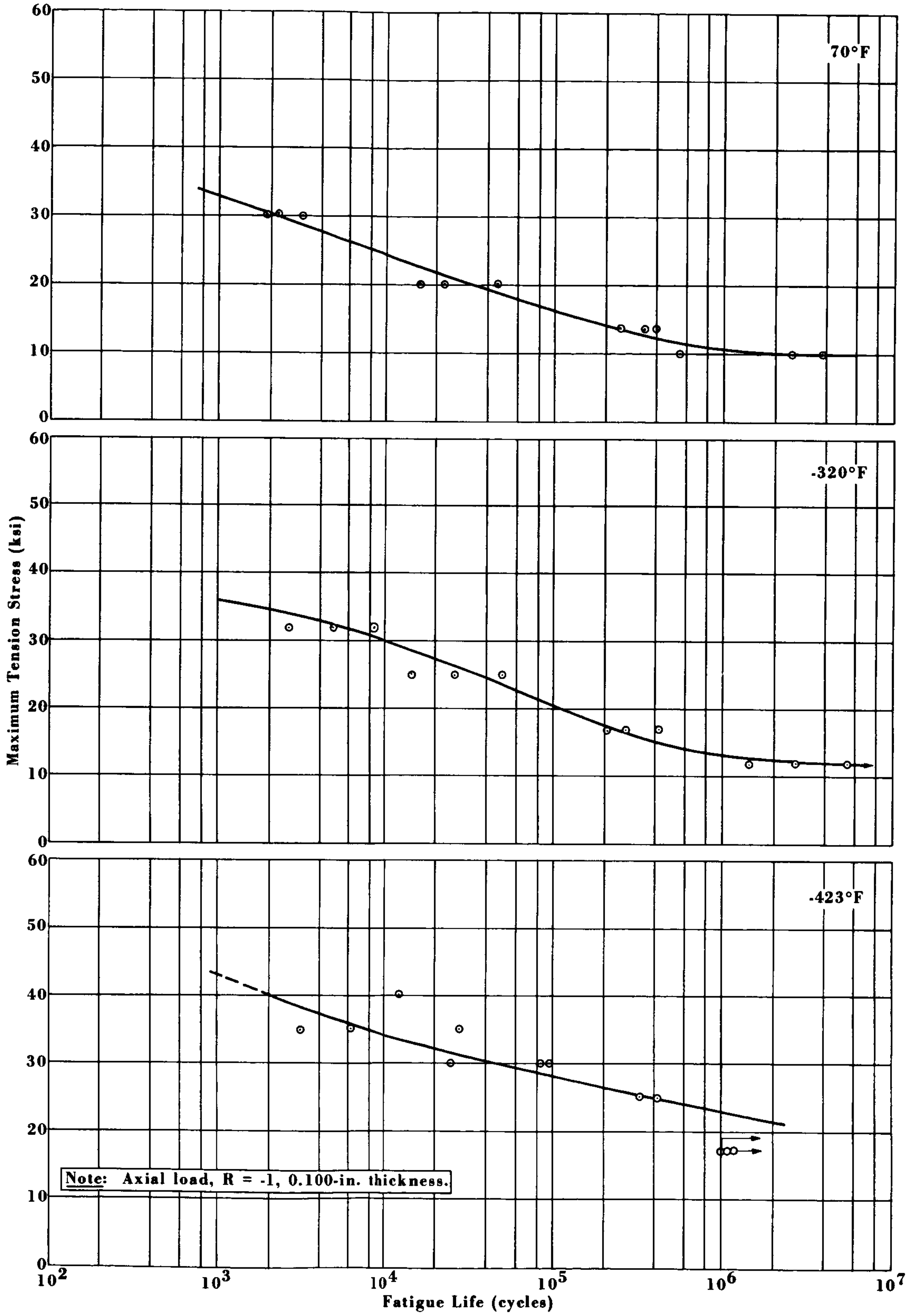

Fig. 38 Fatigue Properties of Welded 5456-H343 Aluminum Alloy

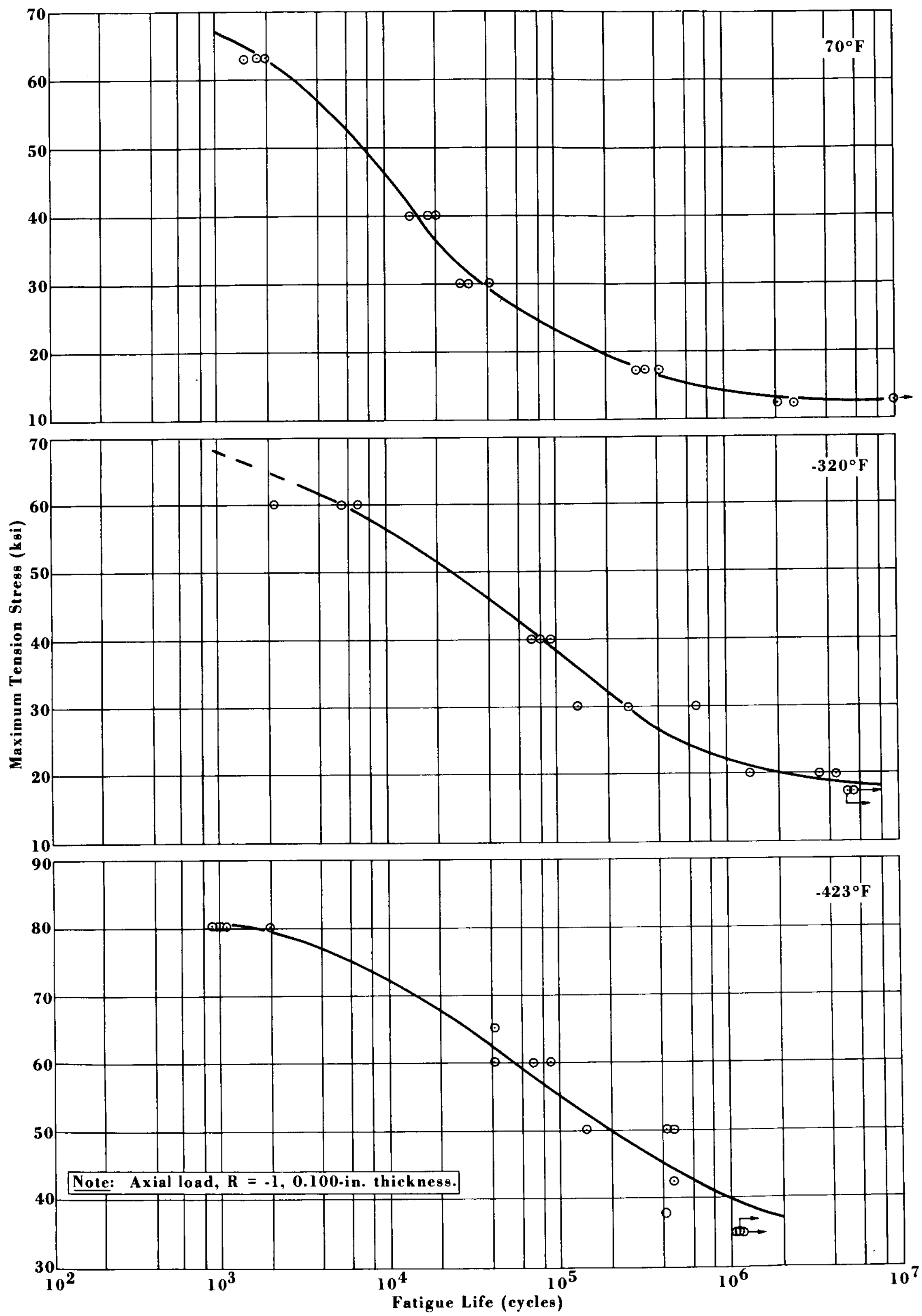

Fig. 39 Fatigue Properties of Unnotched 7075-T6 Aluminum Alloy

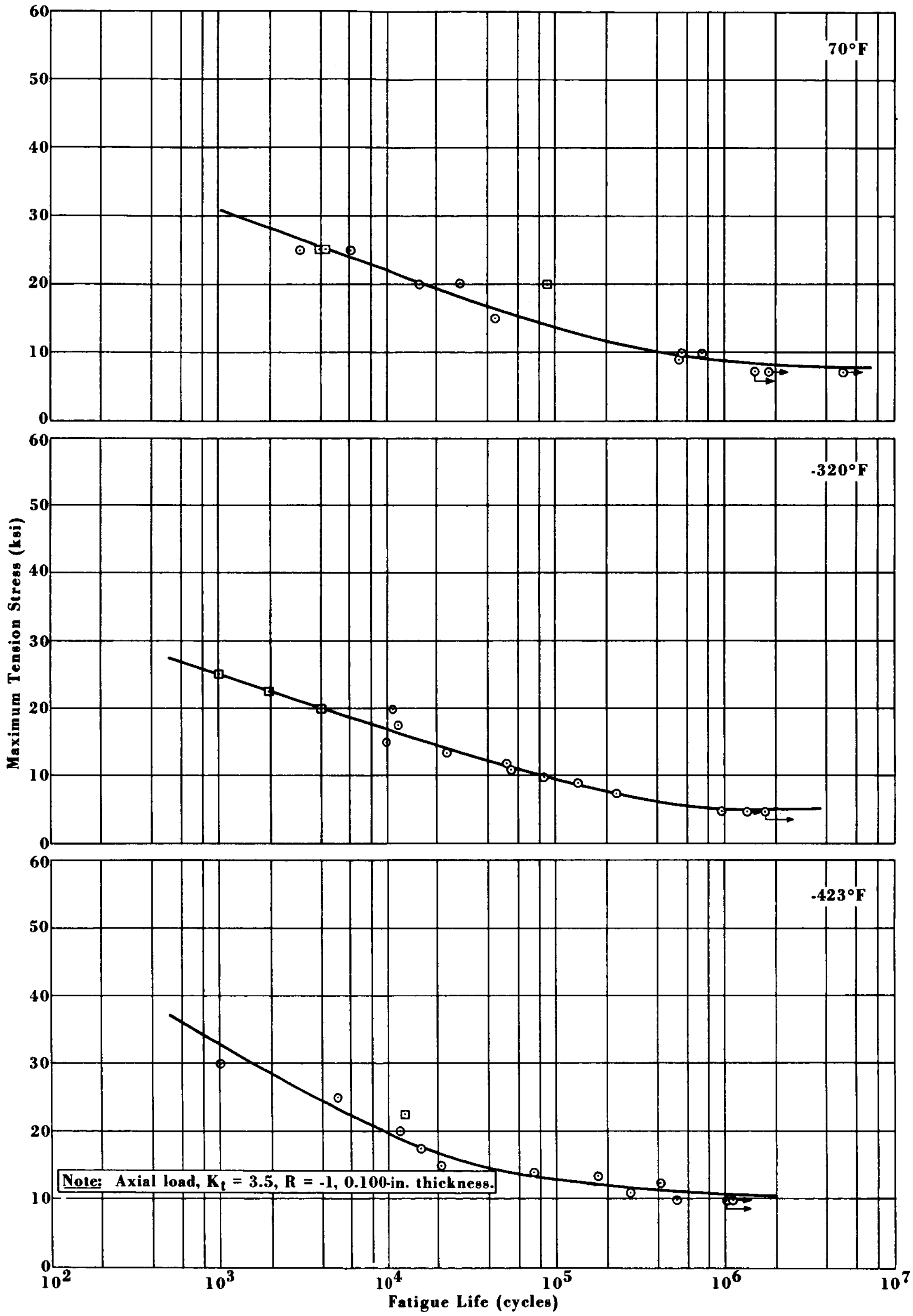

Fig. 40 Fatigue Properties of Notched 7075-T6 Aluminum Alloy

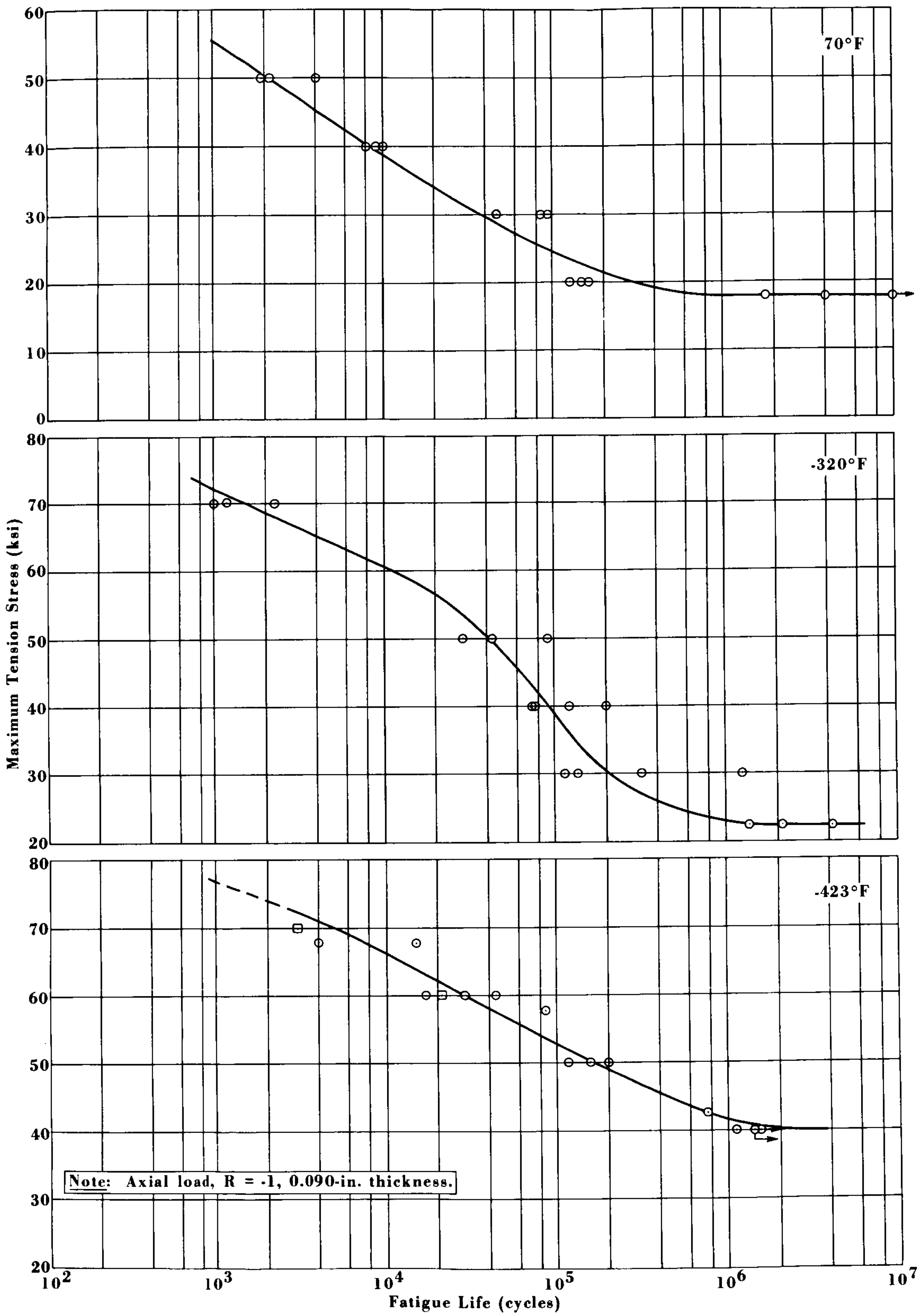

Fig. 41 Fatigue Properties of Unnotched 2020-T6 Aluminum Alloy

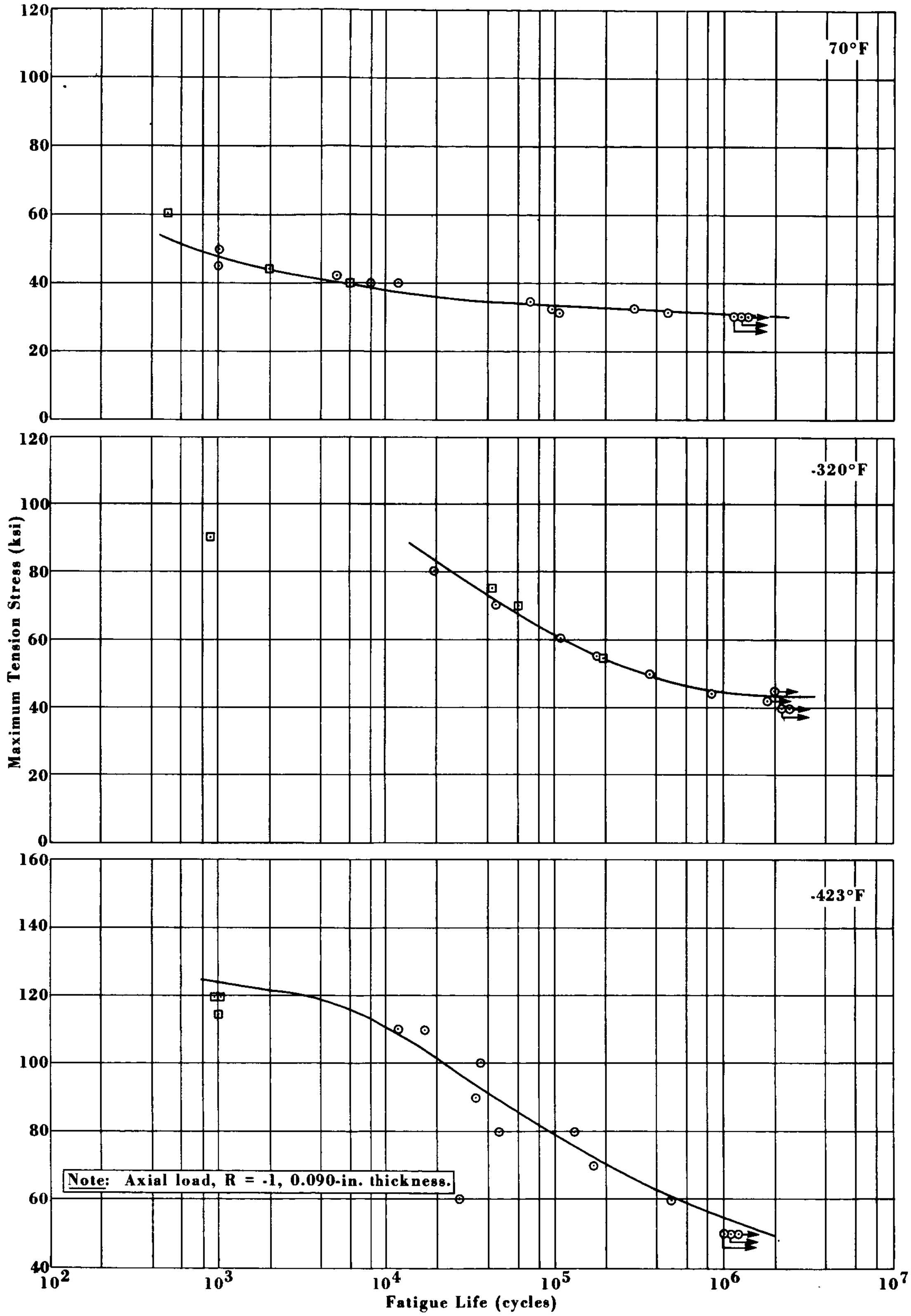

Fig. 42 Fatigue Properties of Unnotched 321 (Annealed) Stainless Steel Alloy

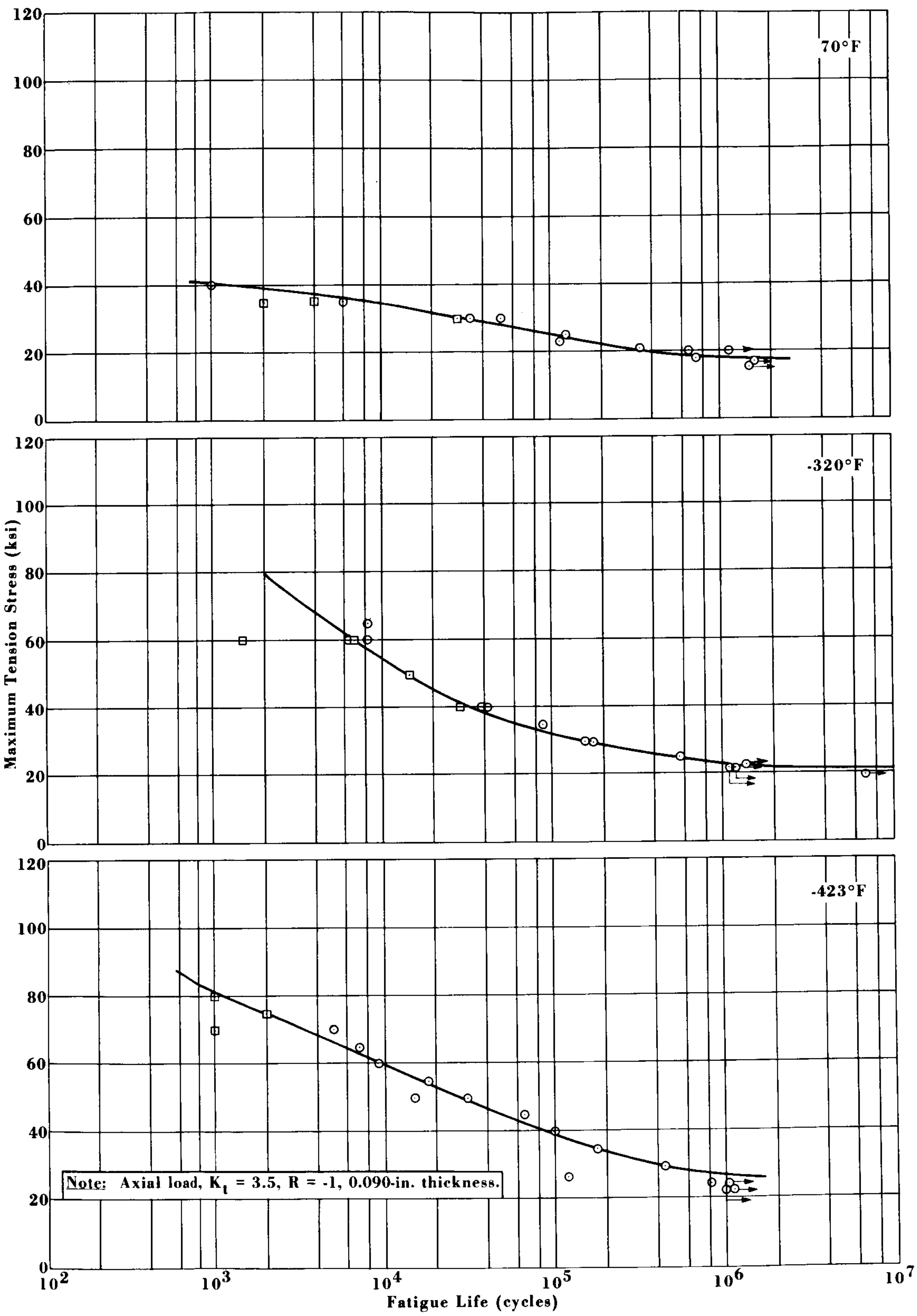

Fig. 43 Fatigue Properties of Notched 321 (Annealed) Stainless Steel Alloy

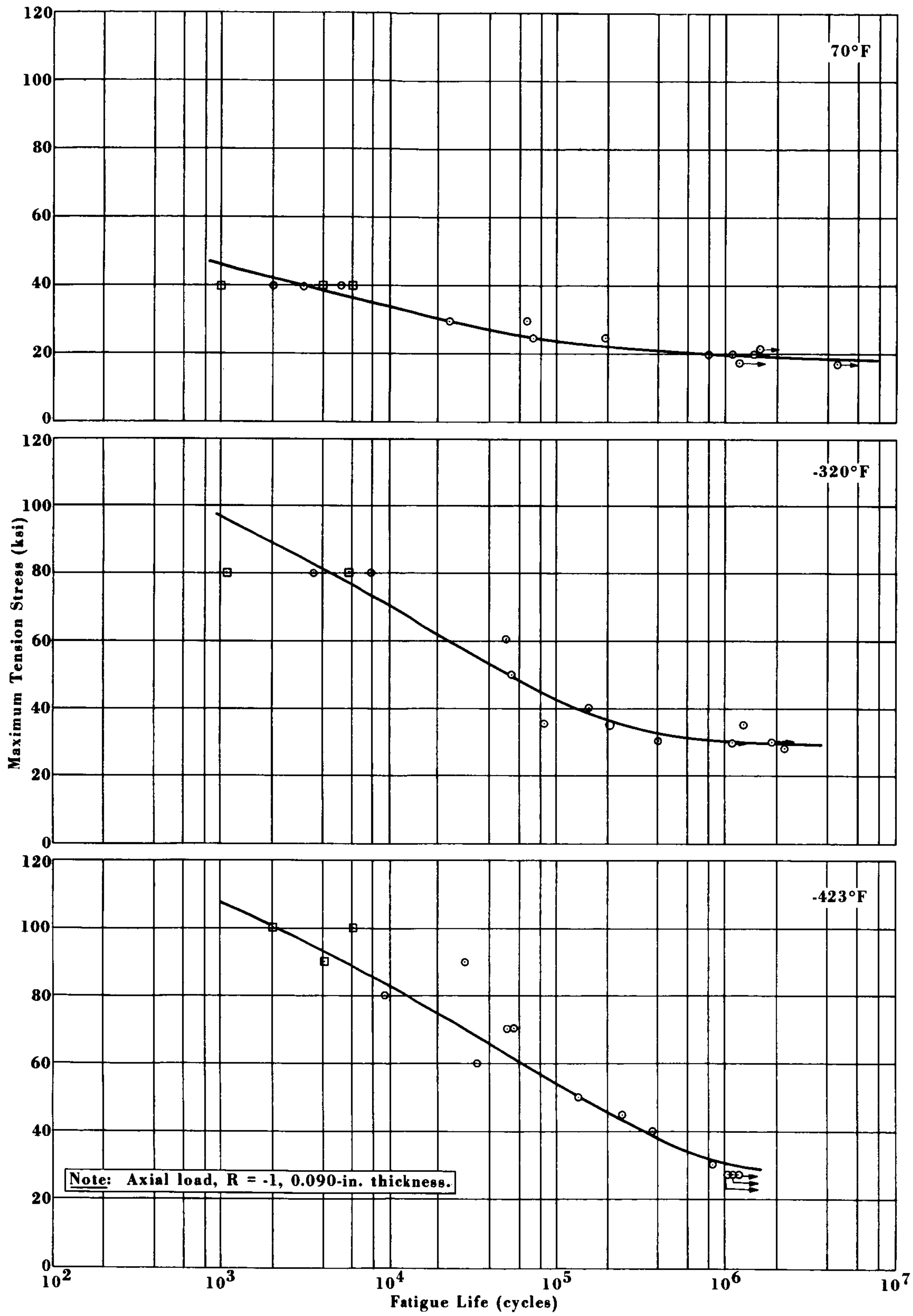

Fig. 44 Fatigue Properties of Welded 321 (Annealed) Stainless Steel Alloy

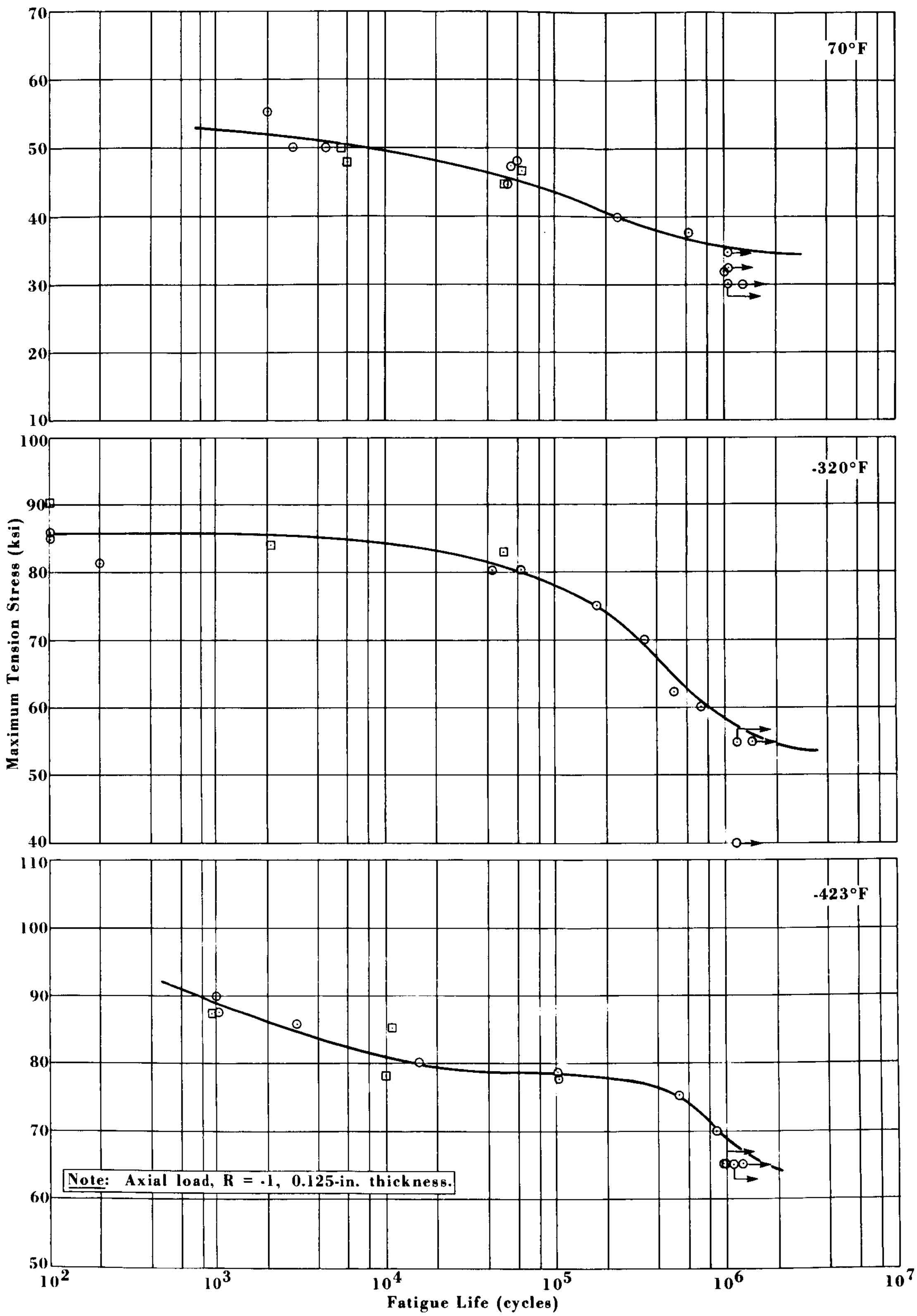

Fig. 45 Fatigue Properties of Unnotched A-286 Stainless Steel Alloy

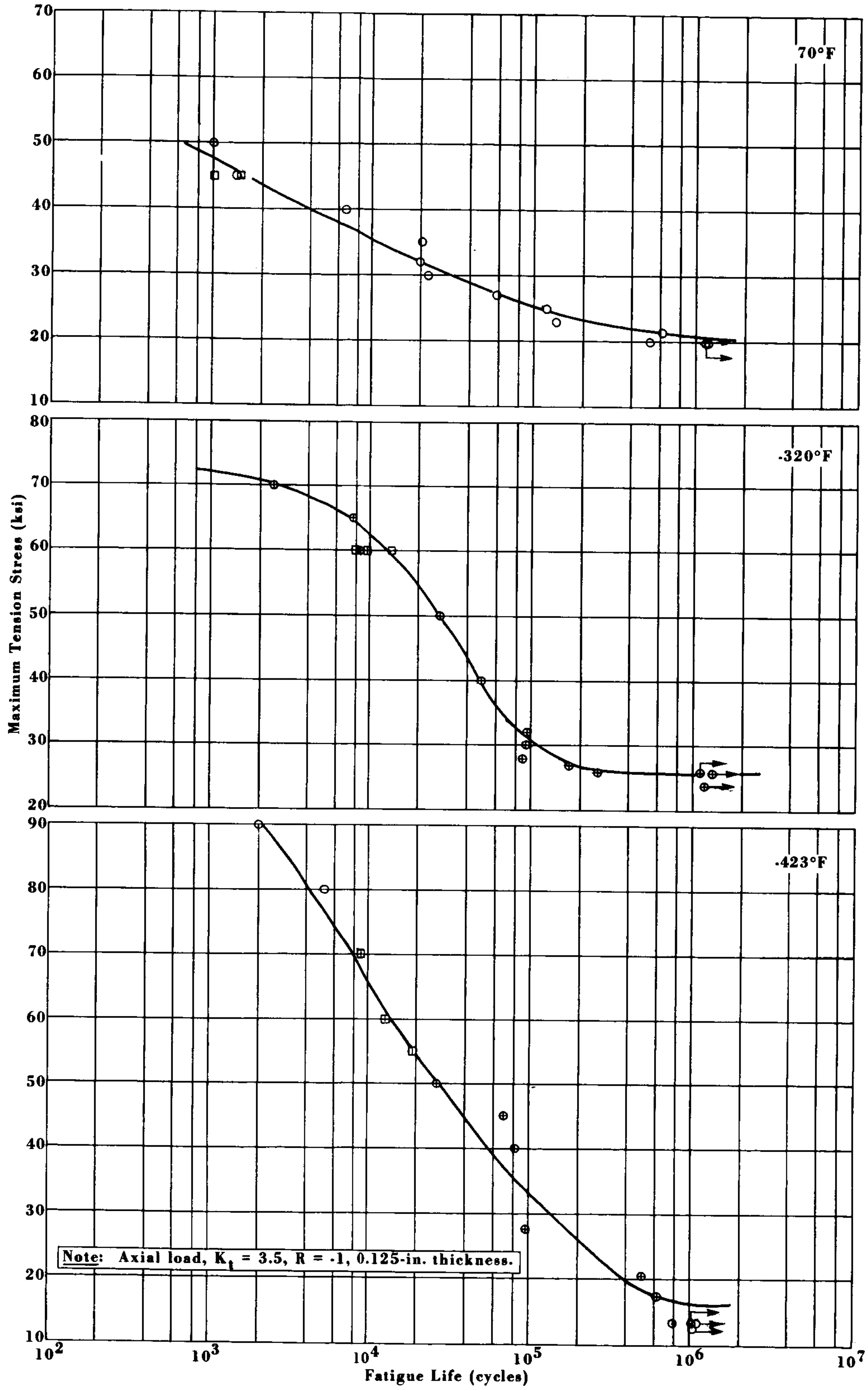

Fig. 46 Fatigue Properties of Notched A-286 Stainless Steel Alloy

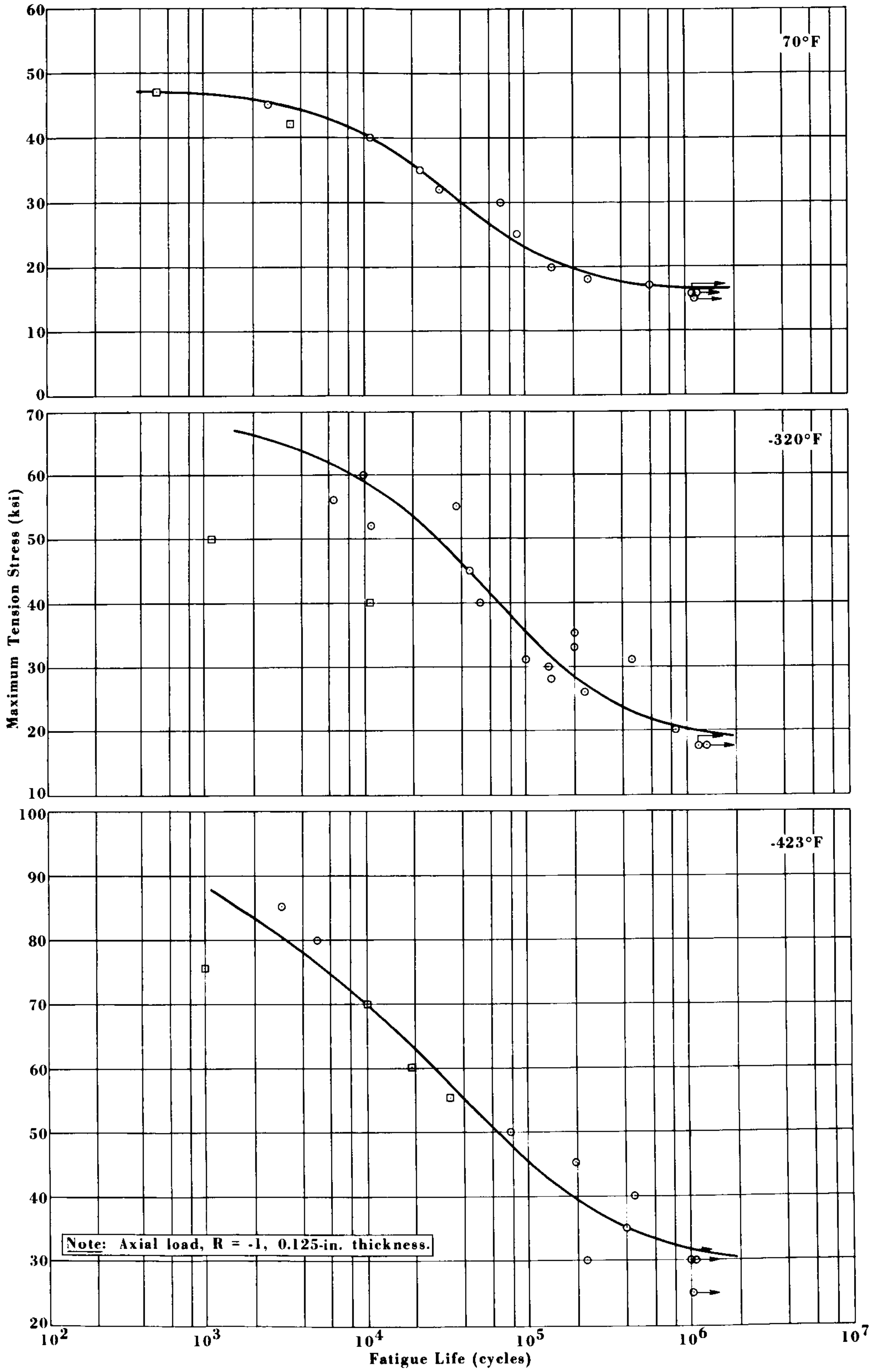

Fig. 47 Fatigue Properties of Welded A-286 Stainless Steel Alloy

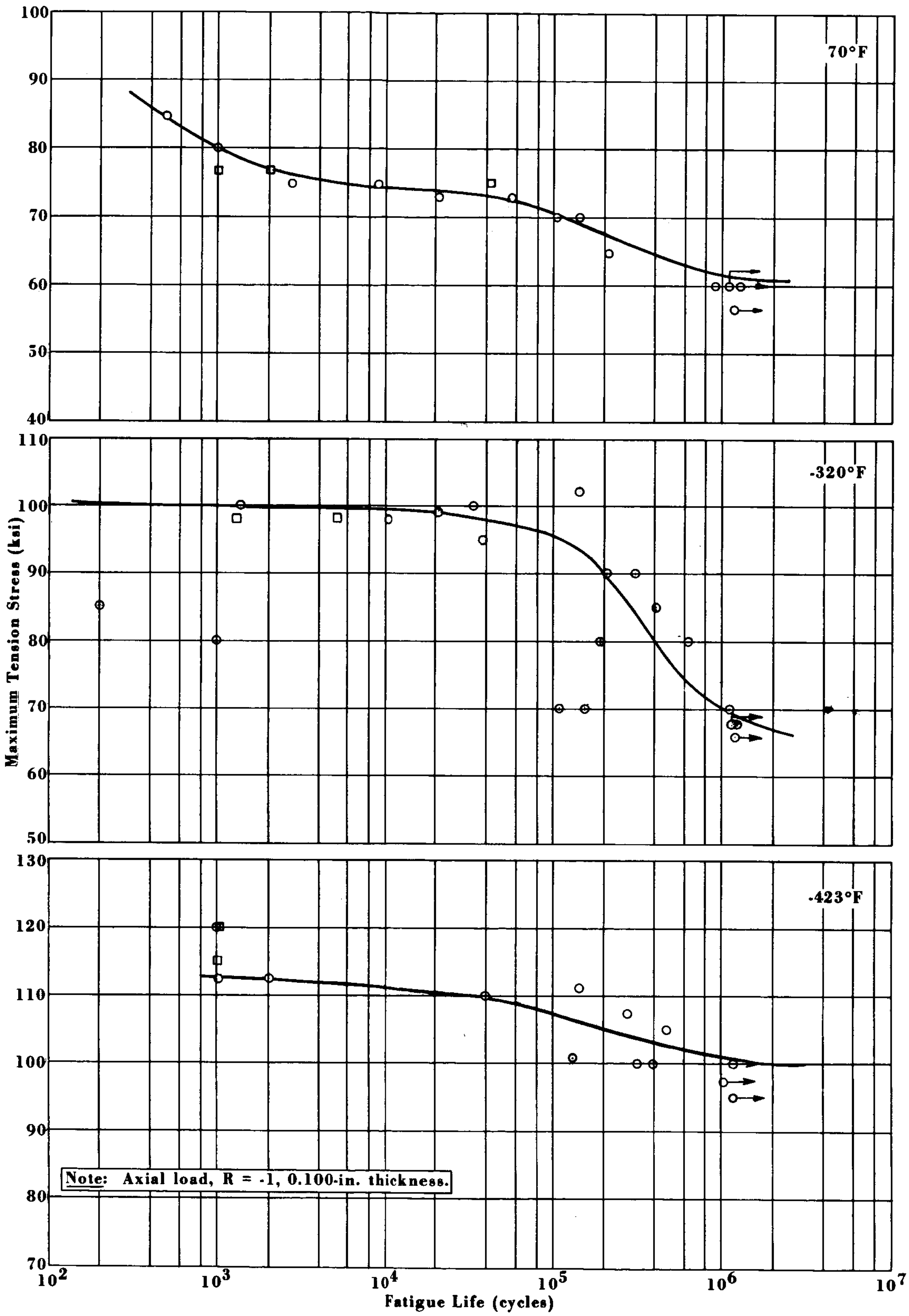

Fig. 48 Fatigue Properties of Unnotched Inconel 718 Nickel Alloy

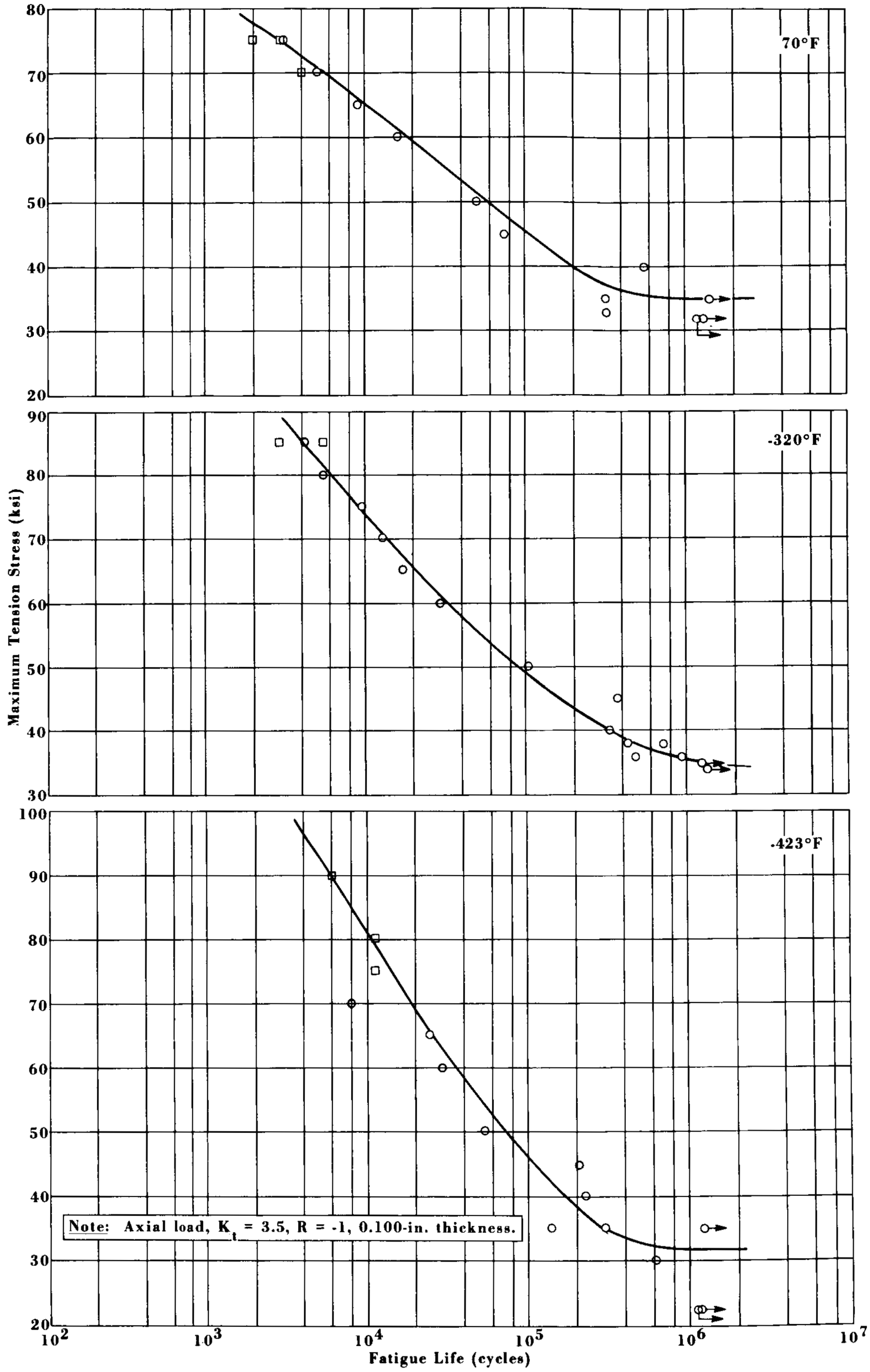

Fig. 49 Fatigue Properties of Notched Inconel 718 Nickel Alloy

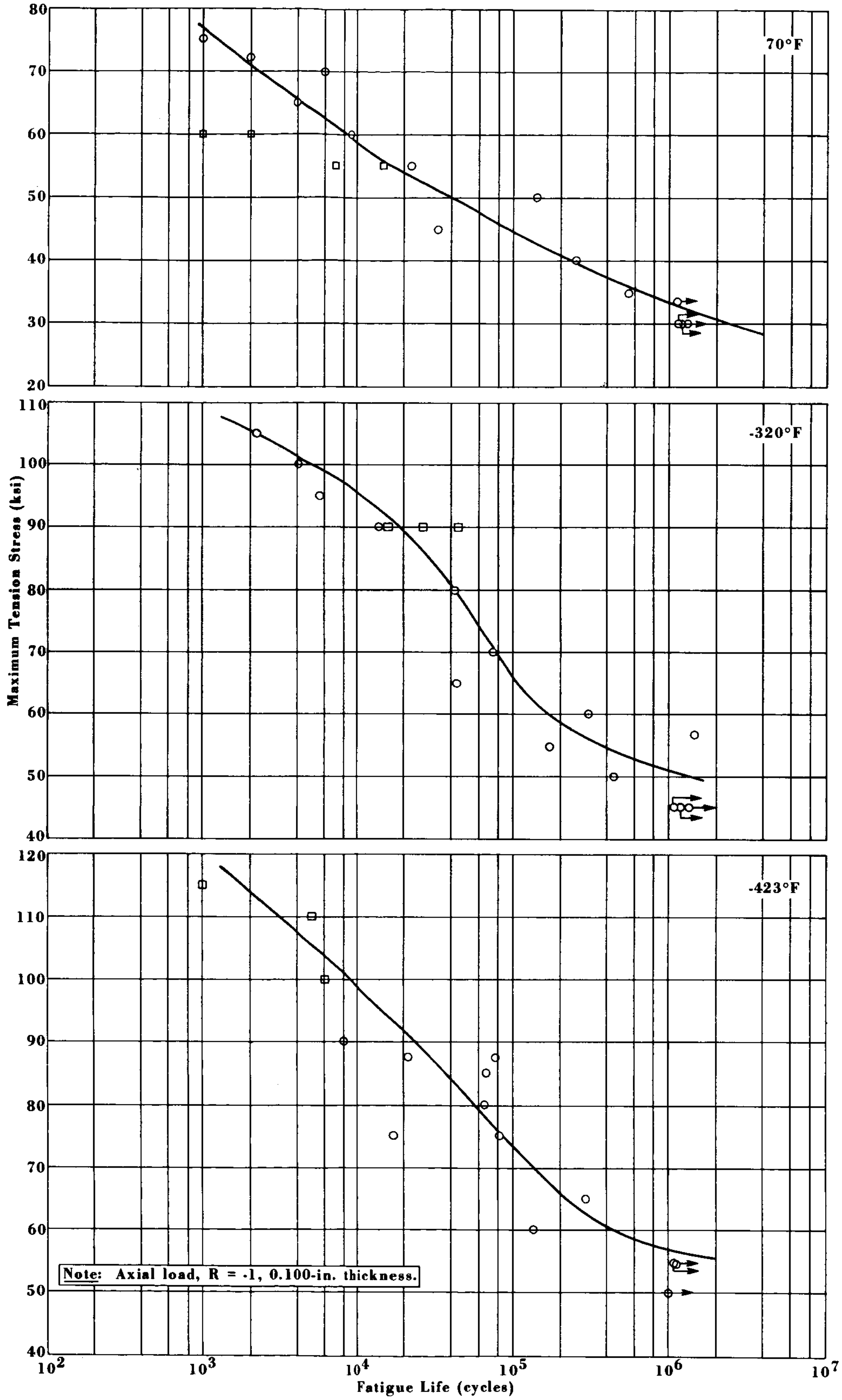

Fig. 50 Fatigue Properties of Welded Inconel 718 Nickel Alloy

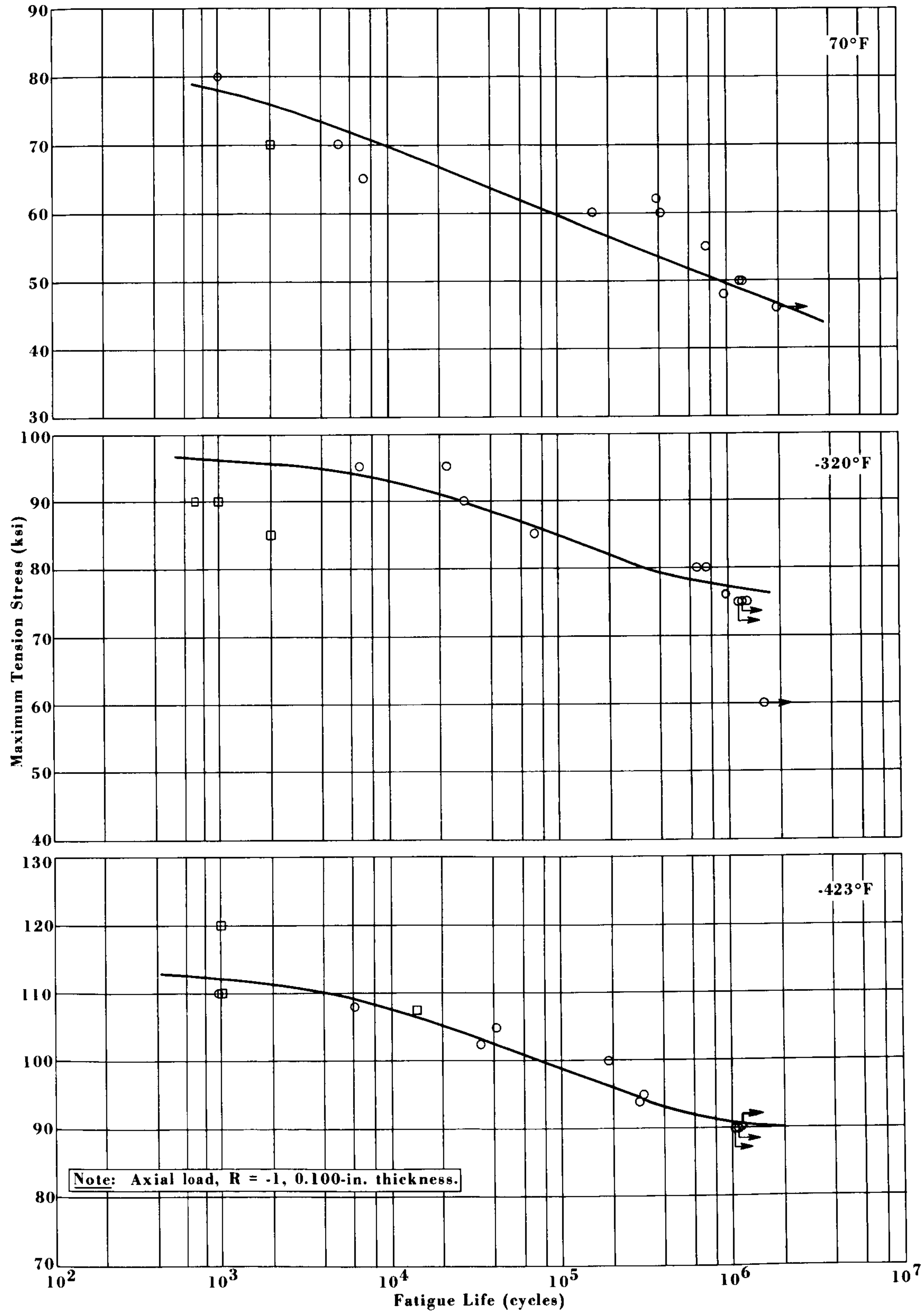

Fig. 51 Fatigue Properties of Unnotched Hastelloy C Nickel Alloy

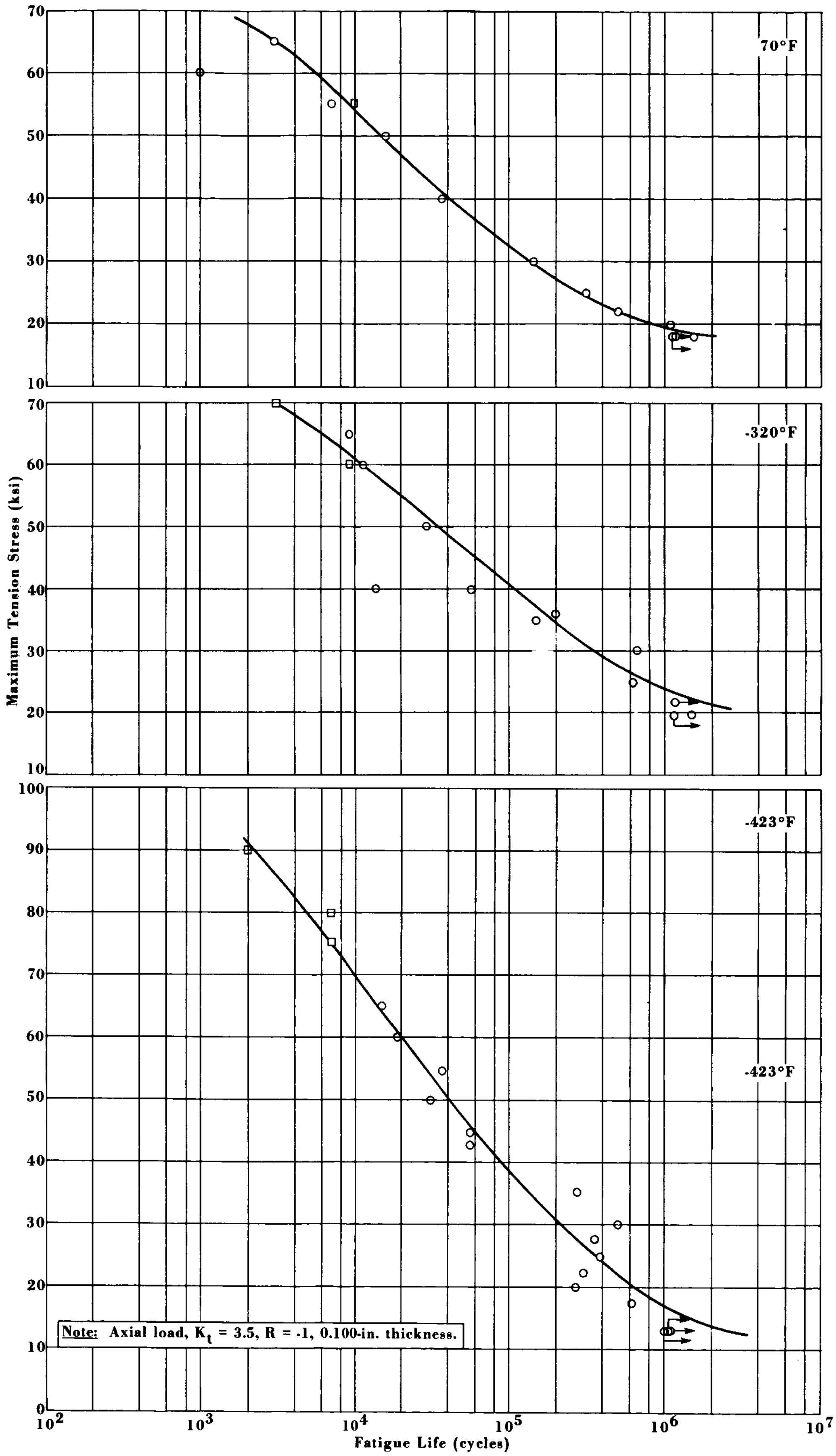

Fig. 52 Fatigue Properties of Notched Hastelloy C Nickel Alloy

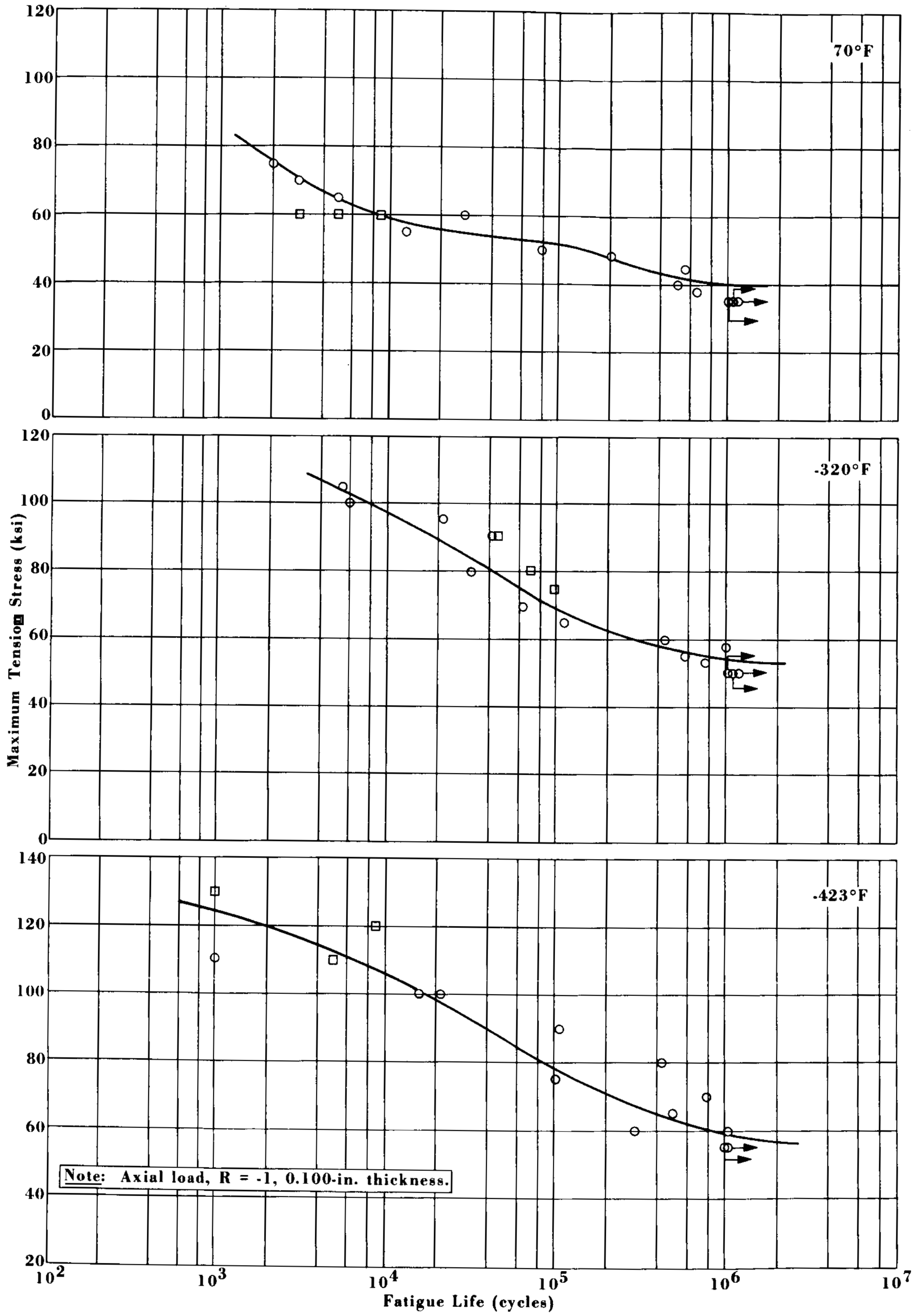

Fig. 53 Fatigue Properties of Welded Hastelloy C Nickel Alloy

VI. DISCUSSION OF RESULTS

A. ALUMINUM ALLOYS

Of the seven aluminum compositions used in this study, five are being used or have been considered for cryogenic service. These alloys are 2014, 2219, 7039, 7106, and 5456. The other two compositions, 2020 and 7075, have not been considered primarily because they are nonweldable grades. In addition, the 7075 exhibits poor toughness characteristics at cryogenic temperatures. However, these last two compositions were included in the study for comparison.

1. Tension Properties

The mechanical properties of the 2014-T6 and 2219-T87 alloys (Fig. 4 and 7, respectively) are similar and in substantial agreement with the data of others (Ref 3 and 4). These alloys are characterized by a greater temperature dependence of strength from -320 to -423°F than from 70 to -320°F. Yield and weld strengths show a relatively constant rate of increase with decreasing temperature. Elongation increases approximately 50% from 70 to -423°F. The principal difference in properties of these alloys is the significantly lower yield strength in the 2219-T87 alloy. The notch strength ratio values are quite high. However, most aluminum alloys exhibit good notch toughness with the relatively low stress concentration factor $(K_t = 3.5)$ used for this work.

The 7039-T6 (Fig. 5) exhibits the characteristic increases in unnotched tension properties observed for the 2014 and 2219 alloys. Notch properties are also similar. Unlike the 2014 and 2219 alloys, weld strength does not increase significantly with decrease in temperature.

The behavior of the 7106-T6 alloy (Fig. 6) is almost identical with that of the 7039-T6 alloy for parent metal and notch properties. Weld strength properties are higher than for the 7039-T6. Weld strength decreases slightly from -320 to -423°F.

The 2219-T62 alloy (Fig. 8) exhibits significantly lower strength, particularly yield strength, than the 2219-T87 composition. This difference results from the absence, in the 2219-T62 temper, of postsolution heat treatment straining used to achieve additional aging response in the 2219-T87 temper. Ductility increases with reduction in temperature, as in the 2014-T6 and 2219-T87 alloys. Weld strength is comparable to that of the 2219-T87. Notch toughness is maintained at high levels down to -423°F.

The 5456-H343 alloy (Fig. 9) exhibits approximately 20% lower ultimate strength than the 2014-2219 alloys. The ratio of yield/ultimate strength is rather low. Elongation is relatively independent of temperature. At 70 to -320°F, weld strength increases, but then decreases with further temperature reduction. This decrease in weld strength and flat ductility curve suggests loss of toughness at low temperatures. The notch data show good retention of toughness down to -423°F. However, the stress concentration (K_t) is not great. Results of other studies (Ref 3 and 5) using sharper notches $(K_t = 6.3\text{-}8)$ have shown lower toughness for this alloy at -423°F than for the 2000 series alloys.

The 7075-T6 material (Fig. 10) shows evidence of the onset of brittle action at -423°F. Ultimate and yield strengths flatten out between -320 and -423°F. Elongation is relatively independent of temperature. Notch tests show a moderate loss of toughness with reduction in temperature. Data obtained by Christian and Watson (Ref 6) using a sharper notch show a significant loss of toughness at low temperatures.

The 2020-T6 alloy (Fig. 11) shows very high strength properties. Room temperature ultimate strength is equal to the strength of 5456-H343 at -423°F. Although this composition is expected to exhibit poor toughness at cryogenic temperatures, the limited evaluation is not sufficient to detect such behavior. Tensile ductility increases to approximately 10% at -423°F.

Modulus data for the seven alloys are given in Fig. 54. Room-temperature results are slightly lower but agree within 4% with data obtained from the Aluminum Association and from producers. Published data are compared with the experimental data tabulated on page 66.

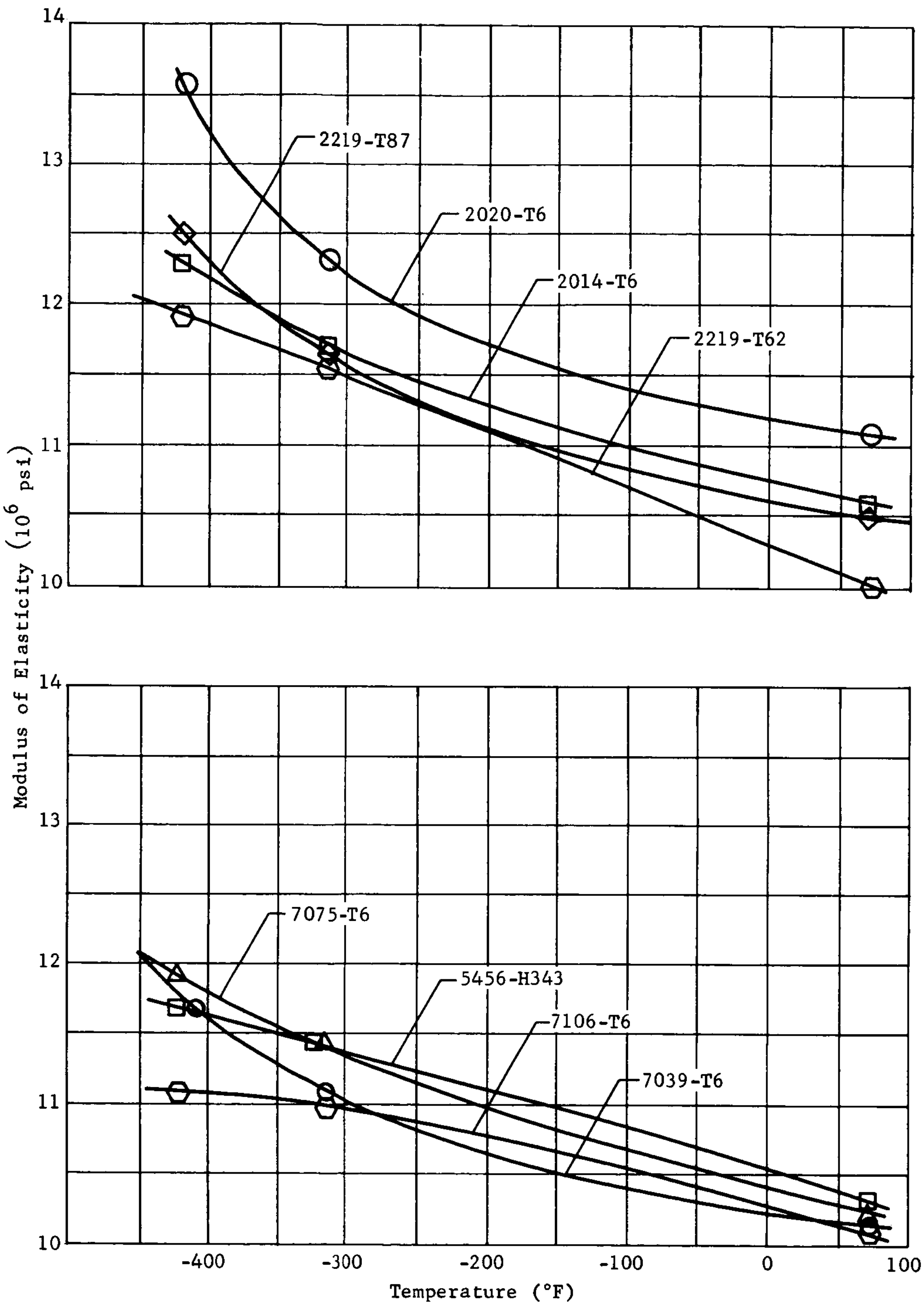

Fig. 54 Comparison of Moduli for Aluminum Alloys at Cryogenic Temperatures

Alloy	Experimental	Published
	Modulus of Elasticity (10^6 psi)	
2014-T6	10.6	10.6
2219-T87	10.5	10.6
2219-T62	10.2	10.6
7039-T6	10.0	10.1
7106-T6	10.1	10.3
5456-H343	10.2	10.3
7075-T6	10.2	10.4
2020-T6	11.1	11.3

The highest modulus material is the 2020 composition. When introduced, this composition was reported to exhibit a 10% improvement over existing alloys. However, subsequent study showed it to be approximately 5%. Nevertheless, this level is still higher than almost all other aluminum alloys.

There are insufficient reliable data in the literature to confirm the cryogenic modulus data.

2. Fatigue Properties

Fatigue data for the aluminum alloys are presented in the figures and tables listed in the following tabulation.

Material	Unnotched		Notched		Welded	
	Figure	Table	Figure	Table	Figure	Table
2014-T6	16, 17	B-1, B-2	18, 19	B-3, B-4	20	B-5
7039-T6	21, 22	B-6, B-7	23, 24	B-8, B-9	25	B-10
7106-T6	26, 27	B-11, B-12	28	B-13	29	B-14
2219-T87	30	B-15	31	B-16	32	B-17
2219-T62	33	B-18	34	B-19	35	B-20
5456-H343	36	B-21	37	B-22	38	B-23
7075-T6	39	B-24	40	B-25	--	--
2020-T6	41	B-26	--	--	--	--

a. 2014-T6

The unnotched 2014-T6 alloy for a stress ratio (R) of -1* exhibits increased strength for 10^6 cycle life of approximately 300% with reduction in temperature from 70 to -423°F. As noted for static behavior, strengthening is greatest between -320 and -423°F. The fatigue ratio† increased from 0.23 to 0.48 with reduction in temperature. The curves obtained at 70 and -423°F were significantly flatter than the -320°F curve, which showed a slight knee. Although the reason for this is not known, a slight misalignment may be responsible. Testing on similar aluminum alloys at -320°F during the second year's effort did not show this behavior. Alignment accuracy achieved during the second year is believed superior to that attained during the first year.

Unnotched 2014-T6 tested in the tension-tension range (R = 0.01) showed a strength increase for 10^6 cycle life with reduction in temperature similar to that shown for the R = -1 condition. Strength levels were 150 to 200% higher than similar tests conducted under fully reversed stressing. A modified Goodman diagram constructed from the data obtained for the two stress ratios is given in Fig. 55. At 70°F, the stress amplitude (S_a) appears to be virtually unaffected by the presence of a mean stress (S_m). However, at -320 and -423°F, the characteristic decrease in stress amplitude with increasing mean stress is observed. At -423°F, the Goodman diagram shows an almost linear decrease of the fatigue life curve.

*Unless otherwise noted, all fatigue tests are for stress ratio (R) = -1.

$$\dagger\text{Fatigue ratio} = \frac{S_N \text{ (fatigue strength at N cycles)}}{S_u \text{ (static tensile strength)}}.$$

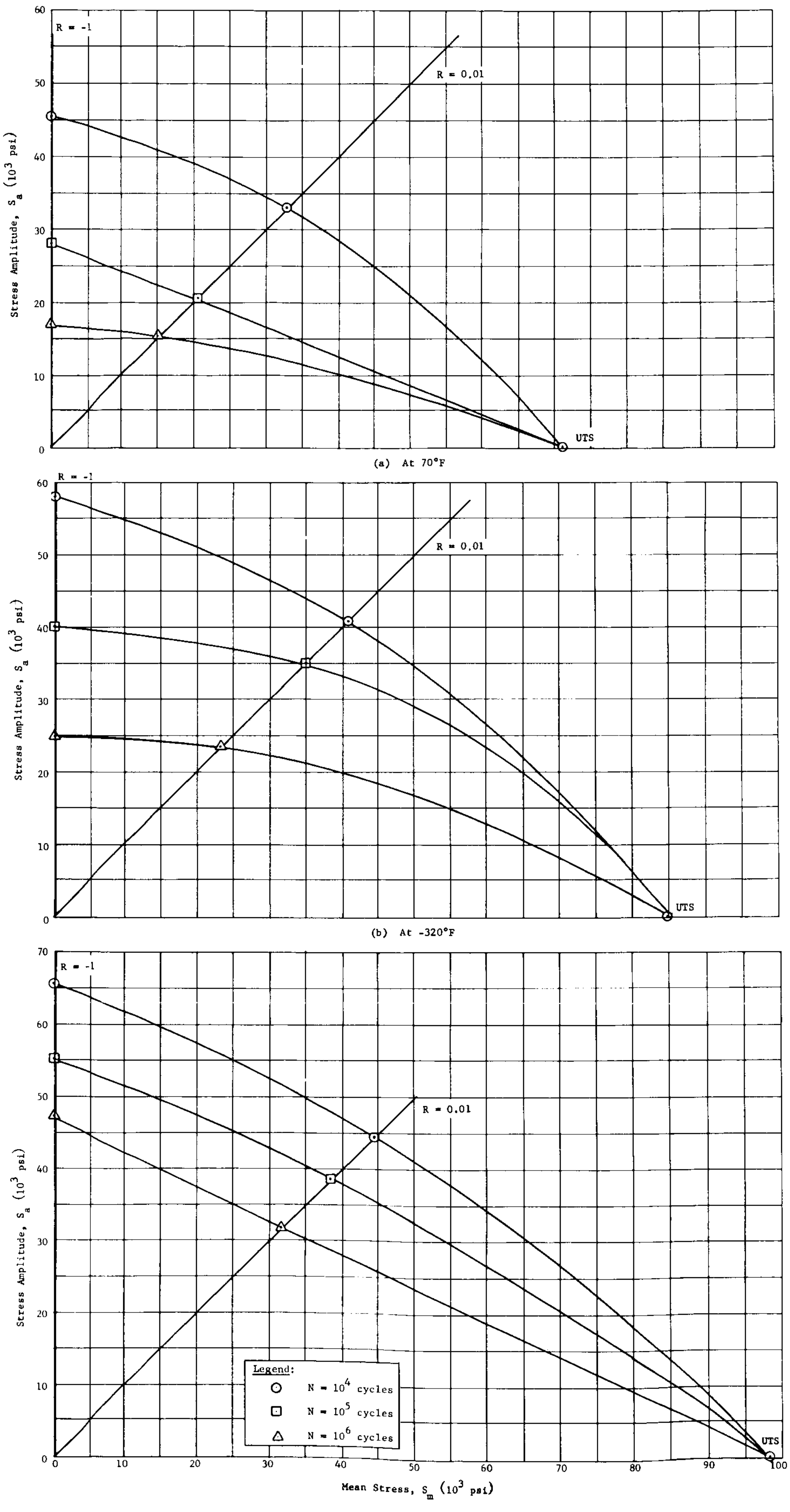

FIG. 55 MODIFIED GOODMAN DIAGRAM FOR 2014-T6 ALUMINUM ALLOY

Notch fatigue testing at two stress concentrations (K_t = 3.5 and 8.0) showed similar S-N diagrams. At 70°F, the curves for the two K_t levels were almost coincidental. Test results obtained at -320°F also showed coincidental curves. At liquid hydrogen temperature (-423°F), the curve for the sharper notch (K_t = 8.0) was slightly lower than observed for the milder notch (K_t = 3.5); however, the difference was small. The notch strength values were significantly lower than those obtained for the unnotched condition. The fatigue notch factor (K_f)* was rather poor, particularly with reduction in temperature. At room temperature, the fatigue notch factor was less than the elastic stress concentration factor (K_t). This agrees with theory and published results. However, at cryogenic temperatures, K_f increases and in a few cases actually exceeds K_t. The significance of this will be discussed later. Note also that K_f increases with number of cycles (N).

Welded joints also show a loss of strength compared to the unnotched material. However, comparing the 70°F static 2014-T6 weld joint efficiency (80%) with the ratio of weld fatigue strength/unwelded fatigue strength (69%), a very good retention of weld strength under dynamic loading is evident. At cryogenic temperatures, a marked decrease in this strength ratio is noted.

*Fatigue notch factor (K_f) =

$$= \frac{\text{fatigue strength of unnotched specimens at N cycles}}{\text{fatigue strength of notched specimens at N cycles}} .$$

b. 7039-T6

The unnotched 7039-T6 composition shows a significant amount of strengthening between 70 and -320°F in the 10^3 to 10^5 cycle range under fully reversed stressing, but minor strengthening from -320 to -423°F. However, at 10^6 cycles the -423°F curve flattens out and a greater strengthening is noted. The fatigue ratio (10^6 cycles) is excellent over the entire temperature range, increasing from 0.31 at 70°F to 0.43 at -423°F.

Unnotched tests in the tension-tension range (R = 0.01) were similar in shape to those performed under fully reversed stressing. Strength levels were approximately 150% of the R = -1 levels. Figure 56 gives a modified Goodman diagram obtained for the two stress ratios. Unlike the data for 2014-T6 at 70°F, the Goodman diagram shows a decrease in stress amplitude with increasing mean stress component.

Notch fatigue testing at two stress concentrations (K_t = 3.5 and 8.0) showed almost identical S-N diagrams. The K_f factors at room temperature showed a significant loss of strength due to a notch. Reduction in temperature resulted in even further loss of notch strength compared to unnotched properties. At 10^6 cycles for the K_t = 3.5 specimens (both -320 and -423°F), the K_f value was slightly above the calculated K_t. As noted for previous alloys K_f showed a general increase with number of cycles.

Testing of welded specimens reveals the principal strengthening occurs between 70 and -320°F, as in the parent metal tests. Only minor strengthening occurs from -320 to -423°F. The fatigue ratio increases from 0.19 to 0.37 with lowering of temperature.

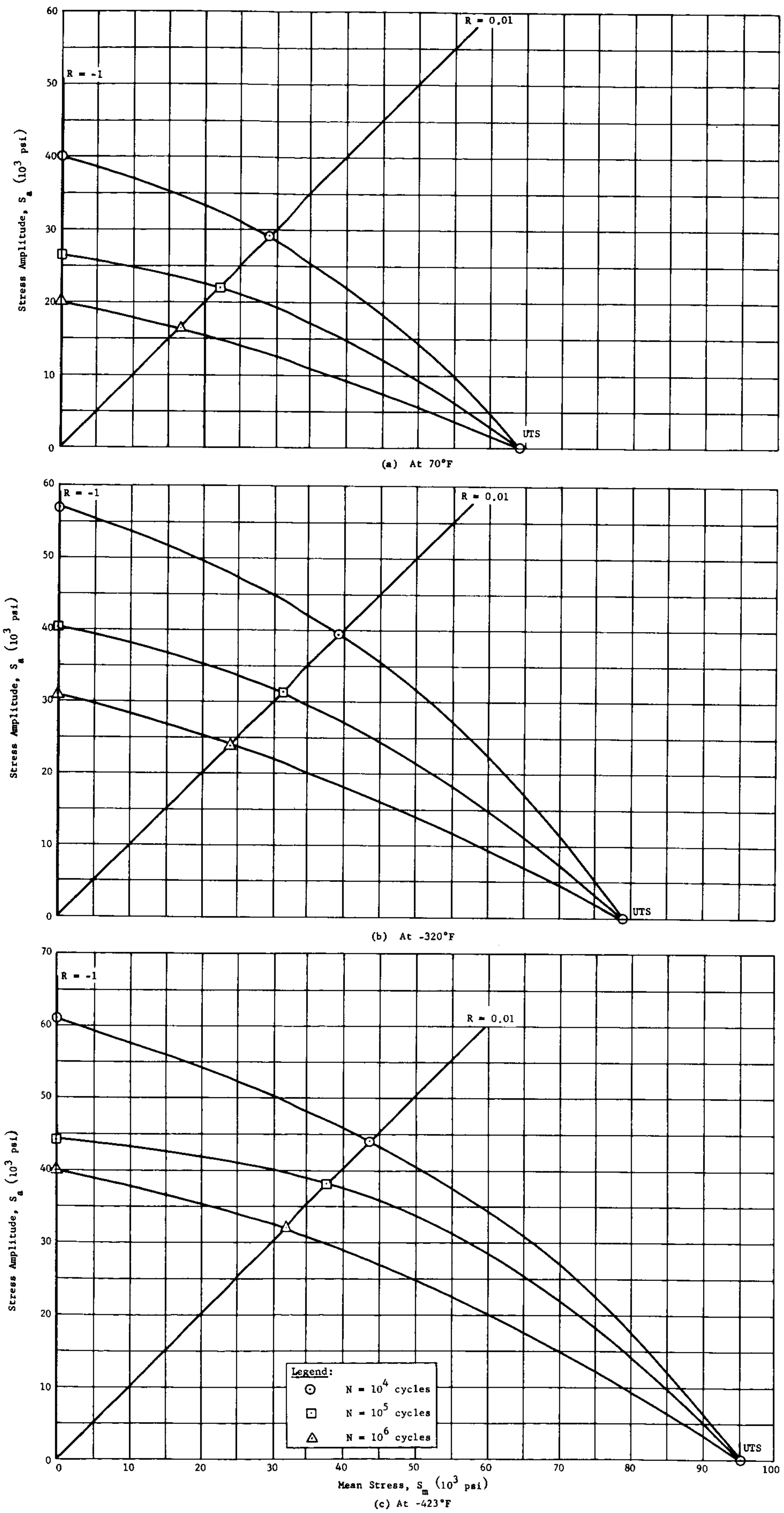

FIG. 56 MODIFIED GOODMAN DIAGRAM FOR 7039-T6 ALUMINUM ALLOY

c. 7106-T6

Fully reversed stressing tests of unnotched 7106-T6 aluminum showed a significant amount of strengthening between 70 and -320°F. Further temperature reduction from -320 to -423°F produced no additional strengthening. The fatigue ratio increases from 0.21 at 70°F to 0.47 at -320°F and then decreases slightly to 0.45 at -423°F.

Tension-tension fatigue tests (R = 0.01) show curves similar in shape to those obtained at R = -1, but strength levels are somewhat higher for the tension-tension condition. Tests performed at -320°F exhibited significant strengthening over the 70°F data, particularly at the high cycle end of the curve. Fatigue data obtained at -423°F showed further strengthening in the low cycle range, but properties similar to those in the -320°F curve in the 10^6 cycle region. A modified Goodman diagram constructed from the above results is presented in Fig. 57.

Notch fatigue testing was conducted only for the milder notch condition ($K_t = 3.5$). The K_f values at 70°F were low. Decreasing temperature caused only a slight increase in K_f. The fatigue notch factors for the alloy at -423°F were the lowest of any aluminum composition evaluated in both the current and previous study.

Weld strength data obtained at 70 and -320°F showed a significant amount of scatter. However, the 70°F results appear to be slightly lower than noted for other aluminum compositions. The cryogenic weld fatigue properties appear to be consistent with other aluminum alloys.

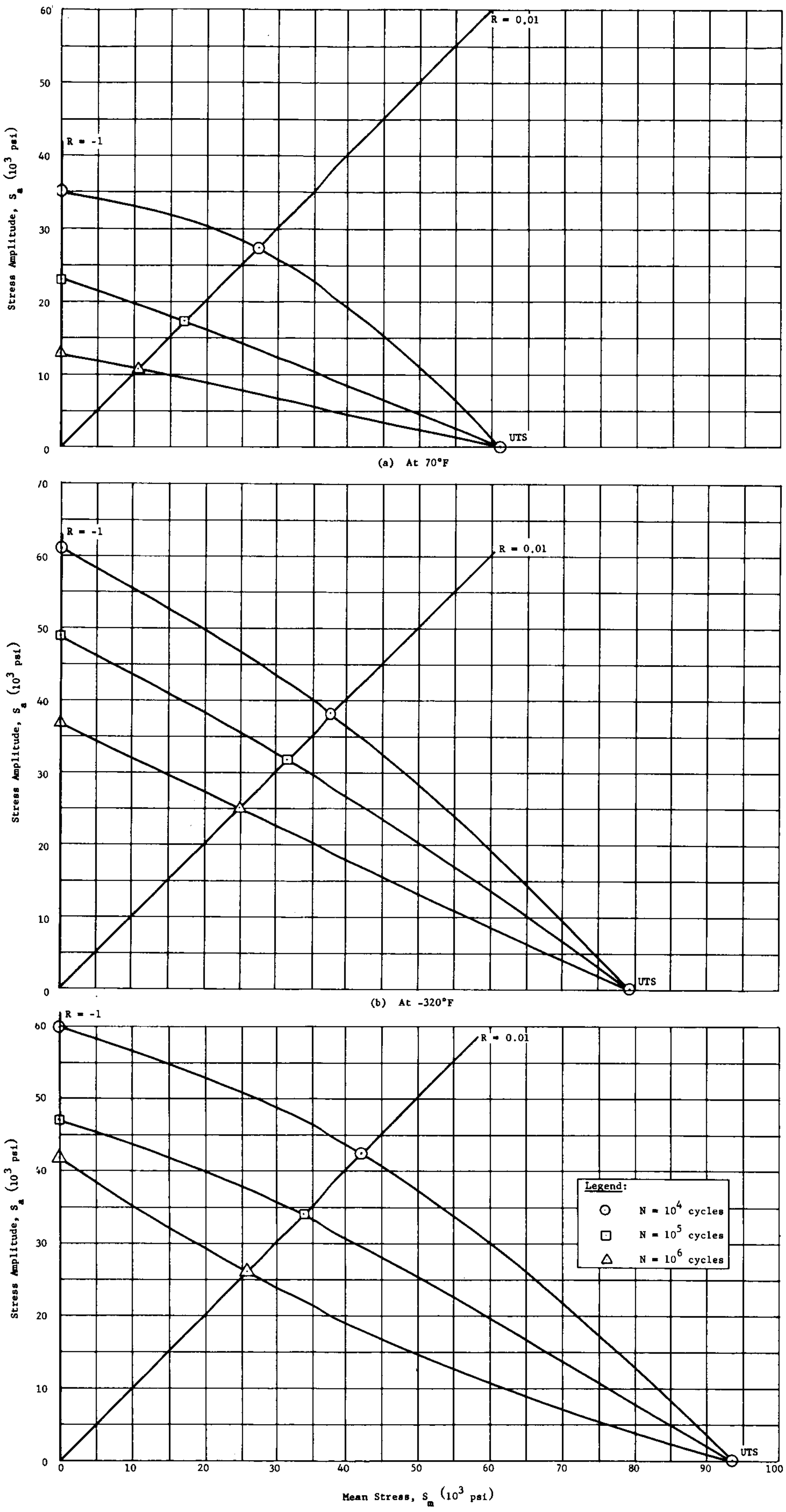

FIG. 57 MODIFIED GOODMAN DIAGRAM FOR 7106-T6 ALUMINUM ALLOY

d. 2219-T87

Unnotched specimens of 2219-T87 alloy show behavior similar to that of the 2014-T6 except that a higher fatigue strength at 70°F (10^6 cycles) is observed. The fatigue ratio is the highest obtained at room temperature for all the aluminum alloys evaluated. The increase in fatigue strength with reduction in temperature is not quite 200%, somewhat lower than the 2014-T6 value. As a result, the fatigue ratio at lower temperatures is not the best of the series. The 2014-T6 alloy, which has similar static strengthening, exhibits a higher fatigue ratio at -423°F. A decrease in fatigue ratio is indicated at -320°F; however, the magnitude of this decrease is not known because of the uncertain fatigue strength at 10^6 cycles.

The knee at -320°F is apparent, but somewhat flatter than found in the 2014-T6. The portion of the curve for fatigue life exceeding 10^5 cycles is presented as a spread band because of conflicting data points. The lower portion of the band gives a strength level lower than attained at 70°F. The upper stress level, 25,000 psi, is closer to the anticipated strength based on comparison with data for similar compositions.

The results of notch fatigue tests ($K_t = 3.5$) show behavior almost identical with the 2014-T6 alloy. The strengthening with reduction in temperature at the lower cycle portion of the curve is even less noticeable than for 2014-T6. The fatigue notch factor (K_f) increased from 2.8 to 5.0 (above the K_t value) with decreasing temperature at 10^6 cycles. At 10^3 cycles, an insignificant increase from 1.6 to 1.8 is noted.

The weld behavior is characterized by similarly flat curves showing major strengthening between -320 and -423°F. The fatigue strength at 70°F (10^6 cycles) is similar to the value for 2014-T6, but superior at -423°F. The fatigue ratio (10^6 cycles) increases from 0.20 to 0.28 as temperature is lowered.

e. 2219-T62

As anticipated, 2219-T62 exhibits slightly lower unnotched fatigue strength properties than its companion material, 2219-T87. This small decrease is approximately proportional to the lower static strength of the -T62 material. The knee observed for 2219-T87 and 2014-T6 at -320°F was not apparent in this test series conducted during the second year. Curves at all three temperatures were rather flat, and quite similar in shape. The fatigue ratio was almost identical to the 2219-T87 data. Unlike the data for the previous alloy, where the magnitude of the decrease in fatigue ratio was uncertain, this series shows a decrease of approximately 10% at -320°F.

Notch fatigue tests $(K_t = 3.5)$ showed strengthening with reduction in temperature at 10^3 cycles. The curves converged rapidly and showed little temperature dependency of strength from 10^4 through 10^6 cycles. The notch factor (K_f) at 10^6 cycles increases from 2.4 to 4.1 (slightly above the K_t value) with decreasing temperature.

The behavior of welded specimens agreed extremely well with that observed for the 2219-T87 specimens. Strengths at 10^6 cycles for each temperature agreed within 2 ksi. The shapes of the corresponding curves were very similar. This behavior is expected, since the static weld behavior of as-welded 2219 is essentially independent of temper. The 10^6 cycle strength values of -T62 and -T87 at -423°F were the highest attained in the aluminum weld studies.

f. 5456-H343

The behavior of unnotched 5456-H343 is characterized by the -320°F knee observed during the first year's testing. The strength values at 10^6 cycles for all temperatures are similar to those obtained for 2014-T6. The fatigue ratio increases from 0.28 at 70°F to 0.53 at -423°F. The -423°F value is the highest attained in the testing of unnotched aluminum alloys. Although the -423°F fatigue strength is similar to that found for 2014-T6, the static strength is significantly lower; hence, the superior fatigue ratio.

Notch fatigue test results for the mild notch $(K_t = 3.5)$ showed rather good retention of properties at 70°F as evidenced by a low K_f value. At -320°F, the K_f values were quite high, even for the short cycle tests. The loss of notch properties at -320°F was worse than that observed at -423°F. No reason for this anomalous behavior is apparent.

Testing of welded material showed similarly shaped flat curves for all temperatures. Strengthening at 10^6 cycles was greater between -320 and -423°F than from 70 to -320°F. The fatigue ratio was constant at 0.22 for both 70 and -320°F and then increased to 0.42 at -423°F for all aluminum alloys evaluated.

g. 7075-T6

Unnotched fatigue behavior of this composition was characterized by similarly shaped, steep curves. The strengths at 10^6 cycles were among the lowest obtained. The fatigue ratios at 70 and -320°F were the lowest found in this study. At -423°F, the fatigue ratio (0.40) corresponded to the value obtained for the tougher 2000 series alloys. However, a study of the static tensile results shows a flattening of the tensile strength between -320 and -423°F that suggests the onset of brittle behavior. Therefore, with little static property strengthening, the fatigue ratio can be deceivingly good.

Notch fatigue tests with a K_t of 3.5 showed good retention of strength at 70°F, as evidenced by low K_f values. However, at -320 and -423°F, the K_f values were at or above the level of the theoretical stress concentration factor, suggesting severe loss of notch toughness.

h. 2020-T6

The unnotched 2020-T6 alloy showed strength values comparable to the 5456 composition. However, because of the much higher static tensile properties, 2020-T6 exhibits relatively high fatigue ratio values. The knee at -320°F is typical of other aluminum alloys tested during the first year.

i. Comparison of Results

A summary of unnotched test results is presented in Table 5. This table presents the fatigue strength and fatigue ratio at 10^6 cycles for each material in the parent metal and welded condition. A bar graph presentation of the data is given in Fig. 58.

The data for the unnotched parent metal tests show that the two 2219 compositions and 7039-T6 exhibit the highest fatigue ratio at room temperature. At -423°F, the 2014-T6 and 5456-H343 are superior. The 7039-T6 and 7106-T6 exhibit fatigue ratios of slightly lower level while the 2219, 7075, and 2020 compositions have the lowest ratios at -423°F.

The data for welded alloys show that the 2219-T62 exhibits the highest 70°F fatigue ratio. At -423°F, both 2219-T62 and 5456-H343 exhibit the best behavior.

The notch data are summarized in Table 6 and Fig. 59. Several interesting trends are apparent from these results. According to fatigue theory and most experimental data, the elastic stress concentration factor (K_t) for structural materials exceeds the fatigue notch factor (K_f). When $K_t = K_f$, the material is as brittle as theoretically possible. A review of the room temperature data shows that K_f is always lower than K_t. With reduction in temperature, the K_f value for a given number of cycles increases. In several cases, particularly at -423°F, the K_f value is equal to or in excess of the K_t. This suggests that notch fatigue specimens become more brittle with reduction in temperature, which agrees with our understanding of cryogenic mechanical property behavior.

The anomalous behavior of K_f exceeding K_t is difficult to explain. Two possibilities exist for the explanation of this phenomenon. The first is that the theory does not apply for extremely low temperatures. The second is that the test method is not completely adequate to study the specific problem.

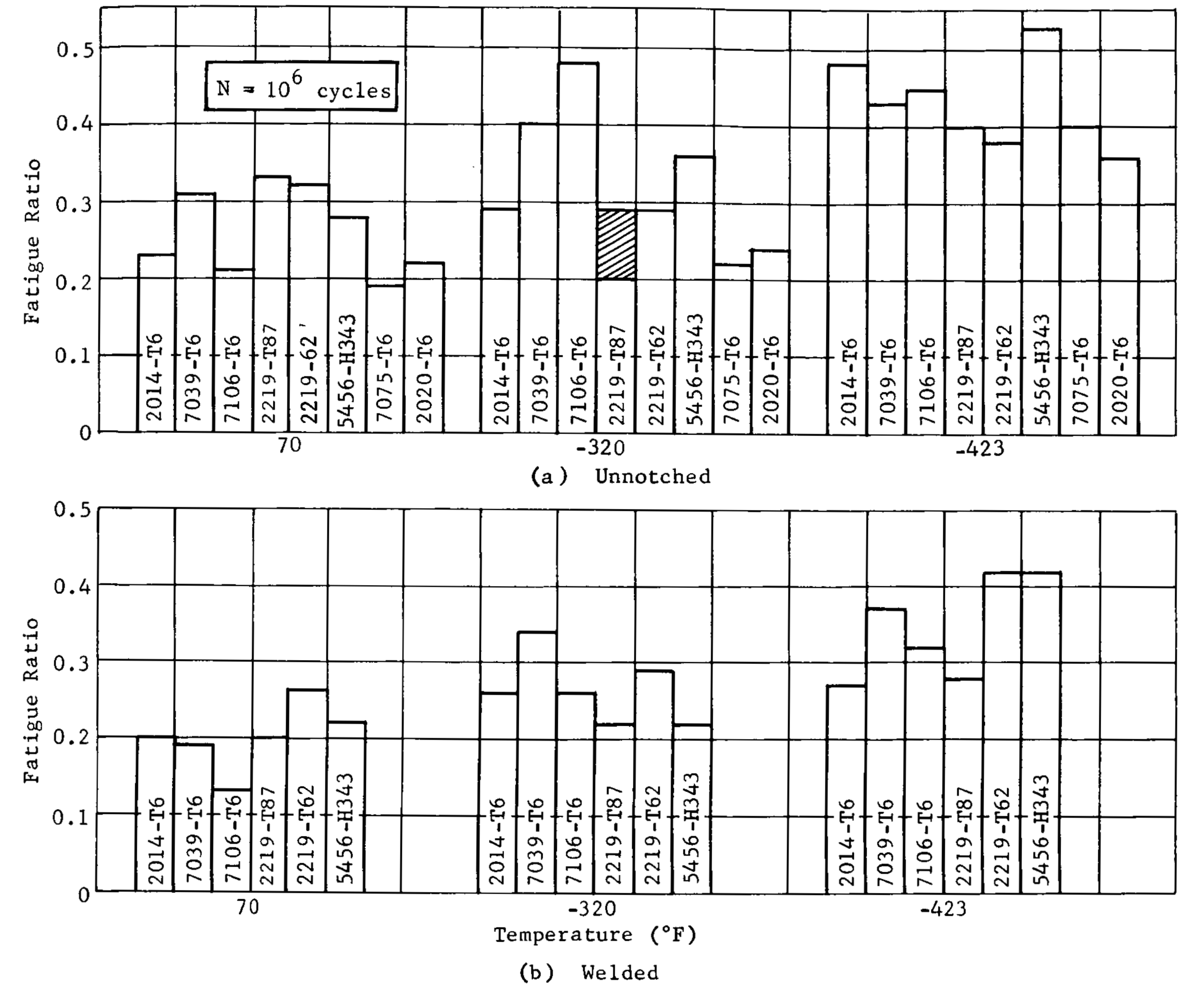

Fig. 58 Comparison of Fatigue Ratios for Aluminum Alloys

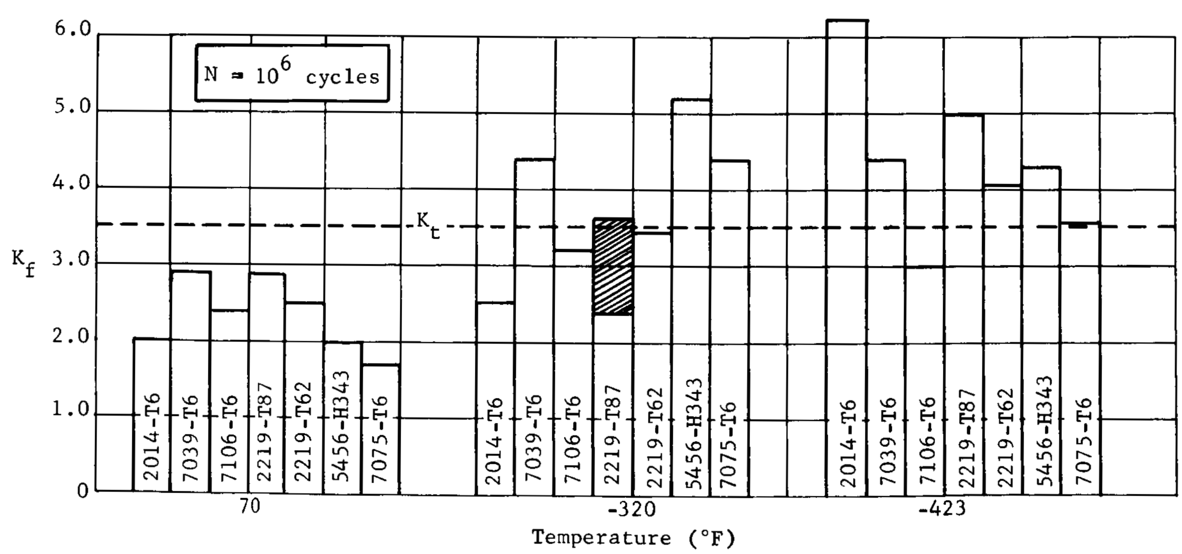

Fig. 59 Comparison of Fatigue Notch Factors for Aluminum Alloys

Table 5 Comparison of Unnotched Fatigue Properties for Aluminum Alloys*

Material	Temperature (°F)	R	Parent Metal		Welded	
			Stress (ksi)	Fatigue Ratio†	Stress (ksi)	Fatigue Ratio†
2014-T6	70	-1.0	17	0.24	11	0.20
	-320		25	0.29	17	0.26
	-423		47	0.48	19	0.27
	70	0.01	31	0.44	--	--
	-320		47	0.55	--	--
	-423		63	0.65	--	--
7039-T6	70	-1.0	20	0.31	9	0.19
	-320		31	0.40	18	0.34
	-423		40	0.43	22	0.37
	70	0.01	33	0.51	--	--
	-320		48	0.61	--	--
	-423		64	0.67	--	--
7106-T6	70	-1.0	13	0.21	8	0.15
	-320		37	0.47	21	0.34
	-423		42	0.45	20	0.34
	70	0.01	21	0.34	--	--
	-320		50	0.63	--	--
	-423		52	0.56	--	--
2219-T87	70	-1.0	22	0.33	10	0.20
	-320		17 to 25	0.22 to 0.29	14	0.22
	-423		40	0.40	24	0.28
2219-T62	70	-1.0	19	0.32	12	0.26
	-320		22	0.29	16	0.29
	-423		37	0.38	26	0.42
5456-H343	70	-1.0	16	0.28	11	0.22
	-320		26	0.36	13	0.22
	-423		43	0.53	23	0.42
7075-T6	70	-1.0	15	0.19	--	--
	-320		22	0.22	--	--
	-423		40	0.40	--	--
2020-T6	70	-1.0	18	0.22	--	--
	-320		23	0.24	--	--
	-423		41	0.36	--	--

*$N = 10^6$ cycles.

†Fatigue ratio $= \frac{S_N \text{ (fatigue strength at N cycles)}}{S_u \text{ (static tensile strength)}}$.

Table 6 Comparison of Notched Fatigue Properties for Aluminum Alloys

Material	Temperature (°F)	K_t^*	Fatigue Strength (ksi)			$K_f^\dagger$		
			10^4	10^5	10^6	10^4	10^5	10^6
2014-T6	70	3.5	22.0	12.5	8.5	2.2	2.3	2.0
	-320		22.0	11.5	10.0	2.6	3.5	2.5
	-423		27.0	15.0	7.5	2.4	3.7	5.9
	70	8.0	20.5	12.5	6.0	1.6	1.6	2.7
	-320		22.5	14.0	8.0	2.6	2.9	3.1
	-423		22.5	12.5	7.0	2.9	4.4	6.7
7039-T6	70	3.5	17.0	9.0	7.0	2.3	2.9	2.9
	-320		23.0	11.0	7.0	2.5	3.7	4.4
	-423		21.0	12.5	9.0	2.9	3.6	4.4
	70	8.0	21.0	10.5	5.5	1.9	2.5	3.6
	-320		25.0	15.2	10.7	2.3	2.7	2.9
	-423		26.6	18.0	11.5	2.3	2.5	3.5
7106-T6	70	3.5	21.0	10.0	5.5	1.7	2.3	2.4
	-320		26.0	15.0	11.5	2.4	3.3	3.2
	-423		27.0	17.5	14.0	2.3	2.7	3.0
2219-T87	70	3.5	20.0	11.0	7.5	2.1	2.7	2.9
	-320		20.0	11.0	7.0	2.2	3.0	2.4 to 3.6
	-423		20.5	14.5	8.0	2.5	3.6	5.0
2219-T62	70	3.5	21.5	13.0	7.5	1.5	1.8	2.5
	-320		30.5	10.0	6.5	1.3	2.4	3.4
	-423		21.0	13.0	9.0	2.6	2.4	4.1
5456-H343	70	3.5	18.5	11.0	8.0	1.9	2.3	2.0
	-320		13.0	8.0	5.0	3.8	4.1	5.2
	-423		19.0	14.5	10.0	2.8	3.1	4.3
7075-T6	70		22.0	13.5	9.0	2.09	1.73	1.70
	-320	3.5	17.0	9.5	5.0	3.32	4.04	4.46
	-423		19.6	12.8	10.6	3.68	4.31	3.60

$^*K_t$ = stress concentration factor.

† Fatigue notch factor (K_f) =

$$\frac{\text{(fatigue strength of unnotched specimens at N cycles)}}{\text{(fatigue strength of notched specimens at N cycles)}}.$$

Most fatigue testing is performed under more ideal conditions of specimen preparation and alignment. The polished round bar specimen would be expected to give somewhat more consistency than the sheet gage specimen because of the ability to machine more accurate notches. Although great pains are taken to insure freedom from eccentricity, the axial loading of sheet material will inherently be less precise in alignment than the fully reversed bending method or axial loading of round bars. Therefore, with increased brittleness at low temperatures, statistical variations in test results would explain the cases where K_f exceeds K_t.

In an attempt to resolve the question of whether our method was sufficiently accurate, six room temperature tests were conducted in the cryostat to determine whether test results obtained in the more complicated cryostat arrangement would reproduce data obtained during the test program at room temperature using simple grips. Results showed that the data points fell within this scatter band of prior data. Therefore, it appears that the cryostat does not give results of lower quality than those obtained in the conventional manner using the selected sheet gage specimen. Without additional research, it is impossible to determine whether K_f exceeding K_t has a rational theoretical basis. A simple series of experiments could be performed to shed more light on the subject. This would consist of modifying the specimen grip to accommodate polished round bar specimens. Evaluation of several alloys in the 10^6 cycle range and 70 and -420°F should show whether inadequacies in the test method were the cause of the anomalous behavior.

It was also noted that K_f shows a general increase with number of cycles. This suggests that the high-stress, short-time tests cannot be used to predict long-time behavior in the presence of stress raisers.

Another observation was that the sharper notch $(K_t = 8.0)$ did not cause any significant loss of toughness above that caused by the milder notch $(K_t = 3.5)$. As a result, K_f was significantly lower than K_t for the two alloys evaluated with both notch acuities.

j. Fractured Specimens

Testing under axial loads and fully reversed stressing does not leave much of a surface to study after fracture. The rapid pounding of the mating surfaces immediately after fracture destroys a great deal of the surface evidence. However, some observations have been made.

The 5456-H343, 7075-T6, 7039-T6, and 7106-T6 unnotched parent metal fatigue specimens tested at cryogenic temperatures appeared laminated, in addition to the characteristic smooth fatigue surface. This appearance was also noted in the 5456-H343 and 7106-T6 room temperature specimens. The laminations probably open up after failure as a result of the hammering action. This behavior is typical for the strain hardened 5456 alloy even in static tension failure, but is not observed for the 7000 series alloys in tension.

The other parent metal aluminum alloys exhibited the flat, smooth, conchoidal appearance typical of fatigue failures.

Weld fractures initiated at the edge of the weld bead. Notch specimens appeared similar to the unnotched parent metal specimens.

k. Results of Other Studies

Extensive room temperature tests of two alloys evaluated in this program, 2014-T6 and 7075-T6, have been performed throughout the past years. These results, summarized in Ref 7, show a higher stress for failure at 10^6 cycles than reported in this work. The strengths reported for these alloys, 25,000 to 30,000 psi, were primarily obtained with bending techniques. However, some axial data on smooth machined round bars are also included.

Several reasons for the lower strengths obtained in this study must be considered. The endurance limit obtained by bending techniques may be as much as 30% higher than values obtained by axial loading. When round bars are machined, even for axial tests, the surface of the material is removed and defects are removed by polishing. In this study, the surface of the sheet was left in the as-received condition.

The literature is almost void of cryogenic data for comparison purposes. The only data for which a comparison can be made have been generated by Fontana (Ref 8) on 7075-T6 using the flexure technique on polished specimens machined from 0.750-in.-diameter bar. These data, significantly higher than obtained in this work, are compared in the following tabulation.

	Stress at 10^6 Cycles (ksi)	
Temperature (°F)	This Work (Axial Load, R = -1)	Fontana (Flexure, R = -1)
70	15	35
-110	--	38
-320	22	59
-423	41	--

B. STAINLESS STEEL AND NICKEL ALLOYS

The alloys evaluated in this program include the two types of stainless steels suitable for cryogenic service plus two nickel base alloys exhibiting outstanding cryogenic properties. The two age-hardenable alloys (A-286 and Inconel 718) were selected by NASA for evaluation in the solution-treated condition.

1. Tension Properties

The mechanical properties of annealed 321 stainless steel are given in Fig. 12. The unnotched behavior shows the characteristic rapid linear increase in ultimate strength with very little increase in yield strength as temperature is decreased. Elongation shows a small decrease with reduction in temperature, but is still quite high (36%) at -423°F. Notch and weld strengths increase from 70 to -320°F, but decrease somewhat from -320 to -423°F.

The behavior of solution-treated A-286 stainless steel is given in Fig. 13. Ultimate strength increases from 90,000 psi at room temperature to 168,000 psi at -423°F. Yield strength is low (46,000 psi at 70°F). Elongation is high and increases with decrease in temperature. Good weld joint efficiency and notch toughness are shown by the test results.

The properties of solution-treated Inconel 718 are presented in Fig. 14. Ultimate, notch, and weld strength curves are almost identical. Yield strength is low. Elongation is high at 70°F and increases with decreasing temperature.

The behavior of Hastelloy C (Fig. 15) is similar to that of Inconel 718.

2. Fatigue Properties

Fatigue data for the stainless steel and nickel alloys are presented in the figures and tables given in the following tabulation.

Material	Unnotched		Notched		Welded	
	Figure	Table	Figure	Table	Figure	Table
321 Stainless Steel	42	B-27	43	B-28	44	B-29
A-286 Stainless Steel	45	B-30	46	B-31	47	B-32
Inconel 718 Nickel Alloy	48	B-33	49	B-34	50	B-35
Hastelloy C Nickel Alloy	51	B-36	52	B-37	53	B-38

a. 321 Stainless Steel

The unnotched fatigue data for 321 stainless steel show a flat curve at 70°F. Curves obtained at both -320 and -423°F are moderately steep. The fatigue ratio (10^6 cycles) at 70°F is 0.37. This value decreases to 0.21 and 0.23 at -320 and -423°F, respectively. Unlike the aluminum alloys, which show an improvement in fatigue performance at low temperatures as evidenced by an increase in the fatigue ratio, the 321 shows a substantial decrease. However, the absolute strength of the stainless steel increases with reduction in temperature and exceeds the properties obtained in the aluminum alloy study.

Notched test results show a flat curve at 70°F and steeper curves at -320 and -423°F. The 10^6 cycle stress level increases from 18 ksi at 70 to 24 and 27 ksi at -320 and -423°F, respectively. The fatigue notch factor (K_f) is exceptionally good. The value for all temperatures varied from 1.8 to 2.0.

The behavior of welded joints was similar to that observed for the unnotched parent metal. Although weld joint efficiency is high in 321 stainless steel, the welded fatigue specimens attain only approximately two-thirds of the unwelded fatigue strength. The fatigue ratio values are 0.23, 0.15, and 0.24 at 70, -320, and -423°F, respectively.

b. A-286 Stainless Steel

Unnotched fatigue data for A-286 stainless steel showed that curves become flatter with decreasing temperature. At 10^6 cycles, fatigue strength increased significantly with reduction in temperature. The fatigue ratio at 10^6 cycles increased slightly from 0.37 at 70°F to 0.41 at -423°F.

Notch tests performed on mildly notched specimens $(K_t = 3.5)$ showed a transition from flat to steep curves with temperature reduction. At 70°F, the K_f values, 1.4 to 1.7, show good retention of notch fatigue strength. Decrease in temperature resulted in an increasing loss of notch strength. For 10^6 cycles at -423°F, K_f (4.0) slightly exceeded the K_t value.

Evaluation of welded specimens showed knee-shaped curves of increasing steepness with decrease in temperature. The fatigue ratio at 10^6 cycles decreased from 0.19 at 70°F to 0.15 at -320°F. At -423°F, the fatigue ratio increased to 0.21.

c. Inconel 718 Nickel Alloy

The unnotched fatigue curves for Inconel 718 were rather flat at 70 and -423°F. Test results at -320°F show a knee-shaped curve. The fatigue ratio was high (0.45 to 0.53).

The behavior of mildly notched specimens $\left(K_t = 3.5\right)$ was characterized by linear curves of increasing slope with decrease in temperature. The K_f value at 70°F was low (1.2 to 1.8). Although K_f increased with decreasing temperature, the highest value was only 3.0.

Welded Inconel 718 alloy showed linear curves of increasing slope with decrease in temperature. The fatigue ratio (0.28 to 0.31) was independent of temperature.

d. Hastelloy C Nickel Alloy

The behavior of unnotched Hastelloy C is characterized by flat curves at all temperatures. Strengthening increased significantly with each decrement of decreasing temperature. The fatigue ratios $\left(10^6 \text{ cycles}\right)$ were high (0.41 to 0.45) and essentially independent of temperature.

Notched fatigue tests performed at a K_t of 3.5 resulted in steep curves at all temperatures. The fatigue notch factor, K_f, was low at 70°F. K_f increased with decreasing temperature; at -423°F $\left(10^6\right)$, K_f exceeded K_t. As noted frequently, K_f increased with the number of cycles.

Welded specimens showed a linear decrease of strength with number of cycles at 70°F. At -320 and -423°F, the curves become steep. The fatigue ratio (0.31 to 0.36) varied little with temperature change.

e. Comparison of Results

A summary of unnotched test results is presented in Table 7. This table presents the fatigue strength and fatigue ratio at 10^6 cycles for each material in the parent metal and welded condition. Data are presented in bar graph form in Fig. 60.

The data for the unnotched parent metal show the Inconel 718 exhibits the highest fatigue ratio at all temperatures. Hastelloy C showed a slightly lower value at each temperature.

Welded alloy data showed the Hastelloy C exhibits the highest fatigue ratio at each temperature. Inconel 718 showed fatigue ratio values approximately 10% lower.

The notch data are summarized in Table 8 and Fig. 61. At 70°F, all compositions show good notch properties. A-286, 321, and Inconel 718 exhibit similar K_f values in the range 1.6 to 1.8. Hastelloy C shows a higher K_f (2.6). Data obtained at -320°F show behavior patterns very similar to those observed at 70°F, except for a small increase in K_f. At -423°F, 321 stainless steel shows virtually no increase in K_f value. A-286 and Hastelloy C alloys have K_f values that are in excess of the stress concentration factor (K_t). The general trend of an increase in K_f with number of cycles is also noted for the stainless steel and nickel alloys.

Table 7 Comparison of Unnotched Fatigue Properties for Stainless Steel and Nickel Alloys*

Material	Temperature (°F)	Parent Metal		Welded	
		Stress (ksi)	Fatigue Ratio†	Stress (ksi)	Fatigue Ratio†
321 SS	70 -320 -423	32 44 54	0.37 0.21 0.23	20 30 31	0.23 0.15 0.24
A-286	70 -320 -423	36 57 69	0.37 0.40 0.41	17 20 32	0.19 0.15 0.21
Inconel 718	70 -320 -423	62 70 99	0.50 0.45 0.53	33 51 55	0.28 0.32 0.31
Hastelloy C	70 -320 -423	49 77 91	0.41 0.44 0.45	37 54 62	0.31 0.36 0.35

*$N = 10^6$ cycles.

†Fatigue ratio = $\frac{S_N \text{(fatigue strength at n cycles)}}{S_u \text{(static tensile strength)}}$.

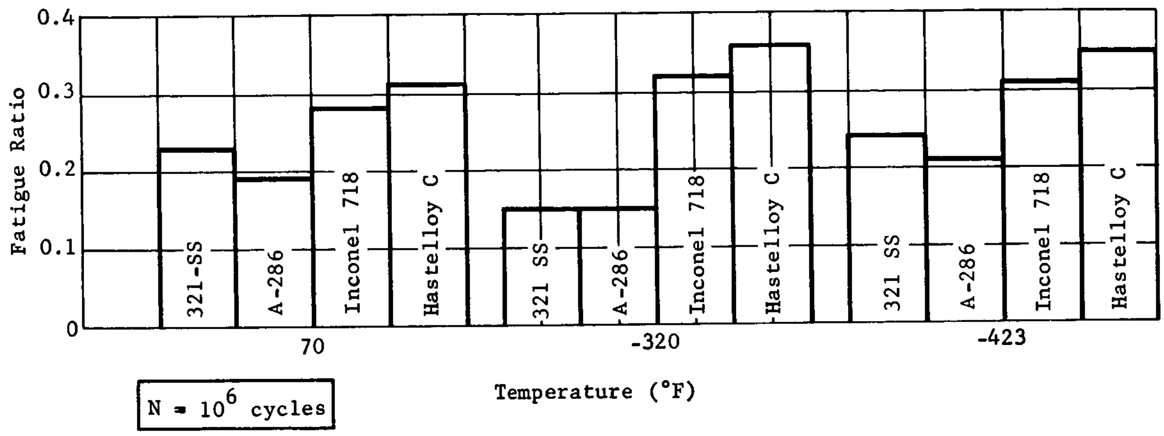

(a) Welded

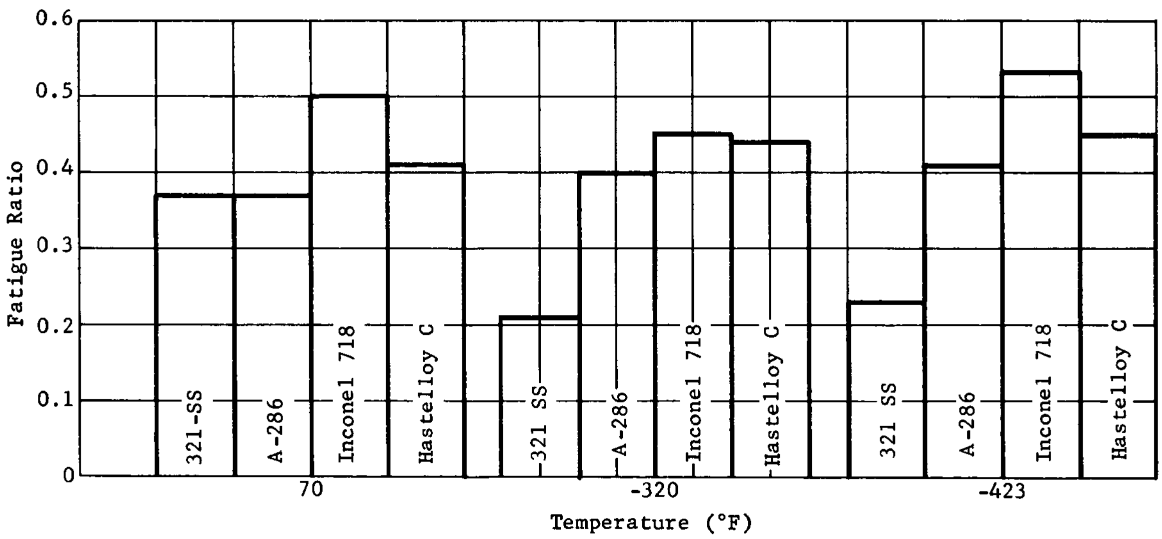

(b) Unnotched

Fig. 60 Comparison of Fatigue Ratios for Stainless Steel and Nickel Alloys

Table 8 Comparison of Notched Fatigue Properties for Stainless Steel and Nickel Alloys

Material	Temperature (°F)	K_t*	Fatigue Strength (ksi)			K_f†		
			10^4	10^5	10^6	10^4	10^5	10^6
321 SS	70	3.5	34.0	25.5	18.0	1.1	1.3	1.8
	-320		54.0	32.0	22.3	---	1.9	2.0
	-423		59.5	38.0	26.3	1.8	2.1	2.1
A-286	70	3.5	35.0	25.0	21.0	1.4	1.7	1.7
	-320		62.5	30.0	26.0	1.4	2.6	2.2
	-423		66.0	33.0	14.0	1.2	2.4	4.9
Inconel 718	70	3.5	65.0	45.0	35.0	1.1	1.6	1.8
	-320		73.5	49.0	35.0	1.3	1.9	2.0
	-423		81.0	45.5	32.5	1.4	2.3	3.1
Hastelloy C	70	3.5	54.0	32.7	19.5	1.3	1.8	2.5
	-320		61.0	40.7	24.0	1.5	2.1	3.2
	-423		69.5	39.0	17.2	1.5	2.5	5.3

*K_t = Stress concentration factor.

†Fatigue notch factor (K_f) =

$$\frac{\text{(fatigue strength of unnotched specimens at N cycles)}}{\text{(fatigue strength of notched specimens at N cycles)}}.$$

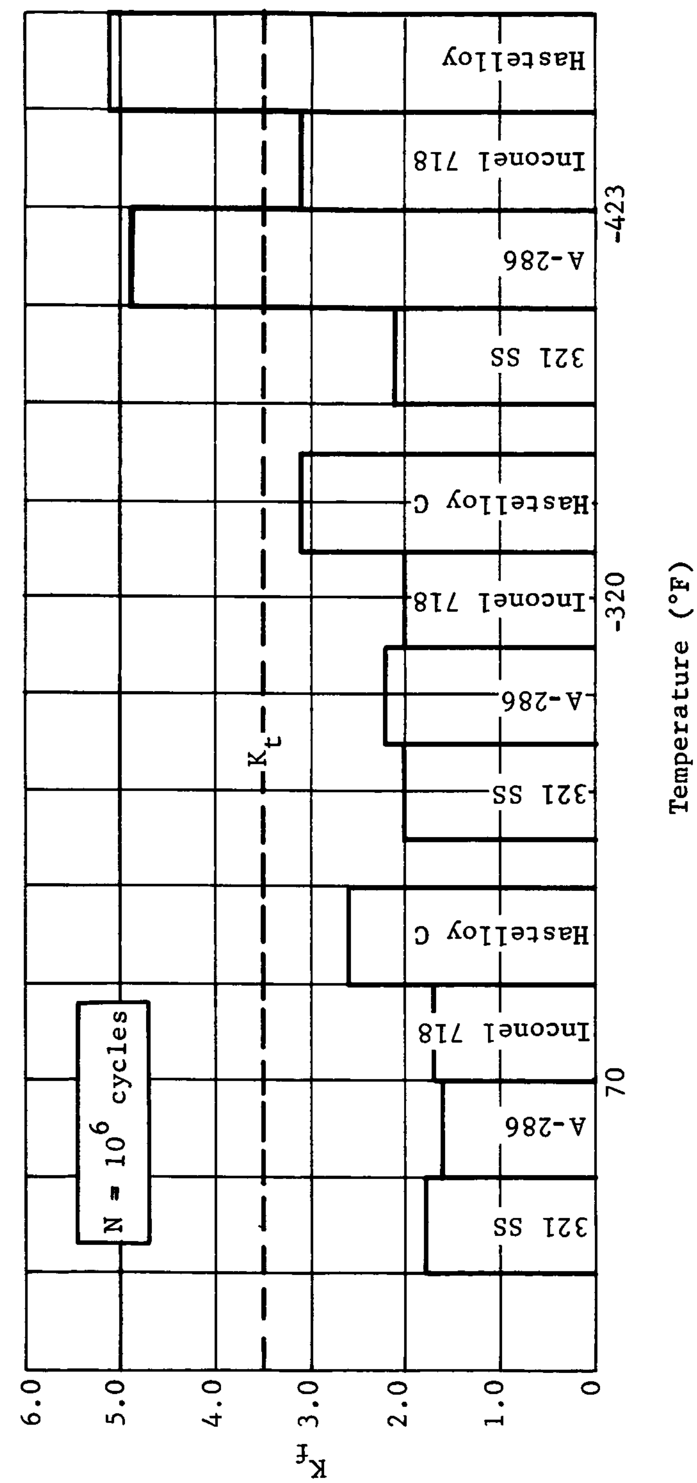

Fig. 61 Comparison of Fatigue Notch Factors for Stainless Steel and Nickel Alloys

VII. CONCLUSIONS

This program has demonstrated that tension/compression fatigue properties can be obtained under axial loading for flat sheet materials at temperatures down to -423°F. Data obtained for the aluminum alloys show:

1) Unnotched 2219 and 7039-T6 exhibit good properties at 70°F;

2) Unnotched 2014-T6 and 5456-H343 were superior at -423°F;

3) Fatigue ratio increases with decrease in temperature for unnotched and welded specimens;

4) Introduction of a mild notch reduces fatigue strength significantly. However, at room temperature, reduction in fatigue strength was less than the theoretical maximum;

5) At cryogenic temperatures, the reduction in fatigue strength decreased significantly; the apparent reduction factor (K_f), in some cases equalled or exceeded the theoretical maximum (K_t);

6) In general, the fatigue notch factor (K_f) increased with number of cycles (N);

7) Notched 2014-T6, 7075-T6, and 5456-H343 showed the best 70°F notched fatigue behavior;

8) The best retention of notch fatigue properties at -423°F was shown by 7106-T6 and 7039-T6;

9) Welded joints decrease fatigue properties. This decrease is greater than the decrease of strength in static weld behavior compared to parent metal, but not as great as when a machined notch is introduced;

10) The 2219-T62 alloy showed the highest welded fatigue ratio at 70 and -423°F. The 5456-H343 was comparable to the 2219-T62 at -423°F.

Test results for the stainless steel and nickel alloys show:

1) The highest unnotched fatigue ratios are exhibited by Inconel 718 and Hastelloy C for the parent metal and welded conditions;

2) The 321 stainless steel shows outstanding notch toughness under cyclic loading at all temperatures;

3) K_f increases with decreasing temperature and increasing number of cycles.

The following materials appear to be satisfactory for cyclic service at cryogenic temperatures.

<u>Aluminum Alloys</u>

2014-T6

2219-T87

2219-T62

7039-T6

7106-T6

5456-H343

<u>Stainless Steel Alloys</u>

321

A-286

<u>Nickel Alloys</u>

Inconel 718

Hastelloy C

Aluminum alloys 2020-T6 and 7075-T6 appear to be somewhat questionable for service at -423°F because of their behavior under static testing.

REFERENCES

1. R. D. Keys: "A Multiple Tensile Specimen Test Device for Use in Liquid Hydrogen." Advances in Cryogenic Engineering, Vol 7, Plenum Press, New York, New York, 1962.

2. R. E. Peterson: Stress Concentration Design Factors, John Wiley and Sons, Inc, New York, New York, 1962.

3. F. R. Schwartzberg, T. F. Kiefer, and R. D. Keys: Determination of Low-Temperature Fatigue Properties of Structural Metal Alloys. Martin-CR-64-74. Martin Company, Denver, Colorado, October 1964.

4. F. R. Schwartzberg and R. D. Keys: "Axial Fatigue Testing of Sheet Materials Down to -423°F." Materials Research and Standards, Vol 4, No. 5, New York, New York, 1964.

APPENDIX A

TENSILE DATA

Table A-1 Tensile Properties of 2014-T6 Aluminum Alloy at Cryogenic Temperatures

Temperature (°F)	Ultimate Strength (ksi)	Yield Strength, 0.2% Offset (ksi)	Elongation in 2 in. (%)	Modulus of Elasticity (psi x 10^6)	Weld Strength (ksi)	Notch Strength* (ksi)	Notch Strength Ratio
70	71.8 70.4 70.9 71.0 avg	67.3 66.3 65.9 66.5 avg	10.5 10.0 9.5 10.0 avg	10.6	55.1 55.3 59.0 56.5 avg	77.0 77.7 77.8 77.5 avg	1.09
-320	85.3 84.9 85.9 85.4 avg	76.4 75.8 75.8 76.0 avg	11.5 12.0 12.0 11.8 avg	11.7	66.2 64.6 67.0 65.9 avg	91.2 91.2 90.4 90.9 avg	1.06
-423	100.0 99.0 96.3 98.4 avg	83.0 82.8 80.7 82.2 avg	14.0 13.5 13.5 13.7 avg	12.3	74.3 72.2 69.5 68.5 71.2 70.5 71.1 avg	102.0 102.5 101.0 101.9 avg	1.04

$^*K_t = 3.5.$

Table A-2 Tensile Properties of 7039-T6 Aluminum Alloy at Cryogenic Temperatures

Temperature (°F)	Ultimate Strength (ksi)	Yield Strength 0.2% Offset (ksi)	Elongation in 2 in. (%)	Modulus of Elasticity (psi x 10^6)	Weld Strength (ksi)	Notch Strength* (ksi)	Notch Strength Ratio
70	64.4	55.8	12.0		47.9	69.9	1.09
	64.5	58.4	12.5		45.2	70.0	
	63.4	58.7	13.0		46.6	69.6	
	64.0	58.6	12.5		46.8		
	64.5	59.0	12.0		49.5		
	64.0	58.2	12.5	10.0	44.5		
	64.1 avg	58.1 avg	12.4 avg		46.8 avg	69.8 avg	
-320	79.2	67.9	18.0		50.3	86.9	1.10
	79.9	68.2	20.0		48.0	87.3	
	80.0	68.5	19.0		56.7	87.3	
	77.7	64.7	18.5		55.8		
	78.0	64.7	20.0		57.3		
	79.0	67.5	19.5	11.6	53.6		
	78.9 avg	66.9 avg	19.1 avg		52.8 avg	87.2 avg	
-423	95.4	74.3	23.0		54.2	94.0	0.98
	95.3	74.0	25.1		56.3	93.6	
	95.1	73.1	23.5		51.1	93.0	
	94.5	74.7	23.0		54.2		
	97.4	73.7	24.0		55.0		
	94.7	74.0	23.5	11.9	51.9		
	95.4 avg	74.0 avg	23.7 avg		53.8 avg	93.5 avg	

*K_t = 3.5.

Table A-3 Tensile Properties of 7106-T6 Aluminum Alloy at Cryogenic Temperatures

Temperature (°F)	Ultimate Strength (ksi)	Yield Strength 0.2% Offset (ksi)	Elongation in 2 in. (%)	Modulus of Elasticity (psi x 10^6)	Weld Strength (ksi)	Notch Strength* (ksi)	Notch Strength Ratio
70	61.3 61.0 60.8 61.0 avg	55.7 55.4 55.3 55.5 avg	15.0 14.0 14.5 14.5 avg	10.1	54.2 53.4 53.9 53.8 avg	66.9 66.8 66.3 66.7 avg	1.09
-320	79.7 78.8 79.5 79.3 avg	66.2 67.3 67.2 66.9 avg	19.5 20.5 20.0 20.0 avg	11.0	59.3 64.1 61.1 61.5 avg	83.6 84.9 84.1 84.2 avg	1.06
-423	93.7 93.3 93.2 93.4 avg	70.4 71.7 71.3 71.1 avg	25.0 24.0 25.0 24.7 avg	11.1	58.4 58.1 59.1 58.5 avg	91.4 92.0 91.6 91.7 avg	0.98

*$K_t = 3.5$.

Table A-4 Tensile Properties of 2219-T87 Aluminum Alloy at Cryogenic Temperatures

Temperature (°F)	Ultimate Strength (ksi)	Yield Strength 0.2% Offset (ksi)	Elongation in 2 in. (%)	Modulus of Elasticity (psi x 10^6)	Weld Strength (ksi)	Notch Strength* (ksi)	Notch Strength Ratio
70	66.6 66.9 66.5 66.7 avg	55.2 55.7 55.2 55.4 avg	11.0 11.0 10.5 10.8 avg	10.5	45.2 50.4 50.6 48.7 avg	69.5 69.1 69.1 69.2 avg	1.04
-320	85.4 85.0 85.0 85.1 avg	65.3 66.0 66.0 65.8 avg	12.5 13.0 12.5 12.7 avg	11.6	63.2 61.0 63.0 62.4 avg	87.2 85.6 86.6 86.5 avg	1.02
-423	100.4 101.0 96.1 99.2 avg	71.0 70.6 68.5 70.0 avg	15.0 15.0 13.5 14.5 avg	12.5	72.2 65.9 70.0 65.5 68.7 64.2 67.7 avg	98.4 99.2 94.2 97.3 avg	0.98

*K_t = 3.5.

Table A-5 Tensile Properties of 2219-T62 Aluminum Alloy at Cryogenic Temperatures

Temperature (°F)	Ultimate Strength (ksi)	Yield Strength 0.2% Offset (ksi)	Elongation in 2 in. (%)	Modulus of Elasticity (psi x 10^6)	Weld Strength (ksi)	Notch Strength* (ksi)	Notch Strength Ratio
70	59.0 58.8 59.0 58.9 avg	41.5 41.2 42.2 41.6 avg	11.0 11.5 11.0 11.2 avg	10.2	45.0 45.7 46.7 45.8 avg	63.6 62.6 63.7 63.3 avg	1.07
-320	76.6 79.9 76.9 77.7 avg	51.9 59.3 54.6 55.3 avg	14.5 13.0 13.5 13.7 avg	11.1	54.7 53.4 53.5 53.9 avg	81.0 75.9 77.8 78.2 avg	1.01
-423	96.0 96.0 96.0 96.0 avg	56.7 55.6 56.1 56.2 avg	28.0 29.0 27.5 28.2 avg	11.7	63.6 61.0 64.1 62.9 avg	90.8 91.4 ____ 91.1 avg	0.95

*K_t = 3.5.

Table A-6 Tensile Properties of 5456-H343 Aluminum Alloy at Cryogenic Temperatures

Temperature (°F)	Ultimate Strength (ksi)	Yield Strength 0.2% Offset (ksi)	Elongation in 2 in. (%)	Modulus of Elasticity (psi x 10^6)	Weld Strength (ksi)	Notch Strength* (ksi)	Notch Strength Ratio
70	56.4 56.8 56.5 56.6 avg	43.2 43.6 43.7 43.5 avg	9.5 9.5 9.5 9.5 avg	10.3	52.0 52.3 50.0 51.4 avg	58.3 58.7 59.3 58.8 avg	1.04
-320	72.8 70.8 73.4 72.3 avg	50.7 50.7 50.5 50.6 avg	9.5 7.0 11.0 9.2 avg	11.4	58.5 61.9 57.8 59.4 avg	71.0 71.3 70.4 70.9 avg	0.98
-423	80.4 82.6 80.8 81.3 avg	53.9 54.1 54.0 54.0 avg	8.5 11.5 9.5 9.8 avg	11.7	54.8 58.0 55.9 52.8 53.5 57.3 55.4 avg	78.8 79.4 77.6 78.6 avg	0.97

$*K_t = 3.5$.

Table A-7 Tensile Properties of 7075-T6 Aluminum Alloy at Cryogenic Temperatures

Temperature (°F)	Ultimate Strength (ksi)	Yield Strength 0.2% Offset (ksi)	Elongation in 2 in. (%)	Modulus of Elasticity (psi x 10^6)	Notch Strength* (ksi)	Notch Strength Ratio
70	78.6 79.2 78.5 78.8 avg	71.4 72.5 70.8 71.6 avg	10.5 10.5 10.5 10.5 avg	10.2	96.0 95.8 96.2 96.0 avg	1.22
-320	98.2 99.1 99.5 98.9 avg	85.3 83.7 84.6 84.5 avg	12.5 11.5 10.0 11.3 avg	11.4	94.0 100.9 94.4 96.4 avg	0.97
-423	100.2 95.5 105.9 100.5 avg	88.4 82.1 87.8 86.1 avg	11.5 2.5† 10.5 11.0 avg of 2	11.9	92.7 91.9 83.0 89.2 avg	0.89

*K_t = 3.5.

†Failed through gage mark.

Table A-8 Tensile Properties of 2020-T6 Aluminum Alloy at Cryogenic Temperatures

Temperature (°F)	Ultimate Strength (ksi)	Yield Strength 0.2% Offset (ksi)	Elongation in 2 in. (%)	Modulus of Elasticity (psi x 10^6)
70	82.7 82.3 82.7 82.6 avg	78.9 77.7 79.1 78.6 avg	8.0 8.0 8.0 8.0 avg	11.1
-320	97.5 97.1 98.0 97.5 avg	87.0 87.2 87.6 87.3 avg	7.0 7.0 7.5 7.2 avg	12.3
-423	110.3 110.0 128.0 116.1 avg	94.8 94.6 100.9 96.8 avg	10.0 10.0 12.5 10.8 avg	13.6

Table A-9 Tensile Properties of 321 Stainless Steel Alloy at Cryogenic Temperatures

Temperature (°F)	Ultimate Strength (ksi)	Yield Strength 0.2% Offset (ksi)	Elongation in 2 in. (%)	Modulus of Elasticity (psi x 10^6)	Weld Strength (ksi)	Notch Strength* (ksi)	Notch Strength Ratio
70	85.5 86.6 86.3 86.1 avg	37.4 38.4 38.3 38.0 avg	53.0 55.0 58.0 55.3 avg	26.0	86.8 86.8 86.6 86.7 avg	90.1 90.2 90.8 90.4 avg	1.05
-320	205.3 206.4 206.1 205.9 avg	44.8 45.2 43.0 44.3 avg	46.5 47.5 46.0 46.7 avg	29.5	208.0 208.8 198.3 205.0 avg	225.4 217.1 219.3 220.6 avg	1.07
-423	253.8 235.2 --‡ 244.5 avg	52.5 --† 52.8 52.6 avg	44.0 29.0 --‡ 36.0 avg	30.7	115.0 118.7 155.0 129.6 avg	212.1 153.4 180.9 182.1 avg	0.77

*K_t = 3.5.

†Strain gage failed.

‡Failed in bearing.

Table A-10 Tensile Properties of A-286 Stainless Steel Alloys at Cryogenic Temperatures

Temperature (°F)	Ultimate Strength (ksi)	Yield Strength 0.2% Offset (ksi)	Elongation in 2 in. (%)	Modulus of Elasticity psi x 10^6	Weld Strength (ksi)	Notch Strength* (ksi)	Notch Strength Ratio
70	92.1 87.2 91.8 90.4 avg	49.8 39.4 46.7 45.7 avg	35.5 43.5 36.0 38.3 avg	28.4	87.9 87.8 88.9 88.2 avg	89.2 90.4 90.3 90.0 avg	1.00
-320	139.5 141.4 142.0 141.1 avg	69.4 73.0 76.2 73.6 avg	77.5 73.5 70.0 74.4 avg	29.3	128.8 121.2 135.8 128.6 avg	131.6 133.5 138.4 134.5 avg	0.95
-423	168.8 168.3 167.7 168.4 avg	80.8 86.2 89.7 85.6 avg	62.5 68.5 54.5 62.4 avg	29.5	146.1 145.6 145.7 145.8 avg	152.7 136.5 150.9 146.7 avg	0.87

*K_t = 3.5.

Table A-11 Tensile Properties of Inconel 718 Nickel Alloy at Cryogenic Temperatures

Temperature (°F)	Ultimate Strength (ksi)	Yield Strength 0.2% Offset (ksi)	Elongation in 2 in. (%)	Modulus of Elasticity ($psi \times 10^6$)	Weld Strength (ksi)	Notch Strength* (ksi)	Notch Strength Ratio
70	121.3 120.9 120.9 121.0 avg	74.8 74.9 75.4 75.0 avg	45.0 44.5 44.0 44.5 avg	29.5	121.6 122.0 121.9 121.8 avg	120.2 120.1 120.4 120.2 avg	0.99
-320	166.3 167.6 166.9 166.9 avg	101.0 98.8 102.9 100.9 avg	57.5 58.0 55.5 57.0 avg	30.6	160.9 167.1 156.2 161.4 avg	160.7 160.1 160.1 160.3 avg	0.96
-423	187.7 189.3 188.5 188.5 avg	111.4 103.3 99.6 104.8 avg	59.0 52.5 56.5 56.0 avg	30.6	184.1 174.4 175.8 178.1 avg	175.6 174.0 175.8 175.1 avg	0.93

*$K_t = 3.5$.

Table A-12 Tensile Properties of Hastelloy C Nickel Alloy at Cryogenic Temperatures

Temperature (°F)	Ultimate Strength (ksi)	Yield Strength 0.2% Offset (ksi)	Elongation in 2 in. (%)	Modulus of Elasticity ($psi \times 10^6$)	Weld Strength (ksi)	Notch Strength* (ksi)	Notch Strength Ratio
70	119.5 120.3 120.0 119.9 avg	65.1 66.0 65.0 65.4 avg	50.5 50.5 50.5 50.5 avg	28.4	121.5 117.4 121.4 120.1 avg	117.4 117.2 116.4 117.0 avg	0.98
-320	175.8 176.2 176.2 176.0 avg	99.8 98.8 99.2 99.3 avg	65.0 64.5 65.5 65.0 avg	30.0	154.8 148.2 151.2 151.4 avg	161.3 161.3 160.9 161.2 avg	0.92
-423	202.9 201.9 200.9 201.9 avg	111.8 113.5 98.7 108.0 avg	61.5 59.0 55.0 58.5 avg	30.3	175.4 182.4 179.7 179.2 avg	181.4 178.2 173.6 177.7 avg	0.88

*K_t = 3.5.

APPENDIX B

FATIGUE DATA

Table B-1 Fatigue Properties* of Parent Metal 2014-T6 Aluminum Alloy (R = -1)

Temperature					
70°F		-320°F		-423°F	
Maximum Tension Stress (1000 psi)	Cycles to Failure	Maximum Tension Stress (1000 psi)	Cycles to Failure	Maximum Tension Stress (1000 psi)	Cycles to Failure
50.0	3.00×10^3	65.0	1.80×10^3	65.0	1.00×10^3
50.0	4.00×10^3	65.0	2.00×10^3	65.0	1.00×10^3
50.0	5.00×10^3	65.0	2.60×10^3	65.0	$8.00 \times 10^{3\dagger}$
40.0	2.00×10^4	50.0	3.33×10^4	62.5	1.50×10^4
40.0	2.50×10^4	50.0	4.17×10^4	62.5	2.60×10^4
40.0	3.30×10^4	50.0	6.96×10^4	62.5	3.50×10^4
30.0	1.30×10^5	40.0	8.89×10^4	50.0	2.76×10^5
30.0	1.57×10^5	40.0	9.50×10^4	50.0	3.70×10^5
30.0	3.95×10^5	40.0	1.10×10^5	50.0	4.17×10^5
25.0	1.26×10^5	30.0	2.06×10^5	45.0	1.22×10^6
25.0	1.76×10^5	30.0	2.58×10^5	45.0	1.12×10^6 (disc)
25.0	5.63×10^5	30.0	2.73×10^5	45.0	1.00×10^6 (disc)
20.0	1.20×10^7 (disc)	25.0	1.07×10^6		
20.0	1.19×10^7 (disc)	25.0	2.54×10^6		
17.5	6.62×10^5	25.0	5.02×10^6 (disc)		
17.5	1.03×10^6				
15.0	5.41×10^5				
15.0	1.28×10^6				
15.0	7.00×10^6 (disc)				
15.0	8.59×10^6 (disc)				

*Axial load R = -1.
†Specimen previously run at 45,000 psi for 1.12×10^6 cycles without failure.

Table B-2 Fatigue Properties of Unnotched Parent Metal 2014-T6 Aluminum Alloy (R = 0.01)

Temperature					
70°F		-320°F		-423°F	
Maximum Tension Stress (1000 psi)	Cycles to Failure	Maximum Tension Stress (1000 psi)	Cycles to Failure	Maximum Tension Stress (1000 psi)	Cycles to Failure
75.0	4.00×10^3	85.0	2.20×10^3 e	95.0	5.00×10^3
70.0	6.00×10^3	85.0	2.40×10^3 f	90.0	7.00×10^3 h
70.0	8.00×10^3 b	85.0	3.10×10^3	90.0	2.00×10^4
70.0	1.00×10^4 c	80.0	8.00×10^3	85.0	9.00×10^3 i
60.0	1.20×10^4 d	75.0	4.16×10^4	82.5	2.20×10^4
60.0	1.70×10^4	70.0	1.03×10^5	80.0	5.70×10^4
60.0	2.00×10^4	65.0	1.69×10^5	75.0	2.12×10^5
50.0	4.20×10^4	60.0	1.14×10^5 g	72.5	2.41×10^5
50.0	5.00×10^4	60.0	2.98×10^5	70.0	6.13×10^5
40.0	1.18×10^5	55.0	5.69×10^5	67.5	5.61×10^5
35.0	1.36×10^5	50.0	2.42×10^5	65.0	8.49×10^5
35.0	2.10×10^5	45.0	1.08×10^6	65.0	1.01×10^6 (disc)
30.0	1.31×10^6 (disc)	45.0	2.30×10^6	62.5	8.17×10^5
30.0	1.56×10^6 (disc)	42.0	4.53×10^5	61.0	7.92×10^5
30.0	1.82×10^6 (disc)	42.0	1.93×10^6 (disc)	61.0	8.76×10^5
		42.0	2.39×10^6 (disc)	60.0	1.00×10^6 (disc)
		40.0	1.70×10^6 (disc)		

a. Stress Ratio (R) = 0.01.
b thru i. Specimen previously run at indicated stress for number of cycles shown without failure.

Footnote	Stress (1000 psi)	Cycles
b	30.0	1.82×10^6
c	30.0	1.31×10^6
d	30.0	1.56×10^6
e	42.0	2.39×10^6
f	42.0	1.93×10^6
g	40.0	1.70×10^6
h	60.0	1.00×10^6
i	65.0	1.01×10^6

Table B-3 Fatigue Properties[a] of Notched[b] 2014-T6 Aluminum Alloy (K_t = 3.5)

Temperature					
70°F		-320°F		-423°F	
Maximum Tension Stress (1000 psi)	Cycles to Failure	Maximum Tension Stress (1000 psi)	Cycles to Failure	Maximum Tension Stress (1000 psi)	Cycles to Failure
32.0	1.00×10^3	25.0	4.90×10^3 c	40.0	1.00×10^3 f
30.0	2.00×10^3	25.0	6.20×10^3	35.0	2.00×10^3
28.0	3.00×10^3	25.0	6.30×10^3	30.0	5.00×10^3 g
25.0	5.00×10^3	25.0	6.60×10^3 d	27.5	9.00×10^3 h
25.0	8.00×10^3	25.0	7.20×10^3 e	25.0	1.70×10^4
20.0	1.30×10^4	20.0	1.33×10^4	20.0	3.00×10^4
20.0	2.50×10^4	15.0	3.57×10^4	17.5	2.10×10^4
18.0	2.10×10^4	15.0	6.11×10^4	17.5	5.40×10^4
15.0	6.60×10^4	10.0	9.78×10^4	15.0	9.70×10^4
12.0	1.13×10^5	10.0	1.74×10^5	12.5	2.40×10^5
11.0	1.34×10^5	10.0	1.79×10^5	10.0	6.60×10^5
10.0	5.09×10^5	10.0	4.16×10^5	7.5	6.10×10^5
7.0	1.25×10^6 (disc)	10.0	2.04×10^6 (disc)	5.0	1.00×10^6 (disc)
6.0	1.24×10^6 (disc)	10.0	2.13×10^6 (disc)	5.0	1.02×10^6 (disc)
5.0	1.14×10^6 (disc)	8.0	4.05×10^5	5.0	1.07×10^6 (disc)
		6.0	1.12×10^6 (disc)		

a. Stress ratio (R) = -1.
b. Stress concentation (K_t) = 3.5.

c thru h. Specimen previously run at indicated stress for number of cycles shown without failure.

Footnote	Stress (1000 psi)	Cycles
c	10.0	2.04×10^6
d	6.0	1.12×10^6
e	10.0	2.13×10^6
f	5.0	1.00×10^6
g	5.0	1.07×10^6
h	5.0	1.02×10^6

Table B-4 Fatigue Properties[a] of Notched[b] Parent Metal 2014-T6 Aluminum Alloy ($K_t = 8.0$)

Temperature					
70°F		-320°F		-423°F	
Maximum Tension Stress (1000 psi)	Cycles to Failure	Maximum Tension Stress (1000 psi)	Cycles to Failure	Maximum Tension Stress (1000 psi)	Cycles to Failure
25.0	3.00×10^3	25.0	4.9×10^3	30.0	3.00×10^3 g
25.0	4.00×10^3 c	25.0	5.9×10^3	27.5	4.00×10^3
25.0	7.00×10^3 d	25.0	9.7×10^3 e	25.0	4.00×10^3 h
20.0	1.00×10^4	25.0	1.11×10^4 f	23.0	9.00×10^3
17.0	1.20×10^4	21.0	1.64×10^4	20.0	1.60×10^4 i
15.0	1.50×10^4	20.0	1.82×10^4	20.0	2.30×10^4
12.0	1.73×10^5	17.0	2.60×10^4	17.5	3.50×10^4
10.0	2.41×10^5	14.0	4.04×10^4	15.0	4.90×10^4
8.0	5.68×10^5	12.0	1.92×10^5	13.0	1.14×10^5
8.0	7.25×10^5	11.0	2.18×10^5	12.5	2.67×10^5
6.0	2.57×10^5	8.0	5.61×10^5 j	10.0	3.48×10^5
6.0	5.05×10^5	8.0	1.06×10^6	7.5	6.77×10^5
4.0	1.18×10^6 (disc)	8.0	1.66×10^6 (disc)	5.0	1.00×10^6 (disc)
4.0	1.91×10^6 (disc)	8.0	1.67×10^6 (disc)	5.0	1.10×10^6 (disc)
		6.0	4.03×10^5 j	5.0	1.10×10^6 (disc)

a. Stress Ratio (R) = -1.
b. Stress Concentration (K_t) = 8.0.
c thru i. Specimen previously run at indicated stress for number of cycles shown without failure.

Footnote	Stress (1000 psi)	Cycles
c	4.0	1.18×10^6
d	4.0	1.91×10^6
e	8.0	1.67×10^6
f	8.0	1.66×10^6
g	5.0	1.00×10^6
h	5.0	1.10×10^6
i	5.0	1.10×10^6

j. Machine misaligned.

Table B-5 Fatigue Properties[a] of Welded 2014-T6 Aluminum Alloy

Temperature					
70°F		-320°F		-423°F	
Maximum Tension Stress (1000 psi)	Cycles to Failure	Maximum Tension Stress (1000 psi)	Cycles to Failure	Maximum Tension Stress (1000 psi)	Cycles to Failure
30.0	2.00×10^3	35.0	1.00×10^2	50.0	5.00×10^2
30.0	7.00×10^3	32.0	2.00×10^3	40.0	2.00×10^3
30.0	1.00×10^4	30.0	1.05×10^4	40.0	3.00×10^3
22.0	1.50×10^4	30.0	2.74×10^4	40.0	6.00×10^3
22.0	2.10×10^4	30.0	2.75×10^4	40.0	6.00×10^3 b
22.0	6.90×10^4	20.0	2.51×10^5	35.0	1.80×10^4
15.0	1.70×10^5	20.0	3.42×10^5	35.0	6.80×10^4
15.0	3.29×10^5	20.0	5.51×10^5	35.0	8.40×10^4
15.0	5.14×10^5	10.0	1.59×10^6 (disc)	30.0	1.82×10^5
9.0	1.02×10^6 (disc)	10.0	3.30×10^6 (disc)	30.0	2.65×10^5
9.0	1.03×10^6 (disc)	10.0	5.29×10^6 (disc)	30.0	3.18×10^5
9.0	1.03×10^6 (disc)			25.0	3.44×10^5
				17.5	1.01×10^6 (disc)
				17.5	1.03×10^6
				17.5	1.06×10^6

a. Axial load R = -1.
b. Specimen previously run at 17,500 psi for 1.01×10^6 cycles without failure.

Table B-6 Fatigue Properties[a] of Parent Metal 7039-T6 Aluminum Alloy (R = -1)

Temperature					
70°F		-320°F		-423°F	
Maximum Tension Stress (1000 psi)	Cycles to Failure	Maximum Tension Stress (1000 psi)	Cycles to Failure	Maximum Tension Stress (1000 psi)	Cycles to Failure
40.0	4.00×10^3 b	75.0	1.00×10^3	75.0	1.00×10^3 i
40.0	9.00×10^3 c	70.0	2.00×10^3	70.0	4.00×10^3 j
40.0	1.10×10^4 d	65.0	4.00×10^3 f	65.0	7.00×10^3
40.0	1.40×10^4 e	60.0	7.00×10^3 g	60.0	1.60×10^4
35.0	2.20×10^4	55.0	1.00×10^4	55.0	1.40×10^4 k
35.0	2.40×10^4	52.0	1.20×10^4 f	50.0	3.60×10^4
30.0	5.50×10^4	50.0	2.90×10^4	47.5	5.50×10^4
30.0	6.40×10^4	45.0	3.90×10^4	45.0	1.97×10^5
25.0	5.60×10^4	42.5	6.70×10^4	40.0	1.01×10^5
20.0	2.04×10^5	40.0	1.31×10^5	40.0	4.31×10^5
20.0	1.27×10^6 (disc)	35.0	3.77×10^5	40.0	1.02×10^6 (disc)
18.0	1.21×10^6 (disc)	32.5	9.28×10^5	37.5	1.00×10^6 (disc)
17.0	1.26×10^6 (disc)	30.0	1.00×10^6 (disc)	37.5	1.02×10^6 (disc)
17.0	1.29×10^6 (disc)	30.0	1.02×10^6 (disc)		
		30.0	1.78×10^6 (disc)		

a. Stress ratio (R) = -1.

b thru k. Specimen previously run at indicated stress for number of cycles shown without failure.

Footnote	Stress (1000 psi)	Cycles
b	17.0	1.29×10^6
c	17.0	1.26×10^6
d	18.0	1.21×10^6
e	20.0	1.27×10^6
f	30.0	1.02×10^6
g	30.0	1.00×10^6
h	30.0	1.78×10^6
i	37.5	1.02×10^6
j	37.5	1.00×10^6
k	40.0	1.02×10^6

Table B-7 Fatigue Properties[a] of Unnotched Parent Metal 7039-T6 Aluminum Alloy (R = 0.01)

Temperature					
70°F		-320°F		-423°F	
Maximum Tension Stress (1000 psi)	Cycles to Failure	Maximum Tension Stress (1000 psi)	Cycles to Failure	Maximum Tension Stress (1000 psi)	Cycles to Failure
70.0	1.00×10^3	85.0	3.20×10^3	100.0	2.00×10^3 h
65.0	4.00×10^3	85.0	3.30×10^3 e	95.0	1.00×10^3 i
60.0	7.00×10^3 b	85.0	3.50×10^3 f	90.0	8.00×10^3 j
60.0	8.00×10^3 c	85.0	3.60×10^3 g	85.0	3.00×10^3
60.0	8.00×10^3 d	80.0	6.70×10^3	85.0	1.20×10^4
60.0	1.30×10^4	75.0	1.28×10^4	85.0	3.50×10^4
50.0	4.50×10^4	70.0	3.54×10^4	80.0	2.40×10^4
45.0	7.70×10^4	65.0	8.39×10^4	80.0	1.45×10^5
40.0	1.60×10^5	60.0	2.65×10^5	75.0	1.17×10^5
40.0	2.46×10^5	60.0	4.36×10^5	70.0	6.27×10^5
35.0	4.32×10^5	56.0	1.56×10^5	65.0	6.27×10^5
35.0	6.38×10^5	55.0	5.93×10^5	60.0	9.57×10^5
32.0	1.12×10^6 (disc)	50.0	1.96×10^5	60.0	1.00×10^6 (disc)
32.0	1.21×10^6 (disc)	50.0	1.11×10^6 (disc)	57.5	1.01×10^6 (disc)
30.0	1.53×10^6 (disc)	45.0	1.11×10^6 (disc)	55.0	1.06×10^6 (disc)
		45.0	1.13×10^6 (disc)		

a. Stress Ratio (R) = .01
b thru j. Specimen previously run at indicated stress for number of cycles shown without failure.

Footnote	Stress (1000 psi)	Cycles
b	32.0	1.21×10^6
c	32.0	1.12×10^6
d	30.0	1.53×10^6
e	45.0	1.11×10^6
f	50.0	1.11×10^6
g	45.0	1.13×10^6
h	55.0	1.06×10^6
i	60.0	1.00×10^6
j	57.5	1.01×10^6

Table B-8 Fatigue Properties[a] of Notched[b] 7039-T6 Aluminum Alloy $K_t = 3.5$

Temperature					
70°F		-320°F		-423°F	
Maximum Tension Stress (1000 psi)	Cycles to Failure	Maximum Tension Stress (1000 psi)	Cycles to Failure	Maximum Tension Stress (1000 psi)	Cycles to Failure
25.0	3.0×10^3	40.0	1.00×10^3	35.0	1.00×10^3 h
25.0	4.0×10^3 c	35.0	2.00×10^3 e	30.0	3.00×10^3
25.0	5.0×10^3 d	30.0	3.00×10^3 f	25.0	4.00×10^3 i
20.0	7.0×10^3	25.0	6.00×10^3	22.5	7.00×10^3 j
20.0	7.0×10^3	22.5	8.00×10^3 g	19.6	1.30×10^4
15.0	1.3×10^4	20.0	1.90×10^4	18.5	2.30×10^4
10.0	6.8×10^4	15.0	4.00×10^4	17.5	3.20×10^4
10.0	9.3×10^4	12.5	6.60×10^4	15.0	6.30×10^4
8.0	1.15×10^5	10.0	1.89×10^5	12.5	8.60×10^4
8.0	3.68×10^5	8.5	2.04×10^5	11.0	2.65×10^5
7.0	8.84×10^5	7.5	7.05×10^5	9.0	2.61×10^5
6.0	1.481×10^6 (disc)	6.5	5.07×10^5	9.0	3.04×10^5
6.0	1.646×10^6 (disc)	6.5	1.00×10^6 (disc)	7.5	1.01×10^6 (disc)
6.0	3.397×10^6	6.0	1.00×10^6 (disc)	7.5	1.01×10^6 (disc)
		6.0	1.03×10^6 (disc)	7.5	1.03×10^6 (disc)

a. Stress ratio (R) = -1.
b. Stress concentration $(K_t) = 3.5$.

c thru j. Specimen previously run at indicated stress for number for cycles shown without failure.

Footnote	Stress (1000 psi)	Cycles
c	6.0	1.481×10^6
d	6.0	1.646×10^6
e	6.0	1.00×10^6
f	6.0	1.03×10^6
g	6.5	1.00×10^6
h	7.5	1.03×10^6
i	7.5	1.01×10^6
j	7.5	1.01×10^6

Table B-9 Fatigue Properties[a] of Notched[b] Parent Metal 7039-T6 Aluminum Alloy (K_t = 8.0)

Temperature					
70°F		-320°F		-423°F	
Maximum Tension Stress (1000 psi)	Cycles to Failure	Maximum Tension Stress (1000 psi)	Cycles to Failure	Maximum Tension Stress (1000 psi)	Cycles to Failure
30.0	1.00×10^3 c	32.0	1.90×10^3 f	35.0	1.00×10^3 h
30.0	2.00×10^3 d	32.0	2.10×10^3 g	32.5	2.00×10^3 i
30.0	2.00×10^3 e	30.0	4.30×10^3	30.0	4.00×10^3
30.0	5.00×10^3	27.7	6.20×10^3	29.0	1.00×10^3 j
25.0	6.00×10^3	25.0	1.02×10^4	27.5	8.00×10^3
20.0	3.43×10^5	20.0	2.41×10^4	26.0	1.30×10^4
18.0	2.60×10^4	17.5	5.17×10^4	25.0	1.60×10^4
15.0	5.40×10^4	15.0	1.02×10^5	22.5	3.30×10^4
15.0	5.80×10^4	13.5	3.57×10^5	20.0	4.50×10^4
12.0	6.10×10^4	12.0	5.96×10^5	17.5	1.05×10^5
10.0	1.07×10^5	11.0	9.44×10^5	15.0	2.92×10^5
8.0	1.91×10^5	10.0	4.91×10^5	12.5	6.96×10^5
6.0	6.13×10^5	10.0	1.18×10^6 (disc)	10.0	1.02×10^6 (disc)
5.0	1.11×10^6 (disc)	9.0	9.27×10^5	10.0	1.10×10^6 (disc)
5.0	1.12×10^6 (disc)	8.0	1.14×10^6 (disc)	10.0	1.11×10^6 (disc)
5.0	1.16×10^3 (disc)				

a. Stress Ratio (R) = -1.
b. Stress Concentration K_t = 8.0
c thru j. Specimen previously run at indicated stress for number of cycles shown without failure.

Footnote	Stress (1000 psi)	Cycles
c	5.0	1.16×10^6
d	5.0	1.11×10^6
e	5.0	1.12×10^6
f	10.0	1.18×10^6
g	8.0	1.14×10^6
h	10.0	1.02×10^6
i	10.0	1.10×10^6
j	10.0	1.11×10^6

Table B-10 Fatigue Properties[a] of Welded 7039-T6 Aluminum Alloy

Temperature					
70°F		-320°F		-423°F	
Maximum Tension Stress (1000 psi)	Cycles to Failure	Maximum Tension Stress (1000 psi)	Cycles to Failure	Maximum Tension Stress (1000 psi)	Cycles to Failure
30.0	4.0×10^3	40.0	1.00×10^3 e	40.0	1.00×10^3
25.0	3.0×10^3 b	35.0	3.00×10^3	40.0	2.00×10^3
25.0	8.0×10^3 c	32.5	1.00×10^4	37.5	3.00×10^3 f
25.0	8.0×10^3	30.0	1.40×10^4	36.0	5.00×10^3
20.0	9.0×10^3	27.5	4.00×10^4	36.0	8.00×10^3 g
20.0	2.2×10^4 d	25.0	2.10×10^4	35.0	2.30×10^4
15.0	3.05×10^4 h	24.0	1.58×10^5	30.0	1.63×10^5
15.0	4.45×10^4 h	22.5	3.36×10^5	25.0	2.90×10^5
15.0	7.65×10^4	20.0	5.08×10^5	25.0	7.10×10^5
12.0	2.48×10^5	18.0	8.86×10^5	22.5	5.62×10^5
10.0	1.46×10^5 h	16.5	1.59×10^6	20.0	8.61×10^5
10.0	4.82×10^5	16.0	1.46×10^6	18.0	1.00×10^6 (disc)
8.0	1.135×10^6 (disc)	16.0	1.75×10^6 (disc)	18.0	1.04×10^6 (disc)
8.0	1.480×10^6 (disc)				
8.0	1.553×10^6 (disc)				

a. Stress ratio (R) = -1.

b thru g. Specimen previously run at indicated stress for number of cycles shown without failure.

Footnote	Stress (1000 psi)	Cycles
b	8.0	1.135×10^6
c	8.0	1.553×10^6
d	8.0	1.480×10^6
e	16.0	1.75×10^6
f	18.0	1.00×10^6
g	18.0	1.04×10^6

h. Specimen tested without wedges to preload ends.

Table B-11 Fatigue Properties[a] of Unnotched Parent Metal 7106-T6 Aluminum Alloy (R = -1)

Temperature					
70°F		-320°F		-423°F	
Maximum Tension Stress (1000 psi)	Cycles to Failure	Maximum Tension Stress (1000 psi)	Cycles to Failure	Maximum Tension Stress (1000 psi)	Cycles to Failure
45.0	2.00×10^3 b	68.0	2.30×10^3	70.3	1.00×10^3 g
40.0	4.00×10^3	65.0	3.50×10^3	65.0	5.00×10^3 h
38.0	6.00×10^3	62.0	1.02×10^4	60.0	8.00×10^3
35.0	8.00×10^3 c	60.0	6.40×10^3 d	57.5	2.00×10^4
35.0	9.00×10^3	60.0	9.40×10^3 e	56.4	5.00×10^3 i
31.0	2.50×10^4	60.0	1.03×10^4	55.0	4.30×10^4
28.5	3.10×10^4	60.0	1.10×10^4 f	50.0	4.90×10^4
25.0	5.20×10^4	55.0	1.95×10^4	45.0	1.39×10^5
20.0	1.66×10^5	50.0	8.16×10^4	44.0	5.90×10^4
18.0	3.83×10^5 j	45.0	1.63×10^5	43.5	2.62×10^5
15.0	6.04×10^5 j	44.0	2.61×10^5	42.5	3.98×10^5
14.0	5.82×10^5 j	40.0	6.51×10^5	42.5	1.07×10^6 (disc)
13.0	1.12×10^6 (disc)	36.0	7.72×10^5	40.2	1.05×10^6 (disc)
12.0	9.75×10^5	36.0	1.12×10^6 (disc)	40.0	8.20×10^5
12.0	1.10×10^6 (disc)	36.0	1.21×10^6 (disc)	40.0	1.06×10^6 (disc)
		34.0	1.48×10^6 (disc)		

a. Stress Ratio (R) = -1.
b thru i. Specimen previously run at indicated stress for number of cycles shown without failure.

Footnote	Stress (1000 psi)	Cycles
b	12.0	1.10×10^6
c	13.0	1.12×10^6
d	36.0	1.21×10^6
e	34.0	1.48×10^6
f	36.0	1.12×10^6
g	40.2	1.05×10^6
h	40.0	1.06×10^6
i	42.5	1.07×10^6

j. Failure occurred through grip area.

Table B-12 Fatigue Properties[a] of Unnotched Parent Metal 7106-T6 Aluminum Alloy (R = 0.01)

Temperature					
70°F		-320°F		-423°F	
Maximum Tension Stress (1000 psi)	Cycles to Failure	Maximum Tension Stress (1000 psi)	Cycles to Failure	Maximum Tension Stress (1000 psi)	Cycles to Failure
60.0	2.00×10^3	83.0	2.40×10^3	95.0	1.00×10^3 i
56.0	8.00×10^3	80.0	2.80×10^3	90.0	4.00×10^3 j
50.0	2.30×10^4	78.0	3.40×10^3	87.5	3.00×10^3 k
40.0	3.00×10^3 b,c	75.0	6.70×10^3 f	87.5	5.00×10^3
40.0	7.00×10^3 b,d	75.0	8.80×10^3 g	85.0	1.00×10^4
40.0	1.20×10^4 b,e	75.0	1.08×10^4	80.0	1.40×10^4
40.0	7.50×10^4	75.0	1.84×10^4 h	77.5	2.80×10^4
35.0	9.10×10^4	70.0	3.20×10^4	75.0	4.50×10^4
30.0	8.30×10^4	65.0	4.25×10^4	70.0	9.00×10^4
27.0	2.00×10^5	60.0	1.36×10^5	65.0	1.65×10^5
25.0	1.94×10^5	55.0	3.27×10^5	60.0	1.76×10^5
25.0	3.06×10^5	50.0	6.13×10^5	55.0	5.71×10^5
20.0	1.10×10^6 (disc)	50.0	1.11×10^6 (disc)	50.0	1.00×10^6 (disc)
20.0	1.12×10^6 (disc)	47.0	1.18×10^6 (disc)	50.0	1.08×10^6 (disc)
20.0	1.27×10^6 (disc)	47.0	1.20×10^6 (disc)	50.0	1.10×10^6 (disc)

a. Stress Ratio (R) = 0.01.
b. Specimen failed through grip area.
c thru k. Specimen previously run at indicated stress for number of cycles shown without failure.

Footnote	Stress (1000 psi)	Cycles
c	20.0	1.10×10^6
d	20.0	1.27×10^6
e	20.0	1.12×10^6
f	47.0	1.20×10^6
g	50.0	1.11×10^6
h	47.0	1.18×10^6
i	50.0	1.10×10^6
j	50.0	1.08×10^6
k	50.0	1.00×10^6

Table B-13 Fatigue Properties [a] of Notched[b] Parent Metal 7106-T6 Aluminum Alloy

Temperature					
70°F		-320°F		-423°F	
Maximum Tension Stress (1000 psi)	Cycles to Failure	Maximum Tension Stress (1000 psi)	Cycles to Failure	Maximum Tension Stress (1000 psi)	Cycles to Failure
40.0	0.00	32.0	3.80×10^3	40.0	1.00×10^3
30.0	2.00×10^3	30.0	5.40×10^3 f	40.0	1.00×10^3 g
28.0	2.00×10^3 c	30.0	6.50×10^3	37.5	2.00×10^3
28.0	2.50×10^3	25.0	1.61×10^4	35.0	4.00×10^3
27.0	3.00×10^3 d	22.0	2.15×10^4	30.0	7.00×10^3
25.0	5.50×10^3	20.0	4.72×10^4	27.5	1.00×10^3 h
20.0	1.25×10^4	18.0	5.44×10^4	25.0	1.50×10^4
18.0	1.70×10^4 e	15.0	1.27×10^5	22.5	2.10×10^4 i
15.0	3.70×10^4	14.0	1.69×10^5	20.0	5.80×10^4
12.0	8.25×10^4	13.0	1.76×10^5	17.5	1.18×10^5
10.0	1.04×10^5	12.0	1.12×10^6 (disc)	15.0	4.54×10^5
7.0	4.15×10^5	11.0	9.70×10^5	14.0	3.25×10^5
6.0	1.11×10^6 (disc)	10.0	1.14×10^6 (disc)	12.5	1.05×10^6 (disc)
5.0	3.36×10^5			12.5	1.10×10^6 (disc)
5.0	1.12×10^6 (disc)			12.5	1.17×10^6 (disc)
5.0	1.14×10^6 (disc)				

a. Stress Ratio (R) = -1.
b. Stress concentration factory (K_t) = 3.5.
c thru i. Specimen previously run at indicated stress for number of cycles shown without failure.

Footnote	Stress (1000 psi)	Cycles
c	5.0	1.12×10^6
d	6.0	1.11×10^6
e	5.0	1.14×10^6
f	10.0	1.14×10^6
g	12.5	1.10×10^6
h	12.5	1.17×10^6
i	12.5	1.05×10^6

Table B-14 Fatigue Properties[a] of Welded 7106-T6 Aluminum Alloy

Temperature					
70°F		-320°F		-423°F	
Maximum Tension Stress (1000 psi)	Cycles to Failure	Maximum Tension Stress (1000 psi)	Cycles to Failure	Maximum Tension Stress (1000 psi)	Cycles to Failure
30.0	1.00×10^3	42.0	1.40×10^3	50.0	1.00×10^3
27.0	3.00×10^3	40.0	4.18×10^4 c	45.0	6.00×10^3 f
25.0	1.90×10^4	38.0	5.05×10^4	40.0	8.00×10^3 g
22.0	5.30×10^4 b	35.0	3.70×10^3	37.5	2.00×10^3
20.0	6.80×10^4	35.0	1.28×10^5 d	35.0	1.00×10^3
18.0	1.10×10^4	33.0	1.60×10^3	35.0	1.30×10^4 h
16.0	1.90×10^4	32.0	9.37×10^4 e	32.5	4.50×10^4
15.0	8.00×10^3	31.0	4.90×10^3	30.0	4.50×10^4
15.0	3.10×10^4	30.0	6.00×10^4	27.5	4.10×10^4
15.0	8.40×10^4	28.0	7.80×10^3	25.0	6.69×10^5
10.0	3.60×10^4	25.0	2.88×10^5	22.5	2.55×10^5
7.0	2.63×10^5	20.0	1.90×10^5	20.0	3.12×10^5
7.0	1.15×10^6 (disc)	20.0	5.97×10^5	17.5	1.01×10^6 (disc)
5.0	5.97×10^5	18.0	1.25×10^6 (disc)	17.5	1.12×10^6 (disc)
		18.0	1.14×10^6 (disc)	17.5	1.13×10^6 (disc)
		18.0	1.46×10^6 (disc)		

a. Stress Ratio (R) = -1.
b thru h. Specimen previously run at indicated stress for number of cycles shown without failure.

Footnote	Stress (1000 psi)	Cycles
b	7.0	1.15×10^6
c	18.0	1.25×10^6
d	18.0	1.14×10^6
e	18.0	1.46×10^6
f	17.5	1.01×10^6
g	17.5	1.13×10^6
h	17.5	1.12×10^6

Table B-15 Fatigue Properties[a] of Parent Metal 2219-T87 Aluminum Alloy

Temperature					
70°F		-320°F		-423°F	
Maximum Tension Stress (1000 psi)	Cycles to Failure	Maximum Tension Stress (1000 psi)	Cycles to Failure	Maximum Tension Stress (1000 psi)	Cycles to Failure
50.0	9.00×10^2	55.0	6.00×10^2	62.5	1.50×10^3
46.0	3.00×10^3	55.0	1.70×10^3	62.5	3.00×10^3
46.0	3.00×10^3	55.0	1.90×10^3	62.5	4.00×10^3 [c]
46.0	4.00×10^3	35.0	4.51×10^4	62.5	7.00×10^3
40.0	9.90×10^3	35.0	6.46×10^4	62.5	7.50×10^3
40.0	1.49×10^4	35.0	8.02×10^4	55.0	4.40×10^4
40.0	2.27×10^4	35.0	1.16×10^5	55.0	6.60×10^4
35.0	2.43×10^4	30.0	1.01×10^5	55.0	8.90×10^4
35.0	2.82×10^4	25.0	1.05×10^6 b	50.0	1.24×10^5
35.0	3.19×10^4	25.0	2.05×10^6 b	47.5	1.73×10^5
30.0	4.86×10^4	20.0	5.21×10^6 (disc)	47.5	1.74×10^5
30.0	1.40×10^5	15.0	1.05×10^6	47.5	3.05×10^5
30.0	1.66×10^5	15.0	2.21×10^6	40.0	7.95×10^5
25.0	1.80×10^5	15.0	2.31×10^6	40.0	1.40×10^6 (disc)
25.0	3.08×10^5			40.0	1.46×10^6 (disc)
25.0	6.76×10^5				
22.5	3.56×10^5				
22.5	9.52×10^5				
22.5	3.40×10^6				
20.0	4.45×10^6				
20.0	1.24×10^7 (disc)				

a. Axial load R = -1.
b. Failed through pinholes.
c. Specimen previously run at 40,000 psi for 1.46×10^6 cycles without failure.

Table B-16 Fatigue Properties[a] of Notched[b] 2219-T87 Aluminum Alloy

Temperature					
70°F		-320°F		-423°F	
Maximum Tension Stress (1000 psi)	Cycles to Failure	Maximum Tension Stress (1000 psi)	Cycles to Failure	Maximum Tension Stress (1000 psi)	Cycles to Failure
32.0	1.00×10^3	27.5	2.10×10^3	35.0	1.00×10^3
30.0	1.50×10^3	25.0	3.50×10^3	30.0	2.00×10^3 f
30.0	1.60×10^4 c	25.0	4.30×10^3 e	29.0	5.00×10^3 g
25.0	4.00×10^3	22.5	7.8×10^3	27.5	8.00×10^3 h
25.0	4.00×10^3 d	20.0	1.95×10^4	25.0	1.20×10^4
20.0	1.00×10^4	15.0	4.90×10^4	22.5	1.00×10^4
15.0	3.30×10^4	10.0	7.83×10^4	22.5	1.50×10^4
12.0	9.70×10^4	10.0	8.89×10^4	20.0	2.80×10^4
10.0	1.60×10^5	10.0	7.61×10^5	17.5	3.90×10^4
9.0	3.63×10^5	7.5	3.09×10^5	15.0	1.04×10^5
8.0	7.30×10^5	7.0	3.98×10^5	12.5	1.72×10^5
8.0	1.10×10^6 (disc)	7.0	4.66×10^5	10.0	4.34×10^5
7.0	1.15×10^6 (disc)	5.0	1.07×10^6	7.0	1.00×10^6 (disc)
7.0	7.32×10^6	6.0	6.94×10^6 (disc)	7.0	1.01×10^6 (disc)
				7.0	1.02×10^6 (disc)

a. Stress ratio (R) = -1.
b. Stress concentration (K_t) = 3.5.
c thru h. Specimen previously run at indicated stress for number of cycles shown without failure.

Footnote	Stress (1000 psi)	Cycles
c	8.0	1.10×10^6
d	7.0	1.15×10^6
e	6.0	6.94×10^6
f	7.0	1.01×10^6
g	7.0	1.02×10^6
h	7.0	1.00×10^6

Table B-17 Fatigue Properties[a] of Welded 2219-T87 Aluminum Alloy

Temperature					
70°F		-320°F		-423°F	
Maximum Tension Stress (1000 psi)	Cycles to Failure	Maximum Tension Stress (1000 psi)	Cycles to Failure	Maximum Tension Stress (1000 psi)	Cycles to Failure
30.0	1.00×10^3	32.0	3.10×10^3	45.0	1.00×10^3
30.0	6.00×10^3	32.0	5.50×10^3	45.0	1.00×10^3
30.0	9.00×10^3	32.0	5.70×10^3	45.0	2.00×10^3
20.0	2.40×10^4	25.0	4.10×10^4	45.0	2.00×10^3 c
20.0	3.30×10^4	25.0	4.74×10^4	45.0	5.00×10^3 c
20.0	5.30×10^4	25.0	5.14×10^4	42.5	1.70×10^4
15.0	7.90×10^4	17.5	1.89×10^5	40.0	3.50×10^4
15.0	1.94×10^5	17.5	3.19×10^5	35.0	5.50×10^4
15.0	2.09×10^5	17.5	5.91×10^5	35.0	7.40×10^4
10.0	2.04×10^6	12.5	9.93×10^5	35.0	1.17×10^5
10.0	1.22×10^6	12.5	3.27×10^6	30.0	2.13×10^5
10.0	1.04×10^7 (disc)	12.5	4.57×10^6	30.0	2.36×10^5
				30.0	4.22×10^5
				22.5	7.78×10^5
				22.5	1.04×10^6 (disc)
				22.5	1.13×10^6 (disc)

a. Axial load R = -1.

b. Specimen previously run at 22,500 psi for 1.04×10^6 cycles without failure.

c. Specimen previously run at 22,500 psi for 1.13×10^6 cycles without failure.

Table B-18 Fatigue Properties[a] of Parent Metal 2219-T62 Aluminum Alloy

Temperature					
70°F		-320°F		-423°F	
Maximum Tension Stress (1000 psi)	Cycles to Failure	Maximum Tension Stress (1000 psi)	Cycles to Failure	Maximum Tension Stress (1000 psi)	Cycles to Failure
36.0	4.00×10^{3}	45.0	7.00×10^{2} d	65.0	1.00×10^{3}
35.0	5.00×10^{3}	45.0	1.30×10^{3}	62.0	2.00×10^{3} g
34.0	5.00×10^{3}	43.0	1.50×10^{3} e	60.0	4.00×10^{3} h
32.0	1.00×10^{3}	43.0	1.90×10^{3}	60.0	8.00×10^{3}
30.0	1.50×10^{4}	43.0	2.60×10^{3}	57.0	7.00×10^{3} i
30.0	1.50×10^{4} b	40.0	5.90×10^{3} f	55.0	1.20×10^{4}
30.0	3.20×10^{4} c	40.0	9.90×10^{3}	50.0	3.80×10^{4}
25.0	6.30×10^{4}	40.0	1.23×10^{4}	50.0	9.00×10^{4}
22.0	3.32×10^{5}	35.0	2.37×10^{4}	45.0	5.70×10^{4}
20.0	2.70×10^{5}	35.0	3.85×10^{4}	45.0	8.50×10^{4}
19.0	7.27×10^{5}	30.0	1.35×10^{5}	40.0	$3.93 \quad 10^{5}$
18.5	1.43×10^{6}	30.0	1.58×10^{5}	40.0	4.42×10^{5}
18.0	3.45×10^{6} (disc)	25.0	2.75×10^{5}	35.0	1.02×10^{6} (disc)
15.0	3.14×10^{5} (disc)	25.0	8.68×10^{5}	35.0	1.04×10^{6} (disc)
		20.0	7.68×10^{5}	35.0	1.12×10^{6} (disc)
		20.0	1.33×10^{6}		
		18.0	1.68×10^{6} (disc)		
		18.0	2.02×10^{6} (disc)		
		18.0	2.23×10^{6} (dsic)		

a. Stress ratio (R) = -1.

b thru i. Specimen previously run at indicated stress for number of cycles shown without failure.

Footnote	Stress (1000 psi)	Cycles
b	15.0	3.14×10^{6}
c	18.0	3.45×10^{6}
d	18.0	2.02×10^{6}
e	18.0	2.23×10^{6}
f	18.0	1.68×10^{6}
g	35.0	1.12×10^{6}
h	35.0	1.04×10^{6}
i	35.0	1.02×10^{6}

Table B-19 Fatigue Properties[a] of Notched[b] 2219-T62 Aluminum Alloy

Temperature					
70°F		-320°F		-423°F	
Maximum Tension Stress (1000 psi)	Cycles to Failure	Maximum Tension Stress (1000 psi)	Cycles to Failure	Maximum Tension Stress (1000 psi)	Cycles to Failure
25.0	2.00×10^3 c	30.0	1.20×10^3	40.0	1.00×10^3
20.0	4.00×10^3 d	30.0	2.30×10^3 f	35.0	2.00×10^3
20.0	5.00×10^3 e	20.0	1.20×10^4 g	30.0	4.00×10^3 i
20.0	6.00×10^3	20.0	1.29×10^4 h	25.0	5.00×10^3
20.0	7.00×10^3	10.0	7.43×10^4	22.5	7.00×10^3
15.0	2.20×10^4	10.0	1.05×10^5	20.0	1.70×10^4
15.0	2.80×10^4	10.0	3.70×10^5	17.0	2.20×10^4
15.0	3.00×10^4	7.0	3.45×10^5	16.5	2.80×10^4 j
10.0	1.06×10^5	7.0	5.39×10^5	15.0	7.40×10^4
10.0	1.14×10^5	5.0	1.11×10^6 (disc)	12.5	1.57×10^5
7.5	7.45×10^5	5.0	1.13×10^6 (disc)	10.0	3.85×10^5
7.5	8.78×10^5	5.0	1.70×10^6 (disc)	7.5	1.03×10^6 (disc)
7.5	1.15×10^6 (disc)			7.0	9.20×10^5
7.5	1.26×10^6 (disc)			6.0	1.03×10^6 (disc)
6.0	1.52×10^6 (disc)				

a. Stress ratio (R) = -1.
b. Stress concentration $(K_t) = 3.5$.
c thru j. Specimen previously run at indicated stress for number of cycles shown without failure.

Footnote	Stress (1000 psi)	Cycles
c	6.0	1.52×10^6
d	7.5	1.26×10^6
e	7.5	1.15×10^6
f	5.0	1.70×10^6
g	5.0	1.11×10^6
h	5.0	1.13×10^6
i	6.0	1.03×10^6
j	7.5	1.03×10^6

Table B-20 Fatigue Properties[a] of Welded 2219-T62 Aluminum Alloy

Temperature					
70°F		-320°F		-423°F	
Maximum Tension Stress (1000 psi)	Cycles to Failure	Maximum Tension Stress (1000 psi)	Cycles to Failure	Maximum Tension Stress (1000 psi)	Cycles to Failure
30.0	1.00×10^{3}	40.0	1.4×10^{3} d	50.0	1.00×10^{3}
30.0	1.00×10^{3} b	40.0	1.7×10^{3} e	50.0	2.00×10^{3}
30.0	2.00×10^{3} c	40.0	3.5×10^{3}	50.0	3.00×10^{3} g
27.0	8.00×10^{3}	40.0	4.1×10^{3}	47.5	4.00×10^{3} h
27.0	1.10×10^{4}	30.0	1.15×10^{4} f	45.0	9.00×10^{3}
20.0	5.70×10^{4}	30.0	2.21×10^{4}	42.5	1.20×10^{4} i
20.0	7.60×10^{4}	30.0	4.28×10^{4}	41.0	2.00×10^{4}
20.0	7.80×10^{4}	30.0	5.14×10^{4}	40.0	3.60×10^{4}
15.0	1.54×10^{5}	20.0	2.10×10^{5}	35.0	1.00×10^{5}
15.0	3.03×10^{5}	20.0	4.83×10^{5}	30.0	3.60×10^{4}
15.0	3.20×10^{5}	17.0	3.40×10^{5}	30.0	2.55×10^{5}
12.0	1.19×10^{6}	15.0	1.11×10^{6}	28.5	6.57×10^{5}
12.0	1.50×10^{6} (disc)	15.0	1.81×10^{6}	25.0	4.62×10^{5}
10.0	1.30×10^{6} (disc)	15.0	1.20×10^{6}	25.0	1.02×10^{6} (disc)
10.0	1.46×10^{6}			22.5	1.00×10^{6} (disc)
				22.5	1.08×10^{6} (disc)

a. Stress ratio (R) = -1.

b thru i. Specimen previously run at indicated stress for number of cycles shown without failure.

Footnote	Stress (1000 psi)	Cycles
b	12.0	1.50×10^{6}
c	10.0	1.30×10^{6}
d	15.0	1.11×10^{6}
e	15.0	1.81×10^{6}
f	15.0	1.20×10^{6}
g	22.5	1.00×10^{6}
h	25.0	1.02×10^{6}
i	22.5	1.08×10^{6}

Table B-21 Fatigue Properties[a] of Parent Metal 5456-H343 Aluminum Alloy

Temperature					
70°F		-320°F		-423°F	
Maximum Tension Stress (1000 psi)	Cycles to Failure	Maximum Tension Stress (1000 psi)	Cycles to Failure	Maximum Tension Stress (1000 psi)	Cycles to Failure
40.0	1.50×10^3	52.0	1.50×10^3	55.0	7.00×10^3
38.5	4.00×10^3	52.0	4.50×10^3	55.0	8.00×10^3
38.5	5.00×10^3	52.0	4.60×10^3	55.0	1.00×10^4
38.5	5.00×10^3	50.0	9.10×10^3	50.0	1.60×10^4
35.0	8.00×10^3	50.0	1.64×10^4	50.0	3.20×10^4
35.0	1.10×10^4	50.0	1.65×10^4	50.0	3.30×10^4
35.0	1.40×10^4	40.0	34.2×10^4	45.0	8.90×10^4
30.0	2.83×10^4	40.0	4.37×10^4	42.5	3.05×10^5
30.0	4.30×10^4	40.0	6.21×10^4	42.5	3.20×10^5
30.0	5.25×10^4	30.0	6.87×10^4	42.5	5.19×10^5
25.0	5.25×10^4	30.0	1.32×10^5	40.0	8.86×10^5 (disc)
20.0	1.70×10^5	30.0	2.38×10^5	40.0	9.07×10^5
20.0	4.59×10^5	25.0	7.94×10^5	40.0	1.52×10^6 (disc)
20.0	5.33×10^5	25.0	1.10×10^6		
15.0	1.00×10^6	25.0	4.43×10^6 (disc)		
15.0	1.69×10^6				
15.0	4.96×10^6 (disc)				

a. Axial load R = -1.

Table B-22 Fatigue Properties[a] of Notched[b] 5456-H343 Aluminum Alloy

Temperature					
70°F		-320°F		-423°F	
Maximum Tension Stress (1000 psi)	Cycles to Failure	Maximum Tension Stress (1000 psi)	Cycles to Failure	Maximum Tension Stress (1000 psi)	Cycles to Failure
25.0	1.00×10^3	25.0	1.00×10^3 c	30.0	1.00×10^3
20.0	6.00×10^3	20.0	1.60×10^3 d	25.0	3.00×10^3
20.0	7.00×10^3	20.0	2.30×10^3	22.5	3.00×10^3 f
15.0	2.80×10^4	20.0	3.80×10^3	22.5	3.00×10^3
15.0	3.20×10^4	20.0	6.10×10^3 e	21.5	2.00×10^3 g
15.0	3.60×10^4	15.0	4.50×10^3	20.0	1.30×10^4
10.0	2.09×10^5	10.0	3.71×10^4	18.5	6.00×10^3 h
10.0	3.83×10^5	10.0	8.15×10^4	17.5	2.90×10^4
8.0	3.04×10^5	10.0	3.44×10^5	16.0	5.90×10^4
7.5	1.18×10^6	7.5	1.50×10^5	15.0	9.70×10^4
7.5	1.51×10^6 (disc)	7.5	2.24×10^5	14.0	1.09×10^5
6.0	7.23×10^6 (disc)	5.0	6.88×10^5	12.5	3.06×10^5
		4.0	1.66×10^6 (disc)	9.0	1.02×10^6 (disc)
		4.0	1.96×10^6 (disc)	9.0	1.05×10^6 (disc)
		3.0	1.70×10^6 (disc)	9.0	1.05×10^6 (disc)

a. Stress ratio (R) = -1.
b. Stress concentration (K_t) = 3.5.
c thru h. Specimen previously run at indicated stress for number of cycles shown without failure.

Footnote	Stress (1000 psi)	Cycles
c	4.0	1.66×10^6
d	4.0	1.96×10^6
e	3.0	1.70×10^6
f	9.0	1.02×10^6
g	9.0	1.05×10^6
h	9.0	1.05×10^6

Table B-23 Fatigue Properties[a] of Welded 5456-H343 Aluminum Alloy

Temperature					
70°F		-320°F		-423°F	
Maximum Tension Stress (1000 psi)	Cycles to Failure	Maximum Tension Stress (1000 psi)	Cycles to Failure	Maximum Tension Stress (1000 psi)	Cycles to Failure
30.0	2.00×10^3	32.0	2.60×10^3	40.0	1.20×10^4
30.0	2.00×10^3	32.0	4.80×10^3	35.0	3.00×10^3
30.0	3.00×10^3	32.0	8.40×10^3	35.0	6.00×10^3
20.0	1.60×10^4	25.0	1.44×10^4	35.0	2.70×10^4
20.0	2.20×10^4	25.0	2.54×10^4	30.0	2.40×10^4
20.0	4.50×10^4	25.0	4.94×10^4	30.0	8.70×10^4
13.8	2.45×10^5	17.0	2.04×10^5	30.0	9.90×10^4
13.8	3.33×10^5	17.0	2.62×10^5	25.0	3.30×10^5
13.8	3.90×10^5	17.0	4.21×10^5	25.0	4.12×10^5
10.0	5.35×10^5	12.0	1.41×10^6	17.5	1.00×10^6 (disc)
10.0	2.44×10^6	12.0	2.58×10^6	17.5	1.07×10^6 (disc)
10.0	3.71×10^6	12.0	5.23×10^6 (disc)	17.5	1.19×10^6

a. Axial load R = -1.

Table B-24 Fatigue Properties[a] of Parent Metal 7075-T6 Aluminum Alloy

Temperature					
70°F		-320°F		-423°F	
Maximum Tension Stress (1000 psi)	Cycles to Failure	Maximum Tension Stress (1000 psi)	Cycles to Failure	Maximum Tension Stress (1000 psi)	Cycles to Failure
63.0	1.50×10^3	60.0	2.20×10^3	80.0	1.00×10^3
63.0	1.80×10^3	60.0	5.50×10^3	80.0	1.00×10^3
63.0	2.00×10^3	60.0	6.70×10^3	80.0	1.00×10^3 b
40.0	1.40×10^4	40.0	7.12×10^4	80.0	2.00×10^3
40.0	1.80×10^4	40.0	7.98×10^4	65.0	4.20×10^4
40.0	1.90×10^4	40.0	9.32×10^4	60.0	4.20×10^4
30.0	2.80×10^4	30.0	1.32×10^5	60.0	7.10×10^4
30.0	3.20×10^4	30.0	2.67×10^5	60.0	8.80×10^4
30.0	4.10×10^4	30.0	6.58×10^5	50.0	1.42×10^5
17.5	3.06×10^5	20.0	1.32×10^6	50.0	4.35×10^5
17.5	3.44×10^5	20.0	3.44×10^6	50.0	4.35×10^5
17.5	4.20×10^5	20.0	4.30×10^6	42.5	4.63×10^5
12.5	2.07×10^6	17.5	5.12×10^6 (disc)	37.5	4.05×10^6
12.5	2.57×10^6	17.5	5.35×10^6 (disc)	35.0	1.08×10^6
12.5	1.03×10^7 (disc)			35.0	1.11×10^6 (disc)
				35.0	1.20×10^6 (disc)

a. Axial load R = -1.
b. Specimen previously run at 35,000 psi for 1.11×10^6 cycles without failure.

Table B-25 Fatigue Properties[a] of Notched[b] 7075-T6 Aluminum Alloy

Temperature					
70°F		-320°F		-423°F	
Maximum Tension Stress (1000 psi)	Cycles to Failure	Maximum Tension Stress (1000 psi)	Cycles to Failure	Maximum Tension Stress (1000 psi)	Cycles to Failure
25.0	3.00×10^3	25.0	1.00×10^3 f	30.0	1.00×10^3
25.0	6.00×10^3	22.5	2.00×10^3 g	25.0	5.00×10^3
25.0	4.00×10^3 c	20.0	4.00×10^3 h	22.5	1.30×10^4 i
25.0	4.00×10^3 d	20.0	1.10×10^4	20.0	1.20×10^4
20.0	1.60×10^4	17.5	1.20×10^4	17.5	1.60×10^4
20.0	2.70×10^4	15.0	1.00×10^4	15.0	2.10×10^4
20.0	9.00×10^4 e	13.5	2.30×10^4	14.0	7.40×10^4
15.0	4.40×10^4	12.0	5.20×10^4	13.5	1.74×10^5
10.0	5.52×10^5	11.0	5.50×10^4	12.5	4.07×10^5
10.0	7.22×10^5	10.0	8.80×10^4	11.0	2.72×10^5
9.0	5.37×10^5	9.0	1.38×10^5	10.0	5.13×10^5
7.5	1.78×10^6 (disc)	7.5	2.32×10^5	10.0	1.02×10^6 (disc)
7.5	1.46×10^6 (disc)	5.0	9.70×10^5	10.0	1.07×10^6 (disc)
7.5	5.03×10^6 (disc)	5.0	1.35×10^6 (disc)		
		5.0	1.72×10^6 (disc)		

a. Stress ratio (R) = -1.
b. Stress concentration (K_t) = 3.5.
c thru i. Specimen previously run at indicated stress for number of cycles shown without failure.

Footnote	Stress (1000 psi)	Cycles
c	7.5	5.03×10^6
d	7.5	1.46×10^6
e	7.5	5.37×10^6
f	5.0	1.72×10^6
g	5.0	1.88×10^6
h	5.0	1.35×10^6
i	10.0	1.07×10^6

Table B-26 Fatigue Properties[a] of Parent Metal 2020-T6 Aluminum Alloy

Temperature					
70°F		-320°F		-423°F	
Maximum Tension Stress (1000 psi)	Cycles to Failure	Maximum Tension Stress (1000 psi)	Cycles to Failure	Maximum Tension Stress (1000 psi)	Cycles to Failure
50.0	2.00×10^3	70.0	1.00×10^3	70.0	3.00×10^3 b
50.0	2.00×10^3	70.0	1.20×10^3	67.5	4.00×10^3
50.0	4.00×10^3	70.0	2.30×10^3	67.5	1.50×10^4
40.0	8.00×10^3	50.0	2.90×10^4	60.0	1.70×10^4
40.0	9.00×10^3	50.0	4.31×10^4	60.0	2.10×10^4 c
40.0	1.00×10^4	50.0	9.23×10^4	60.0	2.90×10^4
30.0	4.80×10^4	40.0	7.42×10^4	60.0	4.30×10^4
30.0	8.50×10^4	40.0	7.70×10^4	57.3	8.60×10^4
30.0	9.30×10^4	40.0	1.22×10^5	50.0	1.16×10^5
20.0	1.25×10^5	40.0	1.97×10^5	50.0	1.53×10^5
20.0	1.49×10^5	30.0	1.16×10^5	50.0	1.99×10^5
20.0	1.60×10^5	30.0	1.49×10^5	42.5	7.75×10^5
18.0	1.76×10^6	30.0	3.27×10^5	40.0	1.09×10^6
18.0	3.90×10^6	30.0	1.22×10^6	40.0	1.41×10^6 (disc)
18.0	1.03×10^7 (disc)	22.5	1.37×10^6	40.0	1.50×10^6 (disc)
		22.5	2.13×10^6		
		22.5	4.16×10^6		

a. Axial load R = -1.

b and c. Specimen previously run at indicated stress for number of cycles shown without failure.

Footnote	Stress (1000 psi)	Cycles
b	40.0	1.50×10^6
c	40.0	1.41×10^6

Table B-27 Fatigue Properties[a] of Parent Metal AISI 321 Stainless Steel Alloy

Temperature					
70°F		-320°F		-423°F	
Maximum Tension Stress (1000 psi)	Cycles to Failure	Maximum Tension Stress (1000 psi)	Cycles to Failure	Maximum Tension Stress (1000 psi)	Cycles to Failure
60.0	5.00×10^2 b	90.0	9.00×10^2 e	120	1.0×10^3 i
50.0	1.00×10^3	80.0	1.92×10^4	120	1.0×10^3 j
45.0	1.00×10^3	75.0	4.33×10^4 f	115	1.0×10^3 k
45.0	2.00×10^3 c	70.0	4.50×10^4	110	1.2×10^4
42.0	5.00×10^3	70.0	6.02×10^4 g	110	1.7×10^4
40.0	6.00×10^3 d	60.0	1.09×10^5	100	3.6×10^4
40.0	8.00×10^3	55.0	1.82×10^5	90	3.4×10^4
40.0	1.20×10^4	55.0	1.84×10^5 h	80	4.6×10^4
35.0	7.20×10^4	50.0	3.70×10^5	80	1.31×10^5
33.0	9.80×10^4	45.0	1.99×10^6 (disc)	70	1.69×10^5
33.0	2.98×10^5	44.0	8.38×10^5	60	2.7×10^4
32.0	1.09×10^5	42.0	1.81×10^6 (disc)	60	4.86×10^5
32.0	4.74×10^5	40.0	2.28×10^6 (disc)	50	1.00×10^6 (disc)
31.0	1.14×10^6 (disc)	40.0	2.32×10^6 (disc)	50	1.01×10^6 (disc)
30.0	1.25×10^6 (disc)			50	1.00×10^6 (disc)
30.0	1.31×10^6 (disc)				

a. Stress ratio (R) = -1.
b thru k. Specimen previously run at indicated stress for number of cycles shown without failure.

Footnote	Stress (1000 psi)	Cycles
b	30.0	1.31×10^6
c	31.0	1.14×10^6
d	30.0	1.25×10^6
e	42.0	1.81×10^6
f	45.0	1.99×10^6
g	40.0	2.28×10^6
h	40.0	2.32×10^6
i	50.0	1.00×10^6
j	50.0	1.00×10^6
k	50.0	1.01×10^6

Table B-28 Fatigue Properties[a] of Notched[b] AISI 321 Stainless Steel Alloy

Temperature					
70°F		-320°F		-423°F	
Maximum Tension Stress (1000 psi)	Cycles to Failure	Maximum Tension Stress (1000 psi)	Cycles to Failure	Maximum Tension Stress (1000 psi)	Cycles to Failure
40.0	1.00×10^3	65.0	8.20×10^3	80.0	1.00×10^3 j
35.0	2.00×10^3 c	60.0	1.50×10^3 f	75.0	2.00×10^3 k
35.0	4.00×10^3 d	60.0	6.40×10^3	70.0	1.00×10^3 l
35.0	6.00×10^3	60.0	6.70×10^3 g	70.0	5.00×10^3
30.0	2.80×10^4 e	60.0	8.10×10^3	65.1	7.00×10^3
30.0	3.40×10^4	50.0	1.48×10^4 h	60.0	9.00×10^3
30.0	5.20×10^4	40.0	2.89×10^4 i	55.0	1.80×10^4
25.0	1.22×10^5	40.0	3.91×10^4	50.0	1.50×10^4
23.0	1.17×10^5	40.0	4.12×10^4	50.0	3.10×10^4
21.0	3.42×10^5	35.0	8.97×10^4	45.0	6.60×10^4
20.0	6.59×10^5	30.0	1.57×10^5	40.0	9.70×10^4
20.0	1.12×10^6 (disc)	30.0	1.72×10^5	35.0	1.76×10^5
18.0	7.44×10^5	25.0	5.82×10^5	30.0	4.43×10^5
17.0	1.56×10^6 (disc)	23.0	1.37×10^6 (disc)	27.0	1.19×10^5
16.0	1.49×10^6 (disc)	22.0	1.10×10^6 (disc)	25.0	8.12×10^5
		22.0	1.12×10^6 (disc)	25.0	1.02×10^6 (disc)
		20.0	6.94×10^6 (disc)	23.5	1.00×10^6 (disc)
				23.5	1.03×10^6 (disc)

a. Stress ratio (R) = -1.
b. Stress concentration (K_t) = 3.5.
c thru l. Specimen previously run at indicated stress for number of cycles shown without failure.

Footnote	Stress (1000 psi)	Cycles
c	20.0	1.12×10^6
d	16.0	1.49×10^6
e	17.0	1.56×10^6
f	22.0	1.12×10^6
g	23.0	1.37×10^6
h	22.0	1.10×10^6
i	20.0	6.94×10^6
j	23.5	1.00×10^6
k	23.5	1.03×10^6
l	25.0	1.02×10^6

Table B-29 Fatigue Properties[a] of Welded AISI 321 Stainless Steel Alloy

Temperature					
70°F		-320°F		-423°F	
Maximum Tension Stress (1000 psi)	Cycles to Failure	Maximum Tension Stress (1000 psi)	Cycles to Failure	Maximum Tension Stress (1000 psi)	Cycles to Failure
40.0	1.00×10^3 b	80.0	1.10×10^3 e	100.0	2.00×10^3 g
40.0	2.00×10^3	80.0	3.60×10^3	100.0	6.00×10^3 h
40.0	3.00×10^3	80.0	5.70×10^3 f	90.0	4.00×10^3 i
40.0	4.00×10^3 c	80.0	7.90×10^3	90.0	2.90×10^4
40.0	5.00×10^3	60.0	5.06×10^4	80.0	9.00×10^3
40.0	6.00×10^3 d	50.0	5.49×10^4	70.0	5.20×10^4
30.0	2.30×10^4	40.0	1.58×10^5	70.0	5.20×10^4
30.0	6.60×10^4	35.0	8.61×10^4	60.0	3.40×10^4
25.0	7.20×10^4	35.0	2.01×10^5	50.0	1.33×10^5
25.0	1.90×10^5	35.0	1.30×10^6	45.0	2.45×10^5
22.0	1.53×10^6 (disc)	30.0	4.10×10^5	40.0	3.61×10^5
20.0	7.89×10^5	30.0	1.12×10^6 (disc)	30.0	8.22×10^5
20.0	1.07×10^6	30.0	1.90×10^6 (disc)	27.5	1.0×10^6 (disc)
20.0	1.45×10^6	28.0	2.24×10^6	27.5	1.005×10^6 (disc)
18.0	1.20×10^6 (disc)			27.5	1.103×10^6 (disc)
18.0	4.50×10^6 (disc)				

a. Stress ratio (R) = -1.

b thru i. Specimen previously run at indicated stress for number of cycles shown without failure.

Footnote	Stress (1000 psi)	Cycles
b	22.0	1.53×10^6
c	18.0	1.20×10^6
d	18.0	4.50×10^6
e	30.0	1.90×10^6
f	30.0	1.12×10^6
g	27.5	1.01×10^6
h	27.5	1.00×10^6
i	27.5	1.10×10^6

ble B-30 Fatigue Properties[a] of Unnotched Parent Metal A-286 Stainless Steel Alloy

Temperature					
70°F		-320°F		-423°F	
Maximum Tension Stress (1000 psi)	Cycles to Failure	Maximum Tension Stress (1000 psi)	Cycles to Failure	Maximum Tension Stress (1000 psi)	Cycles to Failure
55.0	2.00×10^3	90.0	Failed Immediately	90.0	1.00×10^3
50.0	3.00×10^3	90.0	1.00×10^2 f	87.5	1.00×10^3
50.0	4.50×10^3	86.0	1.00×10^2	87.5	1.00×10^3 i
50.0	5.50×10^3 b	85.0	1.00×10^2	86.0	3.00×10^3
48.0	6.00×10^3 c	84.0	2.10×10^3 g	85.0	1.10×10^4 j
48.0	6.00×10^4	83.0	4.80×10^4 h	80.0	1.60×10^4
47.5	5.60×10^4	81.0	2.00×10^2	78.5	1.03×10^5
47.0	6.20×10^4 d	80.0	4.29×10^4	78.0	1.00×10^4 k
45.0	5.00×10^4 e	80.0	6.28×10^4	77.5	1.06×10^5
45.0	5.10×10^4	75.0	1.77×10^5	75.0	5.33×10^5
40.0	2.35×10^5	70.0	3.34×10^5	70.0	8.95×10^5
38.0	6.18×10^5	62.0	5.03×10^5	65.0	9.98×10^5
35.0	1.11×10^6 (disc)	60.0	7.30×10^5	65.0	1.03×10^6 (disc)
32.5	1.13×10^6 (disc)	55.0	1.16×10^6 (disc)	65.0	1.06×10^6 (disc)
32.0	1.01×10^6	55.0	1.42×10^6 (disc)	65.0	1.22×10^6 (disc)
30.0	1.11×10^6 (disc)	40.0	1.13×10^6 (disc)		
30.0	1.37×10^6 (disc)				

a. Stress ratio (R) = -1.
b thru k. Specimen previously run at indicated stress for number of cycles shown without failure.

Footnote	Stress (1000 psi)	Cycles
b	35.0	1.11×10^6
c	30.0	1.11×10^6
d	32.5	1.13×10^6
e	30.0	1.37×10^6
f	40.0	1.13×10^6
g	55.0	1.42×10^6
h	55.0	1.16×10^6
i	65.0	1.03×10^6
j	65.0	1.06×10^6
k	65.0	1.22×10^6

Table B-31 Fatigue Properties[a] of Notched[b] Parent Metal A-286 Stainless Steel Alloy

Temperature					
70°F		-320°F		-423°F	
Maximum Tension Stress (1000 psi)	Cycles to Failure	Maximum Tension Stress (1000 psi)	Cycles to Failure	Maximum Tension Stress (1000 psi)	Cycles to Failure
50.0	1.00×10^3	70.0	2.40×10^3	90.0	2.00×10^3
45.0	1.00×10^3 c	65.0	7.60×10^3	80.0	5.00×10^3
45.0	1.50×10^3 d	60.0	8.00×10^3 e	70.0	9.00×10^3 h
45.0	1.50×10^3	60.0	8.70×10^3	60.0	1.30×10^4 i
40.0	6.50×10^3	60.0	9.70×10^3 f	55.0	1.90×10^4 j
35.0	2.00×10^4	60.0	1.44×10^4 g	50.0	2.70×10^4
32.5	1.95×10^4	50.0	2.75×10^4	45.0	6.90×10^4
30.0	2.20×10^4	40.0	4.91×10^4	40.0	8.10×10^4
27.0	5.75×10^4	32.0	9.52×10^4	27.5	9.60×10^4
25.0	1.18×10^5	30.0	9.26×10^4	20.5	4.97×10^5
23.0	1.34×10^5	28.0	8.90×10^4	17.5	6.16×10^5
21.5	6.12×10^5	27.0	1.72×10^5	13.5	7.99×10^5
20.0	5.11×10^5	26.0	2.59×10^5	13.5	1.02×10^6 (disc)
20.0	1.10×10^6 (disc)	26.0	1.10×10^6 (disc)	13.5	1.07×10^6 (disc)
20.0	1.12×10^6 (disc)	26.0	1.31×10^6 (disc)	12.5	1.04×10^6 (disc)
		24.0	1.18×10^6 (disc)		

a. Stress ratio (R) = -1.
b. Stress concentration (K_t) = 3.5.
c thru j. Specimen previously run at indicated stress for number of cycles shown without failure.

Footnote	Stress (1000 psi)	Cycles
c	20.0	1.10×10^6
d	20.0	1.12×10^6
e	24.0	1.18×10^6
f	26.0	1.10×10^6
g	26.0	1.31×10^6
h	12.5	1.04×10^6
i	13.5	1.07×10^6
j	13.5	1.02×10^6

Table B-32 Fatigue Properties[a] of Welded A-286 Stainless Steel Alloy

Temperature					
70°F		-320°F		-423°F	
Maximum Tension Stress (1000 psi)	Cycles to Failure	Maximum Tension Stress (1000 psi)	Cycles to Failure	Maximum Tension Stress (1000 psi)	Cycles to Failure
47.0	5.00×10^2 b	60.0	9.70×10^3	85.0	3.00×10^3
45.0	2.50×10^3	56.0	6.30×10^3	80.0	5.00×10^3
42.0	3.50×10^3 c	55.0	3.70×10^4	75.0	1.00×10^3 g
40.0	1.00×10^4	52.0	1.09×10^4	70.0	1.00×10^4
35.0	2.20×10^4	50.0	1.10×10^3 e	65.0	5.00×10^3
32.0	0.00×10^1 d	45.0	4.41×10^4	60.0	1.90×10^4 h
32.0	2.90×10^4	40.0	1.04×10^4 f	55.0	3.40×10^4 i
30.0	7.10×10^4	40.0	5.17×10^4	50.0	7.70×10^4
25.0	8.95×10^4	35.0	2.03×10^5	45.0	1.96×10^5
20.0	1.47×10^5	33.0	1.94×10^5	40.0	4.52×10^5
18.0	2.43×10^5	31.0	4.56×10^5	35.0	3.92×10^5
17.0	5.95×10^5	31.0	1.01×10^5	30.0	2.30×10^5
16.0	1.12×10^6 (disc)	30.0	1.47×10^5	30.0	1.01×10^6 (disc)
16.0	1.13×10^6 (disc)	28.0	1.42×10^5	30.0	1.01×10^6 (disc)
15.0	1.12×10^6 (disc)	26.0	2.29×10^5	25.0	1.06×10^6 (disc)
		20.0	8.34×10^5		
		18.0	1.13×10^6 (disc)		
		18.0	1.26×10^6 (disc)		

a. Stress ratio (R) = -1.
b thru i. Specimen previously run at indicated stress for number of cycles shown without failure.

Footnote	Stress (1000 psi)	Cycles
b	16.0	1.12×10^6
c	15.0	1.12×10^6
d	16.0	1.13×10^6
e	18.0	1.13×10^6
f	18.0	1.26×10^6
g	30.0	1.01×10^6
h	25.0	1.06×10^6
i	30.0	1.01×10^6

Table B-33 Fatigure Properties[a] of Unnotched Parent Metal Inconel 718 Nickel Alloy

Temperature					
70°F		-320°F		-423°F	
Maximum Tension Stress (1000 psi)	Cycles to Failure	Maximum Tension Stress (1000 psi)	Cycles to Failure	Maximum Tension Stress (1000 psi)	Cycles to Failure
85.0	5.00×10^2	102.0	1.41×10^5	120.0	1.00×10^3
80.0	1.00×10^3	100.0	1.40×10^3	120.0	1.00×10^3 g
77.0	1.00×10^3 b	100.0	3.31×10^4	115.0	1.00×10^3 h
77.0	2.00×10^3 c	99.0	2.01×10^4	112.5	1.00×10^3 i
75.0	3.00×10^3	98.0	1.30×10^3 e	112.5	2.00×10^3
75.0	9.00×10^3	98.0	5.10×10^3 f	111.0	1.41×10^5
75.0	4.20×10^4 d	98.0	1.05×10^4	111.0	1.49×10^5
73.0	2.20×10^4	95.0	3.94×10^4	110.0	3.90×10^4
73.0	5.70×10^4	90.0	2.04×10^5	107.5	2.72×10^5
70.0	1.09×10^5	90.0	3.10×10^5	105.0	4.64×10^5
70.0	1.55×10^5	85.0	2.00×10^2	100.0	3.08×10^5
65.0	2.14×10^5	85.0	4.02×10^5	100.0	3.87×10^5
60.0	9.32×10^5	80.0	1.00×10^3	100.0	1.16×10^6 (disc)
60.0	1.18×10^6 (disc)	80.0	1.93×10^5	97.5	1.01×10^6 (disc)
60.0	1.36×10^6 (disc)	80.0	6.27×10^5	95.0	1.14×10^6 (disc)
57.0	1.27×10^6 (disc)	70.0	1.09×10^5		
		70.0	1.53×10^5		
		70.0	1.10×10^6		
		68.0	1.13×10^6 (disc)		
		68.0	1.21×10^6		
		66.0	1.18×10^6 (disc)		

a. Stress ratio (R) = -1.
b thru i. Specimen previously run at indicated stress for number of cycles shown without failure.

Footnote	Stress (1000 psi)	Cycles
b	57.0	1.27×10^6
c	60.0	1.18×10^6
d	60.0	1.36×10^6
e	68.0	1.13×10^6
f	66.0	1.18×10^6
g	95.0	1.14×10^6
h	100.0	1.16×10^6
i	97.5	1.01×10^6

Table B-34 Fatigue Properties[a] of Notched[b] Parent Metal Inconel 718 Nickel Alloy

Temperature					
70°F		-320°F		-423°F	
Maximum Tension Stress (1000 psi)	Cycles to Failure	Maximum Tension Stress (1000 psi)	Cycles to Failure	Maximum Tension Stress (1000 psi)	Cycles to Failure
75.0	2.00×10^3 c	85.0	2.80×10^3 f	90.0	6.00×10^3 h
75.0	3.00×10^3	85.0	4.10×10^3	80.0	1.10×10^4 i
75.0	3.00×10^3 d	85.0	5.30×10^3 g	75.0	1.10×10^4 j
70.0	4.00×10^3 e	80.0	5.50×10^3	70.0	8.00×10^3
70.0	5.00×10^3	75.0	9.40×10^3	65.0	2.40×10^4
65.0	9.00×10^3	70.0	1.25×10^4	60.0	3.10×10^4
60.0	1.60×10^4	65.0	1.77×10^4	50.0	5.30×10^4
50.0	5.00×10^4	60.0	3.08×10^4	45.0	2.11×10^5
45.0	7.40×10^4	50.0	1.02×10^5	40.0	2.23×10^5
40.0	5.58×10^5	45.0	3.66×10^5	35.0	1.37×10^5
35.0	3.22×10^5	40.0	3.25×10^5	35.0	2.94×10^5
35.0	1.42×10^6 (disc)	38.0	4.29×10^5	35.0	1.18×10^6 (disc)
33.0	3.28×10^5	38.0	7.10×10^5	30.0	6.02×10^5
32.0	1.19×10^6 (disc)	36.0	4.76×10^5	22.5	1.09×10^6 (disc)
32.0	1.29×10^6 (disc)	36.0	9.21×10^5	22.5	1.13×10^6 (disc)
		35.0	1.21×10^6 (disc)		
		34.0	1.32×10^6 (disc)		

a. Stress ratio = -1.
b. Stress concentration K_t = 3.5.
c thru j. Specimen previously run at indicated stress for number of cycles shown without failure.

Footnote	Stress (1000 psi)	Cycles
c	32.0	1.29×10^6
d	32.0	1.19×10^6
e	35.0	1.42×10^6
f	35.0	1.21×10^6
g	34.0	1.32×10^6
h	22.5	1.09×10^6
i	35.0	1.18×10^6
j	22.5	1.13×10^6

Table B-35 Fatigue Properties[a] of Welded Inconel 718 Nickel Alloy

Temperature					
70°F		-320°F		-423°F	
Maxinum Tension Stress (1000 psi)	Cycles to Failure	Maximum Tension Stress (1000 psi)	Cycles to Failure	Maximum Tension Stress (1000 psi)	Cycles to Failure
75.0	1.00×10^3	105.0	2.20×10^3	115.0	1.00×10^3 i
72.0	2.00×10^3	100.0	4.10×10^3	110.0	5.00×10^3 j
70.0	6.00×10^3	95.0	5.60×10^3	100.0	6.00×10^3 k
65.0	4.00×10^3	90.0	1.40×10^4	90.0	8.00×10^3
60.0	1.00×10^3 b	90.0	1.61×10^4 f	87.5	2.10×10^4
60.0	2.00×10^3 c	90.0	2.64×10^4 g	87.5	7.80×10^4
60.0	9.00×10^3	90.0	4.24×10^4 h	85.0	6.70×10^4
55.0	7.00×10^3 d	80.0	4.43×10^4	80.0	6.50×10^4
55.0	1.50×10^4 e	70.0	7.52×10^4	75.0	8.20×10^4
55.0	2.20×10^4	65.0	4.71×10^4	75.0	1.71×10^4
50.0	1.41×10^5	60.0	3.05×10^5	65.0	2.87×10^5
45.0	3.30×10^4	57.0	1.42×10^6	60.0	1.46×10^5
40.0	2.52×10^5	55.0	1.73×10^5	55.0	1.05×10^6 (disc)
35.0	5.46×10^5	50.0	4.43×10^5	55.0	1.07×10^6 (disc)
34.0	1.11×10^6 (disc)	45.0	1.11×10^6 (disc)	50.0	1.00×10^6 (disc)
30.0	1.14×10^6 (disc)	45.0	1.11×10^6 (disc)		
30.0	1.14×10^6 (disc)	45.0	1.15×10^6 (disc)		
30.0	1.30×10^6 (disc)				

a. Stress ratio (R) = -1.
b thru k. Specimen previously run at indicated stress for number of cycles shown without failure.

Footnote	Stress (1000 psi)	Cycles
b	30.0	1.30×10^6
c	30.0	1.14×10^6
d	30.0	1.14×10^6
e	34.0	1.11×10^6
f	45.0	1.15×10^6
g	45.0	1.11×10^6
h	45.0	1.11×10^6
i	55.0	1.05×10^6
j	50.0	1.00×10^6
k	55.0	1.07×10^6

Table B-36 Fatigue Properties[a] of Unnotched Parent Metal Hastelloy C Nickel Alloy

Temperature					
70°F		-320°F		-423°F	
Maximum Tension Stress (1000 psi)	Cycles to Failure	Maximum Tension Stress (1000 psi)	Cycles to Failure	Maximum Tension Stress (1000 psi)	Cycles to Failure
80.0	1.00×10^3	95.0	6.70×10^3	120.0	1.00×10^3 f
70.0	2.00×10^3 b	95.0	2.25×10^4	110.0	1.00×10^3
70.0	5.00×10^3	90.0	7.00×10^2 c	110.0	1.00×10^3 g
65.0	6.00×10^3	90.0	1.00×10^3 d	108.0	6.00×10^3
62.0	3.74×10^5	90.0	2.77×10^4	107.5	1.40×10^4 h
60.0	1.58×10^5	90.0	7.08×10^4	105.0	4.10×10^4
60.0	4.03×10^5	85.0	2.00×10^3 e	102.5	3.30×10^4
55.0	7.40×10^5	85.0	7.15×10^4	100.0	1.85×10^5
50.0	1.17×10^6	80.0	6.52×10^5	95.0	2.97×10^5
50.0	1.20×10^6	80.0	7.35×10^5	94.0	2.80×10^4
48.0	9.28×10^5	76.0	9.57×10^5	90.0	1.00×10^6 (disc)
46.0	1.90×10^6 (disc)	75.0	1.18×10^6 (disc)	90.0	1.02×10^6 (disc)
		75.0	1.18×10^6 (disc)	90.0	1.07×10^6 (disc)
		75.0	1.28×10^6		
		60.0	1.69×10^6 (disc)		

a. Stress ratio (R) = -1.
b thru h. Specimen previously run at indicated stress for number of cycles shown without failure.

Footnote	Stress (1000 psi)	Cycles
b	46.0	1.90×10^6
c	60.0	1.69×10^6
d	75.0	1.18×10^6
e	75.0	1.18×10^6
f	90.0	1.02×10^6
g	90.0	1.00×10^6
h	90.0	1.07×10^6

Table B-37 Fatigue Properties[a] of Notched[b] Parent Metal Hastelloy C Nickel Alloy

Temperature					
70°F		-320°F		-423°F	
Maximum Tension Stress (1000 psi)	Cycles to Failure	Maximum Tension Stress (1000 psi)	Cycles to Failure	Maximum Tension Stress (1000 psi)	Cycles to Failure
65.0	3.00×10^3	70.0	3.00×10^3 e	90.0	2.00×10^3 g
60.0	1.00×10^3 c	65.0	9.0×10^3	80.0	7.00×10^3 h
55.0	7.00×10^3	60.0	9.2×10^3 f	75.0	7.00×10^3 i
55.0	1.00×10^4 d	60.0	1.12×10^4	65.0	1.60×10^4
50.0	1.60×10^4	50.0	2.89×10^4	60.0	1.90×10^4
40.0	3.70×10^4	40.0	1.37×10^4	54.8	3.80×10^4
30.0	1.43×10^5	40.0	5.72×10^4	50.0	3.20×10^4
25.0	3.17×10^5	36.0	1.99×10^5	45.0	5.60×10^4
22.0	5.05×10^5	35.0	1.49×10^5	42.9	5.60×10^4
20.0	1.07×10^6	30.0	6.62×10^5	35.4	2.84×10^5
18.0	1.53×10^6	25.0	6.28×10^5	30.0	5.09×10^5
18.0	1.15×10^6 (disc)	22.0	1.16×10^6 (disc)	27.5	3.75×10^5
18.0	1.12×10^6 (disc)	20.0	1.13×10^6 (disc)	25.0	3.90×10^5
		20.0	1.46×10^6	22.4	3.16×10^5
				20.0	2.86×10^5
				17.5	6.25×10^5
				13.0	1.02×10^6 (disc)
				13.0	1.07×10^6 (disc)
				13.0	1.12×10^6 (disc)

a. Stress ratio (R) = -1.
b. Stress concentration (K_t) = 3.5.
c thru i. Specimen previously run at indicated stress for number of cycles shown without failure.

Footnote	Stress (1000 psi)	Cycles
c	18.0	1.15×10^6
d	18.0	1.12×10^6
e	22.0	1.16×10^6
f	20.0	1.13×10^6
g	13.0	1.12×10^6
h	13.0	1.07×10^6
i	13.0	1.02×10^6

Table B-38 Fatigue Properties[a] of Welded Hastelloy C Nickel Alloy

Temperature					
70°F		-320°F		-423°F	
Maximum Tension Stress (1000 psi)	Cycles to Failure	Maximum Tension Stress (1000 psi)	Cycles to Failure	Maximim Tension Stress (1000 psi)	Cycles to Failure
75.0	2.00×10^3	105.0	5.50×10^3	130.0	1.00×10^3 h
70.0	3.00×10^3	100.0	6.00×10^3	120.0	9.00×10^3 i
65.0	5.00×10^3	95.0	2.23×10^4	110.0	1.00×10^3
60.0	3.00×10^3 b	90.0	4.09×10^4	105.0	5.00×10^4 j
60.0	5.00×10^3 c	90.0	4.55×10^4 e	100.0	1.70×10^4
60.0	9.00×10^3 d	80.0	3.34×10^4	95.0	2.20×10^4
60.0	3.00×10^4	80.0	6.99×10^4 f	90.0	1.16×10^5
55.0	1.30×10^4	75.0	9.81×10^4 g	80.0	4.43×10^5
50.0	6.90×10^4	70.0	6.27×10^4	75.0	1.03×10^5
48.0	2.03×10^5	65.0	1.19×10^5	70.0	7.90×10^5
45.0	5.58×10^5	60.0	4.41×10^5	65.0	5.00×10^5
40.0	5.20×10^5	57.0	1.01×10^6	60.0	3.11×10^5
38.0	6.79×10^5	56.0	5.71×10^5	60.0	1.04×10^6 (disc)
35.0	1.14×10^6 (disc)	53.0	7.56×10^5	55.0	1.00×10^6 (disc)
35.0	1.17×10^6 (disc)	50.0	1.12×10^6 (disc)	55.0	1.01×10^6 (disc)
35.0	1.19×10^6 (disc)	50.0	1.13×10^6 (disc)		
		50.0	1.16×10^6 (disc)		

a. Stress ratio (R) = -1.
b thru j. Specimen previously run at indicated stress for number of cycles shown without failure.

Footnote	Stress (1000 psi)	Cycles
b	35.0	1.14×10^6
c	35.0	1.17×10^6
d	35.0	1.19×10^6
e	50.0	1.16×10^6
f	50.0	1.12×10^6
g	50.0	1.13×10^6
h	55.0	1.00×10^6
i	55.0	1.01×10^6
j	60.0	1.04×10^6

20 Air Force Materials Laboratory
Wright-Patterson Air Force Base
Dayton, Ohio 45433
Attn: Mr. M. Knight (MAAM)

21 National Aeronautics and Space Administration
Manned Spacecraft Center
Systems Evaluation and Development Division
Houston, Texas 77001
Attn: Mr. J. Kotanchik

22 U. S. Army Materials Research Agency
Watertown Arsenal
Watertown, Massachusetts 02177
Attn: Mr. C. Hickey

23 Belfour Engineering Company
Technical Information Systems
Suttons Bay, Michigan 49682
Attn: Mr. R. C. Braden

24 NBS Cryogenic Engineering Laboratories
Cryogenic Data Center
Boulder, Colorado 80301
Attn: Mrs. J. Mendenhall

25 Aluminum Company of America
Alcoa Research Laboratories
New Kensington, Pennsylvania 15068
Attn: Mr. H. Y. Hunsicker

26 National Aeronautics and Space Administration
NASA Committee on Fatigue Research and Technology
Washington, D. C. 20546
Attn: Mr. Harvey H. Brown, RAL/Secretary

27 National Aeronautics and Space Administration
Langley Research Center
Langley Station
Hampton, Virginia 23365
Attn: Mr. Herbert F. Hardrath

28 National Aeronautics and Space Administration
Langley Research Center
Langely Station
Hampton, Virginia 23365
Attn: Mr. Thomas Coleman

DISTRIBUTION

Copies	To
1 thru 13	National Aeronautics and Space Administration George C. Marshall Space Flight Center Huntsville, Alabama 35812 Attn: PR-EC
14	Air Force Flight Dynamics Laboratory Wright-Patterson Air Force Base Dayton, Ohio 45433 Attn: Mr. L. Kelly (FDTS)
15	Defense Metals Information Center Battelle Memorial Institute 505 King Avenue Columbus, Ohio 43201 Attn: Mr. D. H. Owens
16	Douglas Aircraft Company MSSD, MRPH, Department A-260 3000 Ocean Park Boulevard Santa Monica, California 90405 Attn: Mr. G. V. Bennett
17	Kaiser Aluminum and Chemical Corporation Department of Metallurgical Research Spokane, Washington 99210 Attn: Mr. F. W. DeMoney, Head Mechanical Metallurgy Branch
18	National Aeronautics and Space Administration Lewis Research Center 21000 Brookpark Road Cleveland, Ohio 44135 Attn: Mr. J. Freche (Mail Stop 49-1)
19	General Dynamics/Astronautics 5001 Kearney Villa Road San Diego, California 92123 Attn: Mr. R. W. Tryon, Department 592-1

29 National Aeronautics and Space Administration
Lewis Research Center
21000 Brookpark Road
Cleveland, Ohio 44135
Attn: Mr. Samuel S. Manson

30 Dr. Horace J. Grover
584 Fox Lane
Worthington, Ohio 43201

31 The Boeing Company
Airplane Division
Box 707
Renton, Washington 98056
Attn: Mr. Howard W. Smith,
Assistant Director of Engineering

32 Professor Egon Orowan
Department of Mechanical Engineering (1-306)
Massachusetts Institute of Technology
77 Massachusetts Avenue
Cambridge, Massachusetts 02139

33 Mr. John B. Johnson
1236 Cumberland Avenue
Dayton, Ohio 45406

34 Professor Norman C. Dahl
Department of Mechanical Engineering (3-360)
Massachusetts Institute of Technology
77 Massachusetts Avenue
Cambridge, Massachusetts 02139

35 Hamilton Standard Division
United Aircraft Corporation
Windsor Locks, Connecticut 06096
Attn: Mr. D. F. Phillips, Technical Planning

36 Argonne National Laboratory
High Energy Physics Division, Building D362
9700 South Case Avenue
Argonne, Illinois 60440
Attn: Mr. A. Tamosaitis

37	Brookhaven National Laboratory Associated Universities, Incorporated Upton, Long Island, New York 11973 Attn: Mr. Joseph A. Bamberger
38	National Aeronautics and Space Administration Manned Spacecraft Center Houston, Texas 77001 Attn: Mr. R. E. Johnson
Remaining Copies	Martin Company Denver Division Denver, Colorado 80201 Attn: Libraries Section